Application of IR and NMR spectroscopy to certain complexes of 8-hydroxyquinoline and 8-aminoquinoline

A thesis submitted to the
University of Cape Town
in fulfilment of the requirements for the degree of
Master of Science

by

Cheryl Lynn Knight B.Sc. (Hons.)

Department of Inorganic Chemistry
University of Cape Town
Rondebosch
7700
South Africa

December 1987

To my Parents

Acknowledgements

I would like to extend my sincere thanks and appreciation to:

My supervisor, Professor D.A. Thornton, for his patience, advice and overall guidance of this study.

Dr. G.E. Jackson for his invaluable assistance and interest in the NMR research.

Dr. C. Engelter for her encouragement and interest at all times.

Mark Kelly and Dr. A. Hendry for their friendly advice and help, particularly with the proof-reading of this manuscript.

Mrs. P. Alexander for her proficient typing of this thesis.

The University of Cape Town and the South African Council for Scientific and Industrial Research for financial assistance.

My parents for their immeasurable support and encouragement.

Summary

The IR spectra of twenty-one transition metal complexes of 8-hydroxyquinoline over the range 700 - 50 cm^{-1} are discussed in relation to their known or inferred structures. The complexes are of three types: (a) the *bis*(aquo) complexes of the first row transition metal(II) ions, $[M(ox)_2(H_2O)_2]$ (M = Mn, Fe, Co, Ni, Cu, Zn); (b) the corresponding anhydrous complexes, $[M(ox)_2]_n$ (M = Mn, Co, Ni, Cu, Zn) and (c) the complexes of the metal(III) ions, $[M(ox)_3]$ (M = Sc, V, Cr, Mn, Fe, Co, Ga, Rh and In). Deuterated 8-hydroxyquinoline was synthesized by the Skraup synthesis and has been used to assist in the assignment of the metal-ligand modes. The assignment of these bands was further based on $^{64,68}Zn$ labelling of the *bis*(aquo) zinc chelate and on the effects of metal ion substitution in relation to structural considerations based on crystal field theory.

An investigation of the IR spectra of a series of *tris*, *bis* and *mono*(8-aminoquinoline) complexes of the first transition row metal(II) perchlorates and halides is reported. The complexes are of the type: (a) $[M(aq)_3](ClO_4)_2$ (M = Fe, Co, Ni); (b) $[M(aq)_2(H_2O)_2]X_2$ (M = Fe, X = Cl; M = Co, Ni, Cu, X = Cl, Br) and (c) $[M(aq)X_2]$ (M = Cu, Zn; X = Cl, Br). Deuteration of the amino group of 8-aminoquinoline has enabled assignments of the internal vibrations of the amino group in the high frequency region to be made. This labelling technique also permits differentiation between the two species of metal-nitrogen frequencies, *viz.*, $\nu M\text{-}NH_2$ and $\nu M\text{-}N(py)$. Of particular interest in view of structural implications of Jahn-Teller distortion, is the deviation from the normal Irving-Williams stability sequence observed for the Cu(II) compounds.

In a study of the ^{1}H-NMR spectra of paramagnetic Ni(II) oxine complexes, it was found that the chelates were not fluxional at room temperature. The assignment of the NMR spectra was therefore complex, because several isomers of these chelates were found to co-exist at room temperature. Initial assignments were thus made at 393.1 K (fast exchange conditions) using chemical substitution data. The free energy of activation $\Delta G^{\neq}$, for exchange between the various forms, was calculated using computer simulation. Two mechanisms have been proposed to account for the fluxional behaviour of the chelates.

INDO (Intermediate Neglect of Differential Overlap) calculations of spin density were performed and the results correlated with the experimentally observed NMR shifts. The shifts are interpreted in terms of mechanisms for spin-delocalization into the ligand. It was found that spin-delocalization occurred predominantly *via* a π-mechanism and involved the transfer of spin from the metal into the antibonding orbital (π^*) of the ligand. This probably arises from π-bonding through the nitrogen atom. There was no spectral evidence for π-bonding through the phenolic oxygen atom.

Abbreviations

Abbreviations of ligands used in this study.

aq	=	8-aminoquinoline
ox	=	8-hydroxyquinoline
dmso	=	dimethylsulphoxide

Abbreviations used in the IR study.

B.M.	=	Bohr magneton
CFSE	=	Crystal Field Stabilization Energy
LFT	=	Ligand Field Theory
MOT	=	Molecular Orbital Theory
def.	=	deformation
i.p.	=	in-plane
o.o.p.	=	out-of-plane
IR	=	Infrared
kK	=	kiloKayser
L	=	generalized ligand
M	=	generalized metal
R	=	generalized substituent
X	=	generalized anion
α	=	infrared bending vibration : in-plane
δ	=	infrared bending vibration
γ	=	infrared bending vibration : out-of-plane
ν	=	infrared stretching vibration
ν(ring)	=	infrared stretching vibration or in-plane bend of the ring
ρ	=	infrared bending vibration : rocking

ω	=	infrared bending vibration : wagging
τ	=	infrared bending vibration : twisting

Abbreviations used in the NMR study.

$A_{N.}$	=	Nuclear spin-electron coupling constant
ESR	=	Electron Spin Resonance
δ	=	chemical shift (ppm)
$\Delta G^{\neq}$	=	free energy of activation
K	=	rate constant
INDO	=	Intermediate Neglect of Differential Overlap
NMR	=	Nuclear Magnetic Resonance
ν	=	frequency of diamagnetic resonance
$\Delta\nu^{con}$	=	shift caused by the contact interaction
$\Delta\nu^{dip}$	=	shift caused by the dipolar interaction
ρ_{sN}	=	spin density in the valence s orbital on nucleus N

Structural formulae of ligands

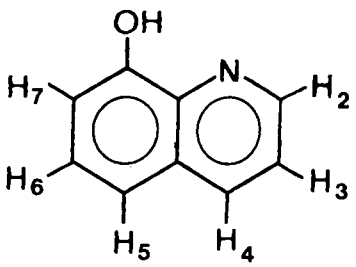

8-hydroxyquinoline (ox)

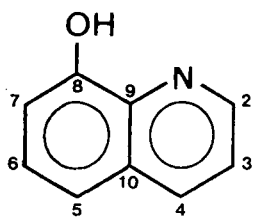

8-hydroxyquinoline (ox)

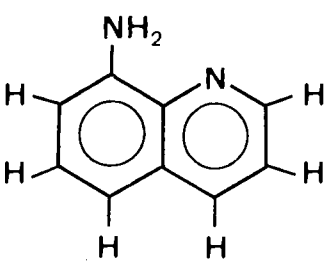

8-aminoquinoline (aq)

Contents

Chapter One

CHAPTER ONE

1. INTRODUCTION

1.1 INFRARED SPECTROSCOPY : A BRIEF OUTLINE OF THE THEORY

A very important aspect of chemistry is the determination of the structure of a compound, and spectroscopy has been shown to be a useful method for structure determination. Streitwieser and Heathcock [1] have defined spectroscopy as an experimental process in which the energy differences between allowed states of a system are measured by detecting the frequencies of the corresponding light (energy) absorbed. The energy difference between the different quantum states depends on the physical phenomenon involved. That is, each phenomenon corresponds to the absorption of light in a different region of the electromagnetic spectrum. Since the range of wavelengths required is so vast, different instrumentation is needed for each spectral region. For Raman and infrared spectroscopy, the physical phenomenon is molecular vibrational energy. These techniques encompass radiation having wavenumbers ranging from roughly 10 000 to 10 cm^{-1}.

If a molecule is to absorb infrared radiation, it must undergo a net change in dipole moment as a result of its vibrational or rotational motion. Only under these circumstances, can the alternating field of the radiation interact with the molecule and cause a change in its motion. For example, the charge distribution about carbon monoxide is not symmetrical; one atom having a greater electron density than the other. Thus, when the distance between the centres fluctuates, as it does in a

vibration, an oscillating electric field is established which can interact with the electric field associated with the radiation. If the frequency of the radiation matches a natural vibrational frequency of the molecule, a net transfer of energy occurs. This results in a change of the amplitude of the molecular vibration and absorption of radiation therefore occurs. Similarly, the rotation of unsymmetrical molecules about their centres of mass will produce a fluctuation in dipole moment; again, interaction with the radiation is possible. At normal pressures, molecules such as oxygen, nitrogen and chlorine do not absorb in the infrared region because there is no net change in dipole moment during the vibration or rotation of these homonuclear species.

The relative positions of atoms in a molecule are not fixed, but fluctuate continuously because of several types of vibrations. In a simple diatomic/triatomic molecule it is possible to define the number and nature of such vibrations and relate these to the energies of absorptions. Analysis becomes extremely difficult, if not impossible, with polyatomic molecules because of the large number of vibrating centres and the possibility of interactions occurring between several centres.

Vibrations fall into the basic categories of stretches and bends. A stretching vibration involves a continuous change in the interatomic distance along the axis of the bond between two atoms. Bending vibrations are characterized by a change in the angle between two bonds and are of four types: scissoring, rocking, wagging and twisting. The various types of vibrations are shown in Fig. 1.1.

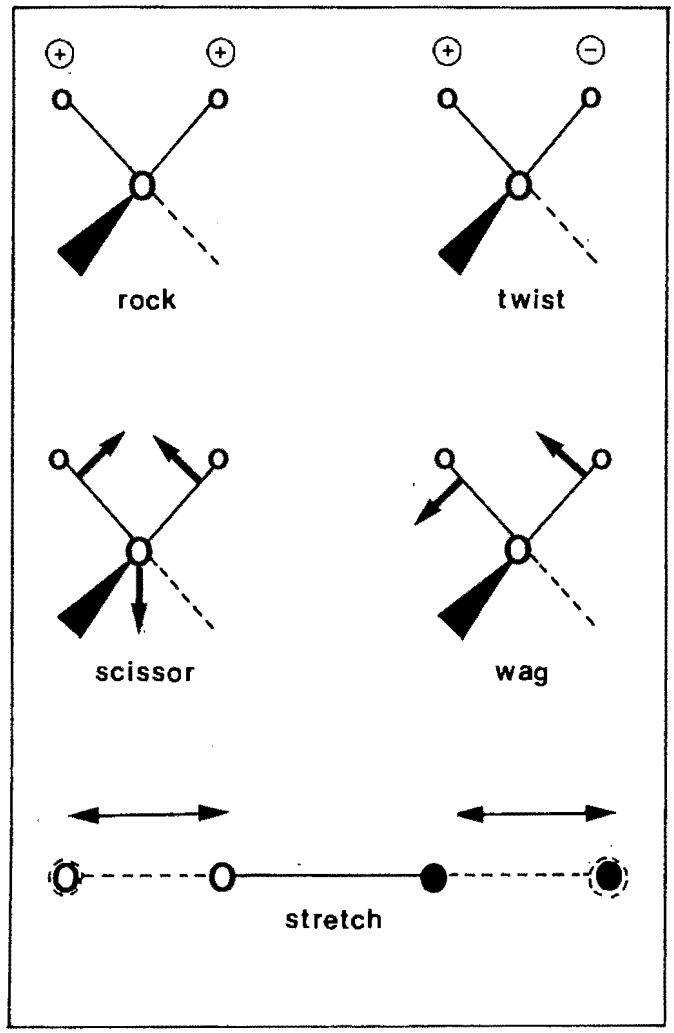

Fig. 1.1 Types of molecular vibrations. Note: ⊕ indicates motion from plane of page toward reader; ⊖ indicates motion from plane of page away from reader.

In a polyatomic molecule, all of the above vibrations are possible. In addition, interaction or coupling of vibrations can occur if the vibrations of a diatomic species have similar energy. The result of coupling is a change in the characteristics of the vibrations involved. As a result, the position of an absorption peak corresponding to a given organic functional group cannot be specified exactly. While coupling may lead to uncertainties in the identification of functional groups contained in a compound,

it is this effect that provides the unique features of an infrared absorption spectrum that are so important for the positive identification of a compound.

1.2 CRYSTAL FIELD ASPECTS OF INFRARED SPECTRA

CRYSTAL FIELD THEORY (CFT) has been developed as a result of the theoretical treatment of bonding in transition metal complexes. The crystal field may be considered to be the result of an electrostatic interaction between the metal ion and ligands in a transition metal complex. LIGAND FIELD THEORY (LFT) is a modified version of CFT and takes into account orbital overlap. The essence of CFT [2] is that the five *d*-orbitals, which are degenerate in energy in the gaseous metal ion become differentiated in the presence of the electrostatic field because of the ligands (see Fig. 1.2). A consequence of this is that transition metal

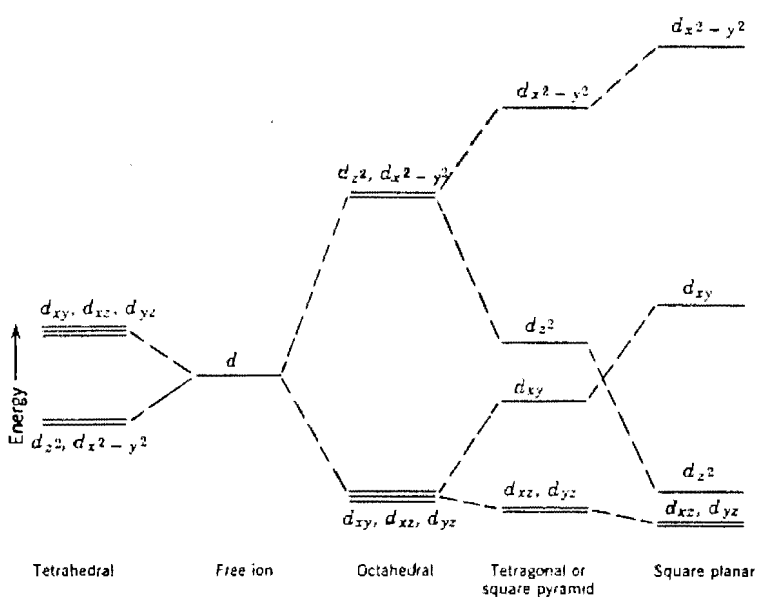

Fig. 1.2 Crystal field splittings of the *d*-orbitals of a central ion in regular complexes of various structures [3].

complexes have different stabilities according to the electron distribution amongst the orbitals. Another approach is MOLECULAR ORBITAL THEORY (MOT) in which the orbitals of the transition metal complex are considered to arise from a linear combination of the appropriate atomic orbitals of the metal ion and the ligands. It gives similar results to LFT. The advantage is that it more readily accounts for π-bonding.

From first principles, crystal field splitting of the orbitals of any element with partially filled p, d or f-orbitals may be considered possible. However, since the p-orbitals are directed equivalently along the x, y and z axes as normally defined, they are not split by the crystal field. The d- and especially the f-orbitals of an element in a complex bear a close enough similarity to the orbitals in the free ion to enable CFT to be applicable. The splitting of d-orbitals is large and the associated stabilization can be as high as 420 kJ/mol. For the f-orbitals, however, the splitting is much smaller and the associated stability is about ten or twenty times smaller than for the d-orbitals. It is thus not surprising that the most studied systems are those consisting of compounds containing $3d$-transition metals. The d-orbitals will therefore be treated in more detail to provide more insight into CFT.

In an octahedral environment, the crystal field splits the five d-orbitals into two sets of orbitals, with an energy difference of $10Dq$. Those orbitals lying in the direction of the ligands are raised in energy with respect to those lying away from the ligands. In this way, three of the orbitals, denoted t_{2g}, are

stabilized by an amount of $4Dq$ and the remaining two e_g orbitals are destabilized by an amount of $6Dq$. By preferentially filling the low-lying levels, the d-electrons can stabilize the system, as compared to the case of the random filling of the d-orbitals. The exceptions are in the cases of d^0, d^{10} and high-spin d^5 in which there is no net stabilization since the effect of the electrons in the t_{2g} orbitals is counterbalanced by the destabilization resulting from the occupancy of the e_g orbitals. The gain in bonding energy achieved by filling the d-orbitals is called the crystal field stabilization energy (CFSE). The CFSE of any transition metal ion in an octahedral environment is given by [2]:

$$10Dq = f \cdot g$$

where f is a measure of the crystal field splitting power of a ligand combination relative to that of $6H_2O$ ($f = 1$) and g is the spectroscopically determined magnitude of $10Dq$ for the octahedrally hydrated metal ion. The CFSEs of metal ions in tetrahedral and square planar environment can be calculated in a similar manner.

The CFSE has been shown to affect the way in which bond distances, lattice energies, heats of ligation and other thermodynamic properties vary throughout an isostructural series of isovalent metal compounds of constant ligand composition. The CFSE actually only contributes a small amount to the total bonding energy such as the electrostatic attraction between a metal ion and ligands as well as the interelectronic repulsions (other than d-orbital electrons). Thus the relatively small crystal

field splitting effect can only be detected when other factors which influence the thermodynamic properties are constant or vary smoothly through the series of complexes being studied.

The frequencies of the vibrational spectra of a series of transition metal complexes are dependent on some mode of vibration of the molecule. These vibrations are determined by the strengths of the vibrating bonds and thus any change in bond strength will influence the force constant and hence the frequency of the related vibrations should be affected (assuming negligible mass effect). The metal-ligand bond strengths depend on the CFSE of a particular complex, variations in CFSE being associated with corresponding variations in bond strength. Thus the metal-sensitive frequencies of a set of metal complexes – that is those which involve some vibration involving metal-ligand bonds - should show some correlation with the CFSE. As the CFSE affects the metal-ligand bond strength, it is plausible that the metal-sensitive frequencies of a series of complexes would show a variation with *d*-orbital population similar to that shown by the thermodynamic properties.

This was shown to be the case by Sacconi and Sabatini [5,6] for metal(II) hydrazine complexes and by Thornton and co-workers [7-16]. νM-O of many β-ketoenolates of trivalent transition metal ions show a correlation with *d*-orbital population which is consistent with the relative values of the CFSE's of metal(III) ions [7]. Similar results have been obtained for the variation of νM-L of metal(II) 2,2'-bipyridyl and 1,10-phenanthroline complexes of the divalent metals [8], divalent metal acetylacetonates and their nitrogen base adducts [9] , di- and trivalent

metal tropolonates [10], the potassium salts of the divalent *tris*(acetylacetonates) [8], the di- and trivalent γ-substituted acetylacetonates [11], metal(III) oxalate and cyanide complexes [13], the metal(II) anthranilates [14], the lanthanide(III) tropolonates [15] and the lithium salts of the lanthanide(III) *tetrakis*(tropolonates) [16]. These latter complexes involve crystal field splitting of the degenerate 4*f*-orbitals. The crystal field splitting effects are small in comparison to the effects observed for the *d*-orbitals.

The heterolytic bonding energy ($-\Delta H$) of complex formation, in the gas phase, from the free ion corresponds to the equation

$$M^{n+}_{(g)} + nL^{-}_{(g)} \rightarrow ML_{n(s)} \quad - \Delta H$$

for an ion M of valency n with a bidentate monobasic ligand L. The heterolytic bonding energy may be divided into a CFSE contribution ($-\delta H$) and an ionic contraction contribution (E_r). This can be expressed as

$$- \Delta H = - \delta H - E_r$$

It is therefore necessary to know the value of $-E_r$ for a particular complex in order to calculate a value for the crystal field contribution from the measured energy ($-\Delta H$). This is provided by the complexes of metal ions with zero CFSE (namely d^0, d^5 (high-spin) and d^{10} configurations for the transition metal ions and the f^0, f^7 and f^{14} configurations for the lanthanides and actinides). In these instances,

$$-\Delta H = -E_r$$

If $-E_r$ increases linearly, then in a plot of $-\Delta H$ against atomic number, interpolation between these points (d^0, d^5 (high-spin) and d^{10}) enables values of $-E_r$ to be estimated for all metal ion configurations. Using these estimates of $-E_r$, values of the CFSE contribution ($-\delta H$) can be obtained. An alternative method of obtaining the CFSE is based upon the method of George and McClure [17]. The contribution of the CFSE to νM-L is taken as the difference between the observed frequency, ν, and the frequency, ν_o, on the interpolation line through the points for the d^0, d^5 (high-spin) and d^{10} or f^0, f^7, and f^{14} configurations.

The value of $\nu - \nu_o$ is considered to be the crystal field contribution to the total frequency and has been shown to yield a good correlation with calculated values of the CFSE [7 - 16].

The complexes of the three ions with zero CFSE generally show an increase in νM-L (*i.e.* ν_o) in the order $d^0 < d^5$ (high-spin) $< d^{10}$ and $f^0 < f^7 < f^{14}$. This is the order expected from the contraction of ionic radii throughout the series, but the opposite expected from their relative atomic masses. Therefore, the effect of ionic radii must outweigh the effect of ionic masses in determining the frequency order. Independent evidence for the small effect has been cited by Hulett and Thornton [18].

It has therefore been established that metal-sensitive vibrations for a series of transition metal complexes, all follow the predicted crystal field order. It should therefore be possible to use this trend to assign metal-sensitive frequencies in a new series of compounds where the metal-sensitive bands have not previously been assigned.

1.3 METHODS USED FOR THE ASSIGNMENT OF BANDS IN THE VIBRATIONAL SPECTRA OF METAL COMPLEXES

The precise assignment of bands in the infrared spectra of metal complexes to vibrations between specific atoms is of great interest as it can give direct information regarding many structural and bonding features. However, such a task applied to the systems as many-bodied as those studied in this work is definitely not easy since the interpretation of the spectra is complicated by intermolecular vibrations, lowering of symmetry and extensive vibrational coupling.

Amongst the vibrations of coordination compounds, the metal-ligand vibrations are the most important since they provide direct information about the structure of the complex and the nature of the metal-ligand bonds. These vibrations generally appear below 600 cm^{-1} as a result of the high mass of the metal atom and the relatively weak nature of the M-L bond. Various methods can be used to assign (a) internal ligand vibrations and (b) metal-ligand vibrations.

1.3.1 *Internal ligand vibrations*

1.3.1.1 The most theoretical approach to the assignment of the bands in a spectrum is *via* a normal coordinate treatment of the molecule. This requires initial experimental observation of the vibrational frequencies and their assignments. A normal coordinate analysis can then be used to predict theoretical vibrational frequencies and assignments. In this way, it is possible to check the initial experimental vibrational frequencies and assignments [19].

1.3.1.2 The characteristic light absorption of molecules in the infrared region depends partially on the masses of their constituent atoms. The substitution of an atom by its isotope will therefore result in a change of the frequency of the vibrations involving the particular isotopic species. The spectral results obtained in this manner can be interpreted with a high degree of confidence in the analysis of the spectra.

The expected isotopic shifts can be calculated, to a first approximation, by assuming the labelled atom to be part of a simple harmonic oscillator. If ν is expressed in wavenumbers, the vibrational frequency of a diatomic molecule can be represented by the equation

$$\nu = 1/2\pi c\,(f/\mu)^{\frac{1}{2}}$$

while the vibrational frequency of the corresponding isotopically labelled system can be given by

$$\nu^{i} = 1/2\pi c\,(f/\mu^{i})^{\frac{1}{2}}$$

where ν = vibrational frequency (as a wavenumber)

f = harmonic force constant

c = velocity of light

μ = reduced mass of the molecule.

The superscript i refers to the labelled system. If one then assumes that the force constants of the bonds are unchanged by isotopic replacement (which to a first approximation, is the case) then the expected isotopic shifts may be

calculated from

$$\nu^{i}/\nu = (\mu/\mu^{i})^{\frac{1}{2}}$$

Obviously, the larger the relative mass difference, the greater the isotopic shifts of the respective bands. The biggest isotopic shifts are observed for the deuterated and tritiated molecules where the m^{i}/m ratios are the largest (m^{i} = mass of the heavier isotope and m = mass of the unlabelled atom(s)). Shifts of up to 1 000 cm^{-1} (1 300 cm^{-1} for tritiation) have been observed. With other labelled atoms where the m^{i}/m ratios are smaller (*e.g.* $^{15}N/^{14}N$) shifts are considerably less, but may yet be as large as 40 cm^{-1}, for example, in an $^{18}O/^{16}O$-labelled system [20]. The smaller shifts are quite easily resolved with present-day commercial instruments (for sharp bands shifts of 1 - 2 cm^{-1} are meaningful).

1.3.2 *Metal-ligand vibrations*

While both of the methods used for the assignments of the internal ligand vibrations discussed above, may also be used, the following techniques (although somewhat empirical) are of some value.

1.3.2.1 Since M-L vibrations are absent in the free ligands, a comparison of the spectra of the free ligand and its metal complexes may provide assignments of the M-L modes. This method has the distinct disadvantage that some ligand vibrations activated by complex formation may appear in the same region as the M-L vibrations [21].

1.3.2.2 The M-L vibrations are expected to appear in the same region for complexes of identical metals and similar ligands. This method has been used to assign νCu-N in the compounds CuX_2L_2 (X = Cl, Br; L = substituted pyridine), νNi-O in substituted pyridine adducts of Ni(II) acetylacetonates, νM-O in metal-β-ketoenolates and νPt-N in the complexes *trans*-$[PtBr_2(Y)(L)]$ (where Y = ethylene or CO, and L = a substituted aniline) [22-25].

1.3.2.3 The metal-ligand vibrations in a series of isostructural isovalent transition metal complexes of constant ligand composition are metal-sensitive and shift according to the properties of the metals. Hence the infrared bands which parallel the order of the CFSEs of the metal can be assigned to metal-ligand modes [10,12].

1.3.2.4 The aforementioned technique of isotopic labelling (see Section 1.3.1.2) was applied specifically to the use of isotopically labelled ligands. However, this method can equally be applied to isotopically labelled metal ions [20]. Two distinct approaches may be used, independently or in combination: the metal ion and/or the ligand donor atom may be replaced by an isotopically labelled species.

This method is specifically suited to labelling the metal-ligand vibrations. Its major disadvantage is not only that the shifts (which are generally quite small due to the relatively small m^i/m ratios) may fall within the range of experimental error, but also that the methods fail to

distinguish between different types of metal-ligand vibrations which arise in complexes with different donor atoms *e.g.* between νM-N and νM-Cl in $[M(py)_2Cl_2]$ complexes. Moreover, suitable stable metal isotopes are often of limited availability and extremely expensive.

The advantage of labelling the ligand donor atom as opposed to the metal atom are firstly, that the isotopically induced shifts are generally larger owing to a more favourable m^i/m ratio and, secondly, that the available ligands can often be obtained in larger quantities than the metal isotopes (available, usually, as their oxides) with a consequent reduction in the difficulties of complex preparation and spectral measurement. A drawback of labelling the ligand donor atom is that some bands originating in ligand vibrations may be incorrectly assigned to νM-L. This difficulty can be particularly problematical if the isotopically-induced shifts are large and the shifted band is 'buried' in a mass of internal ligand bands.

It should be noted that the observed frequency shifts which result from labelling are subject to factors such as the extent to which the labelled atoms participate in the particular vibration, the number and nature of the atoms in the molecule that have been labelled and the extent of hydrogen bonding. The observed shift will be greatest if the molecule is simple with no vibrational coupling occurring, that is, with each band being as vibrationally pure as possible.

It has been shown that the isotopic labelling method of assigning the bands in infrared spectra is by far the most unambiguous and simple technique [26]. The isotopic labelling carried out in this research involved both the labelling of the ligand as well as the metal atom (in suitable cases).

1.3.2.5 Clearly, a combination of theoretical and practical data is necessary for an exhaustive solution of the assignment problem. Even a relatively simple group theoretical study of a specific complex is useful in the interpretation of isotopic shift data.

The concept of symmetry is important to almost every area of life in our universe. Many difficult problems can be simplified if the molecule has some symmetry properties. For instance, when molecules and ions crystallize, they usually yield structures with well-defined symmetry. The quantitative discussion of symmetry is called group theory [27-31]. The application of group theory to molecules gives useful information regarding the properties of the molecules. In order to classify molecules according to their symmetry, it is necessary to list all of their symmetry elements. Thus the name of the point group to which a molecule belongs, is determined by the symmetry of the elements that characterize it.

Group theory considers a molecule to be an isolated unit. However, a molecule in the solid state cannot be regarded as an isolated unit because it is subject to the symmetry restrictions of its solid environment. These additional

effects can split degenerate vibrations, change the activities of various modes and generate lattice modes which arise from translatory and rotatory motions of the molecules within the crystal. Hence, to perform a rigorous vibrational analysis, the entire array of molecules needs to be taken into account which is a daunting task. Fortunately, site group and factor group analysis make certain assumptions that give a valid approximation.

In the site group analysis, the surroundings of the molecule are considered to be static, but its symmetry is imposed on the molecule. Site symmetry, which is usually lower than molecular symmetry, can be obtained if the space, the number of molecules per unit cell and the point group of the isolated molecules are known. Factor group analysis is the more rigorous of the two approximations since it accounts for lattice modes and solid state splitting of the nondegenerate vibrations of the free molecule. Halford [32], and Adams and Newton [33] have published useful data for the use of these two analyses.

Despite the more rigorous approach of factor group analysis, simple group theoretical considerations may provide useful information regarding the expected number and type of infrared bands (*e.g.* whether a fundamental, that is stretches and bends, is infrared or Raman active) in the molecule. This information is extremely helpful for the assignment of bands in the infrared spectra.

1.4 THE RATIO ν^D/ν^H USED IN THE ASSIGNMENT OF THE C-H/D AND RING VIBRATIONS IN METAL COMPLEXES

It has been well established that most of the bands which originate in the internal vibrations of heterocyclic bases also occur on an almost band-for-band basis in the spectra of their metal complexes [34]. Moreover, it has recently been shown that the ν^D/ν^H ratios of heterocyclic bases and their corresponding metal complexes can be used as a method for assignments in infrared spectra. The ratio (ν^D/ν^H) between the frequencies of the corresponding bands in the infrared spectra of deuterated and unlabelled molecules serves as a useful tool to distinguish between the C - H stretching (or bending) modes and the ring stretching (or bending) modes in aromatic and heterocyclic compounds [20].

Thornton and colleagues [35,36] have examined the ν^D/ν^H ratio for several complexes of heterocyclic bases. The results of their study may be summarized as follows:

(a) the ratio ν^D/ν^H varies from 0.68 to 0.85 for C - H modes
(b) the ratio ν^D/ν^H lies within the range 0.85 to 1.00 for the ring modes.

Distinction between the above modes and metal-ligand modes, or vibrations arising from the modes of other functional groups or other coordinated ligands is also possible since the latter generally yield ν^D/ν^H ratios close to unity. Where apparently anomalous ratios are observed, the possibility of incorrect assignments or vibrational coupling must be considered.

1.5 NMR OF PARAMAGNETIC COMPLEXES

1.5.1 *General characteristics*

Nuclear Magnetic Resonance (NMR) spectra can, with few exceptions, be recorded for paramagnetic complexes in solution [37,38]. These spectra provide information regarding the structure of the complexes, the distribution of the unpaired electrons and also the reactive centres in the molecule. Inter- and intra-molecular exchange phenomena, *e.g.*, ligand exchange rate constants and rotation barriers, can be determined in this way. NMR studies of paramagnetic complexes are therefore a rich source of molecular information.

Paramagnetic spectra differ from diamagnetic spectra in three principal ways [39]. Firstly, the chemical shift scale is several orders of magnitude greater than for the analogous diamagnetic compounds. Proton chemical shifts of 200 ppm (from TMS) and even larger at room temperature are common. It is the observation of these large isotropic shifts from the corresponding diamagnetic resonance positions which is the most interesting feature of paramagnetic NMR spectra. Secondly, spin-spin coupling is rarely observed in these spectra. The half-widths of the NMR signals are between one and several thousand Hz for dissolved paramagnetic species. Finally, the isotropic shifts can be linearly related to $1/T$, reflecting a Curie or near Curie behaviour.

1.5.2 *Origin of the isotropic shift*

There are several ways in which the nuclei in metal complexes

can be influenced by unpaired electrons. These effects can be roughly divided into two interactions:

(a) shifts arising from a Fermi contact interaction and,

(b) shifts arising from a pseudo-contact (dipolar) interaction between the electronic and nuclear magnetic moments.

The effect of these nuclear electron interactions is great because of the large magnetic moment of the unpaired electrons.

The Fermi contact interaction may be defined as the interaction of the nuclear magnetic moment with the unpaired electron density on that nucleus, causing spin density to reach the resonating nucleus, or the ligands of the paramagnetic metal, in the following ways (Fig. 1.3):

(a) Electron density may be donated from the *d*-orbitals of the metal to vacant antibonding orbitals of the ligands which have σ- or π-character. This mechanism has been found to contribute to the isotropic shift for the pyridine, pyridine *N*-oxide and picoline adduct complexes of many 3*d*-metals [40-42].

(b) Electron density in the highest occupied orbitals of the ligand or ligands is transferred into unoccupied or unfilled *d*-orbitals of the metals. This mechanism is, in particular, possible for the more highly charged 3*d*-metal ions. A positive spin density also remains in the ligand *d*-orbitals, so it is often difficult to differentiate between mechanisms (a) and (b).

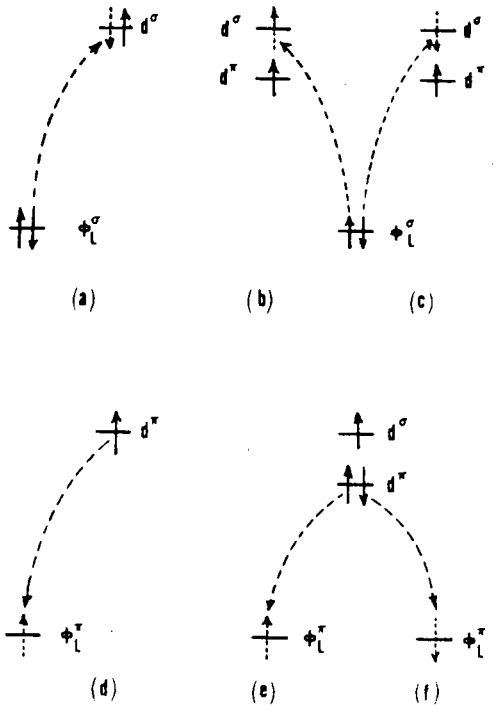

Fig. 1.3 Spin transfer mechanisms (a) L→M σ-spin transfer into a singly occupied *d*-orbital (b) parallel and (c) antiparallel L→M σ-spin transfer from a doubly occupied ligand orbital into a vacant *d*-orbital (d) M→L π-spin transfer from a singly occupied *d*-orbital into a vacant ligand orbital (e) parallel and (f) antiparallel M→L π-spin transfer from a doubly occupied *d*-orbital into a vacant ligand orbital [39].

The study of the NMR spectra of paramagnetic compounds can often be complicated by intra-molecular (and also inter-molecular in solid studies) dipole-dipole interactions which affect the magnitude and sign of the isotropic shifts in an extremely complicated way. The pseudo-contact (dipolar) contribution to the overall isotropic shifts can only be

determined in relatively simple cases. It is noteworthy that, in complexes where there is extensive electron delocalization, the pseudo-contact contribution to the total shift should be small. This is because the pseudo-contact model is based on the assumption that a point charge is localized on the metal ion [43]. The observed isotropic NMR shift of a paramagnetic compound is the sum of the shifts caused by the contact and dipolar interactions, $\Delta\nu^{con}$ and $\Delta\nu^{dip}$ respectively, and can be represented by

$$(\Delta\nu^{iso}/\nu) = (\Delta\nu^{con}/\nu) + (\Delta\nu^{dip}/\nu)$$

where ν is the frequency of the corresponding diamagnetic resonance [39]. Depending on the paramagnetic system under study, the relative contributions of contact and dipolar shifts will vary. In magnetically isotropic systems, such as <u>purely</u> octahedral Ni(II) complexes, the dipolar shift is zero. The isotropic shift is then purely contact in origin [44] and is related to the hyperfine coupling constant A_N by

$$(\Delta\nu^{iso}/\nu) = -[A_N g_{av.}{}^2 \beta^2 S(S+1)]/[g_N \beta_N 3kT]$$

where $g_N = 5.58$

$\beta_N = 5.05 \times 10^{-17} JG^{-1}$

$g_{av.} = \mu_{eff.}/\sqrt{S(S+1)}$

$\beta = 9.27 \times 10^{-21} JG^{-1}$

S = sum of electron spins

A_N = nuclear spin-electron coupling constant

k = Boltzmann constant

T = temperature.

Experimentally, the magnitude of A_N can be determined from the hyperfine splitting of the electron spin resonance (ESR) spectra of radicals. Dipolar shifts are present in magnetically anisotropic systems such as Co(II) octahedral complexes. The dipolar contribution to the isotropic shift will then be given by

$$(\Delta\nu^{dip}/\nu) = -D(\chi_{||}-\chi_{\perp})/[(3\cos^2\theta-1)/r^3]$$

where D = positive quantity (dependent on temperature and on various relaxation times)

$\chi_{||}, \chi_{\perp}$ = parallel and perpendicular components, respectively, of the magnetic susceptibilities

r = distance from the magnetic ligand nucleus (N) to the paramagnetic metal

θ = angle between the line joining the nucleus, metal and the principal molecular magnetic axis.

The last equation is valid for axially symmetric systems but, in general, axial symmetry is assumed with or without good reason.

In the analysis of paramagnetic spectra the contact resonance shifts are of interest since these can be interpreted in terms of a spin transfer mechanism (σ or π), by which the unpaired electrons are delocalized from the paramagnetic metal into the ligand system. The contact shift

can be mathematically related [39] to the spin density through the hyperfine coupling constant which is directly proportional to the spin density at the nucleus (N) by

$$A_N = (k|\phi_{sN}(r_N)|^2 \rho_{sN}$$

where $k = (4\pi/3) g\beta\gamma_N \hbar <S_z>^{-1}$

$<S_z>$ = average spin

ρ_{sN} = spin density in the valence s orbital on nucleus (N)

$|\phi_{sN}(r_N)|^2$ = density at the nucleus.

The factor $k|\phi_{sN}(r_N)|^2$ is a constant for each type of magnetic nucleus and has the value 539.86 Gauss for the hydrogen atom. Spin density in the valence orbitals of ligand atoms can be calculated using approximate molecular orbital theory. Information about the spin delocalization mechanism can be obtained by correlating the calculated spin densities with the experimental isotropic shifts. In the case of magnetically anisotropic systems, the contact and dipolar contributions to the isotropic shift must be separated before correlation is possible.

1.5.3 *Methods of assignment*

The process of assigning particular resonances of a paramagnetic spectrum to specific sets of equivalent nuclei is more complicated than for the diamagnetic spectrum. For diamagnetic spectra, there is generally good correlation between chemical shift and electron density. However, this is not the case for paramagnetic spectra. For this reason,

a popular method for making assignments is by chemical substitution. Substitution of a hydrogen by a methyl group is common because the observed shift in the methyl resonance gives very useful information for spectral interpretation. Substitution by deuterium, halogen atoms or even phenyl groups, is also useful. It should be mentioned that whilst the perturbation in the NMR of a diamagnetic substance introduced by replacing a proton by a halogen atom is large, the effect on the remainder of the spectrum of a paramagnetic substance is generally negligible.

Isotropic shifts often obey a Curie (or near Curie) behaviour. This can assist in making assignments. If the diamagnetic reference chemical shifts corresponding to two possible assignments differ significantly, a plot of isotropic shift against $1/T$ will have a zero intercept when $1/T$ is zero for the correct assignment, but not for the incorrect one. Such a procedure has been used in determining the diamagnetic positions for some difficult-to-assign biological molecules [45].

REFERENCES

1. A. Streitwieser and C.H. Heathcock, *Introduction to Organic Chemistry* [Collier-Macmillan] London (1976) ch. 10.

2. B.N. Figgis, *Introduction to Ligand Fields* [Wiley-Interscience] New York 1966.

3. F. Basolo and R.G. Pearson, *Mechanisms of Inorganic Reactions* [Wiley] New York, 2nd ed. (1967) p 376.

4. C.K. Jørgensen, *Absorption Spectra and Chemical Bonding in Complexes* [Pergamon] London (1962) p 110.

5. L. Sacconi and A. Sabatini, *Nature*, 186 (1960) 549.

6. L. Sacconi and A. Sabatini, *J. Inorg. Nucl. Chem.*, 25 (1963) 1389.

7. R.D. Hancock and D.A. Thornton, *J. Mol. Structure*, 4 (1969) 361.

8. G.C. Percy and D.A. Thornton, *J. Mol. Structure*, 10 (1971) 39.

9. R.D. Hancock and D.A. Thornton, *J. S. Afr. Chem. Inst.*, 23 (1970) 71.

10. L.G. Hulett and D.A. Thornton, *Spectrochim. Acta*, 27A (1971) 2089.

11. C.A. Fleming and D.A. Thornton, *J. Mol. Structure*, 17 (1973) 79.

12. G.S. Shephard and D.A. Thornton, *Helv. Chim. Acta*, 54 (1971) 2212.

13. R.D. Hancock and D.A. Thornton, *J. Mol. Structure*, 6 (1970) 441.

14. G.S. Shephard and D.A. Thornton, *J. Mol. Structure*, 16 (1973) 321.

15. L.G. Hulett and D.A. Thornton, *J. Mol. Structure*, 13 (1972) 115.

16. L.G. Hulett and D.A. Thornton, *Chimia*, 26 (1972) 72.

17. P. George and D.S. McClure, *Prog. Inorg. Chem.*, 1 (1959) 381.

18. L.G. Hulett and D.A. Thornton, *J. Inorg. Nucl. Chem.*, 35 (1973) 2661.

19. G.T. Behnke and K. Nakamoto, *Inorg. Chem.*, 6 (1967) 433.

20. S. Pinchas and I. Laulicht, *Infrared Spectra of Labelled Compounds* [Academic Press] London (1971) ch. 7.

21. K. Nakamoto, *Infrared Spectra of Inorganic and Coordination Compounds* [Wiley] New York (1963) part (III).

22. M. Goldstein, E.F. Mooney, A. Anderson and H.A. Gebbie, *Spectrochim. Acta*, 21 (1965) 105.

23. J.M. Haigh, N.P. Slabbert and D.A. Thornton, *J. Inorg. Nucl. Chem.*, 32 (1970) 3635.

24. R.D. Hancock and D.A. Thornton, *J. Mol. Structure*, 4 (1969) 377.

25. G.A. Foulds, P.S. Hall and D.A. Thornton, *J. Mol. Structure*, 117 (1984) 95.

26. G.C. Percy and H.S. Stenton, *J. Chem. Soc. Dalton*, (1976) 1466, 2429.

27. F.A. Cotton, *Chemical Applications of Group Theory* [Wiley Interscience] New York, 2nd ed. (1971).

28. E.B. Wilson, J.C. Decius and P.C. Cross, *Molecular Vibrations* [McGraw-Hill] New York (1955).

29. J.R. Ferraro and J.S. Ziomek, *Introductory Group Theory and its Applications to Molecular Structure* [Plenum] New York (1969).

30. D.C. Harris and M.D. Bertolucci, *Symmetry and Spectroscopy* [Oxford University Press] New York (1978).

31. A. Vincent, *Molecular Symmetry and Group Theory* [Wiley] New York (1977).

32. R.S. Halford, *J. Chem. Phys.*, 14 (1946) 8.

33. D.M. Adams and D.C. Newton, *Tables for Factor Group and Point Group Analysis* [Beckman-RIIC Ltd.] Croydon (1970).

34. L.P. Bicelli, *Ann. Chim.*, 48 (1958) 749.

35. A.T. Hutton and D.A. Thornton, *Spectrochim. Acta*, 34A (1978) 645.

36. G.A. Foulds, J.B. Hodgson, A.T. Hutton, M.L. Niven, G.C. Percy, P.E. Rutherford and D.A. Thornton, *Spectroscopy Letters*, 12 (1979) 25.

37. H.J. Keller and K.E. Schwarzhans, *Angew. Chem.*, intern. Ed., 9 (1970) 196.

38. K.E. Schwarzhans, *Angew. Chem.*, intern. Ed., 9 (1970) 946.

39. G.N. La Mar, W. DeW. Horrocks and R.H. Holm (eds.), *NMR of Paramagnetic Molecules* [Academic Press] London (1973).

40. J.A. Happe and R.L. Ward, *J. Chem. Phys.*, 39 (1963) 1211.

41. R.H. Holm, G.C. Everett and W. DeW. Horrocks, *J. Amer. Chem. Soc.*, 88 (1966) 1071.

42. G.N. La Mar and G. van Hecke, *J. Amer. Chem. Soc.*, 91 (1969) 3442.

43. N. Bloembergen and W.C. Dickinson, *Phys. Rev.*, 79 (1950) 179.

44. R.J. Fitzgerald and R.S. Drago, *J. Amer. Chem. Soc.*, 90 (1968) 2523.

45. K.J. Würthrich, R.G. Schulman, B.J. Wyluda and W.S. Caughey, *Proc. Nat. Acad. Sci.*, 62 (1969) 636.

Chapter Two

CHAPTER TWO

2. PHYSICAL METHODS

2.1 INFRARED SPECTRA

The mid-IR spectra were determined as Nujol mulls (4 000 - 180 cm^{-1}) and as hexachlorobutadiene (HCBD) mulls (3 500 - 3 000; 1 500 - 1 300 cm^{-1}) between caesium iodide plates on a Perkin-Elmer 983 spectrophotometer. The far-IR spectra were obtained as Nujol mulls between polyethylene plates on a Digilab FTS - 16B/D interferometer (500 - 50 cm^{-1}). The quoted wavenumber precision of the Perkin-Elmer spectrophotometer is better than 1 cm^{-1} and the reproducibility better than 0.3 cm^{-1}. The Digilab interferometer has similar specifications, its added advantage is that it extends to a much lower wavenumber limit than the Perkin-Elmer system and that it has the capability of storing the recorded spectra.

2.2 ^{1}H-NUCLEAR MAGNETIC RESONANCE SPECTRA

The ^{1}H-NMR spectra were obtained on a VXR-200 MHz Fourier Transform spectrometer in the range -20 ppm to 160 ppm, with respect to deuterated dimethylsulphoxide (dmso), which was also used as the solvent. The spectra were recorded in the temperature range 297.5 to 393.1 K.

2.3 MASS SPECTRA

Mass spectra were measured on a VG Micromass 16F instrument operating in the electron impact mode, with an electron beam energy 70 eV and ion accelerating voltage 3 kV, and with ion

source temperature in the region 175 - 185°C.

2.4 MICROANALYSIS

Microanalyses were performed on a Heraeus Universal Combustion Analyzer, Model CHN-Micro, by Mr WRT Hemsted of the Department of Organic Chemistry. The calculated values are based on the assumption that the effect of mass change (due to labelling) on the heat conductivity of nitrogen or water vapour is negligible.

2.5 COMPUTATION

All computations were performed at the Computer Centre of the University of Cape Town on a Univac 1100/81 computer.

CHAPTER THREE

3. ISOTOPIC LABELLING APPLIED TO THE INFRARED SPECTRA OF THE METAL 8-QUINOLINOL COMPLEXES

3.1 INTRODUCTION

8-Quinolinol, also known as 8-hydroxyquinoline or oxine, was first introduced as an analytical reagent in 1926. Its parent molecule is quinoline, a member of the condensed ring *N*-heterocyclic compounds. Oxine differs from other hydroxy-substituted quinolines in that the steric relationship of the hydroxyl group in the eight position relative to the ring nitrogen enables many metal ions to form chelates with oxine. Metals such as copper, zinc, cadmium, aluminium, bismuth, uranium, manganese, iron and nickel, amongst others, form insoluble chelates [1]. 8-Hydroxyquinoline therefore has many analytical applications as summarized by Hollingshead [2]. The position of the hydroxyl group in the eight position may also explain the antifungicidal and antibacterial activity of oxine and its substituted derivatives [3]. Metal oxinates have been the subject of various spectrochemical investigations including infrared [3-12], X-ray crystallography [13-20], ultraviolet [21], nuclear magnetic resonance [22,23] and mass spectrometry studies [24,25].

The infrared and Raman spectra of the quinoline molecule have been studied by various workers [26-29], but vibrational studies of substituted quinolines are far less common [30,31]. In the present study, we have investigated the infrared spectra of oxine and its transition metal chelates. One of the earliest reports of the ligand oxine was by Sharma and colleagues in

1980 [32]. The spectrum was analyzed by assuming C_s symmetry for the molecule and the fundamental infrared frequencies and probable modes of vibration were discussed. Srivastava and coworkers [33] have recently published more detailed assignments for oxine. A correlation of the fundamental vibrational frequencies of oxine with naphthalene and quinoline was also presented. The most recent and complete vibrational study on oxine is by Marchon *et al.* who presented both IR and Raman data in the region 4 000 - 160 cm^{-1} for both oxine and oxine-OD [34].

The first infrared spectral study of the metal chelates of oxine was by Stone in 1954 [3]. He reported the IR spectra of the bismuth and magnesium oxinates in an attempt to correlate the large solubility difference with the structures as determined from the spectra. Charles and coworkers [4] studied the IR spectra of 8-hydroxyquinoline, 2- and 4-methyl-8-hydroxyquinoline and several metal chelates derived from these reagents. In general, the spectra of the chelates from a specific ligand were found to be quite similar. A characteristic band at about 1 100 cm^{-1} was found to be sensitive to metal ion substitution; this band was therefore assigned to the C-O vibration. Phillips and Deye [5] examined the IR spectra of chelates or salts of oxine with a variety of metals in the range 760 - 220 cm^{-1}. In agreement with Charles *et al.*, the spectra were found to be characterized by close resemblance of band positions, with a few exceptions due to hydration and the presence of oxygen-containing cations. Magee and Gordon reported the IR spectra of oxine and a variety of metal chelates between 5 000 - 250 cm^{-1} [6-8]. The bands at 1 548, 1 515 and

1 508 cm^{-1} were assigned to νC=C and νC=N vibrations. The peaks around 780 cm^{-1} as well as those in the region 1 200 - 1 000 cm^{-1} were attributed to ring vibrations and C-H deformation modes. A significant peak in the range 870 - 850 cm^{-1} in the spectra of the metal oxinates was found to vary quite significantly with the metal and was therefore assigned to the νM-O vibration. No mention was made of νM-N.

The absorption frequencies of oxine and about sixteen metal oxinates in the range 900 - 400 cm^{-1} were reported by Tackett and Sawyer [9]. This included the spectra of α- and β-$Cu(ox)_2$. The α-form was found to have the same absorption bands as the other divalent metal chelates, whereas the β-form showed some unique peaks in the region 850 - 620 cm^{-1}. Below this range, however, the spectra of both forms were almost identical. The difference was explained by the assumption that the α-form contained oxine in a *cis*-planar configuration which could be converted to the *trans*-planar β-form by heating. Tentative assignments for some of the bands in this region were made by comparing the spectrum of oxine with various substituted pyridines, naphthalenes, benzenes and phenols, the vibrations of which have been assigned by normal coordinate analysis.

One of the first assignments of M-L vibrations was given by Larsson and Eskilsson who assigned the bands near 300 and 400 cm^{-1} in the Fe(III) and Co(III) oxinate spectra, respectively, as the M-L vibrations [10]. The assignments were made by comparison with the ligand spectrum; the νM-L bands were expected in the low frequency region due to the rigidity and

mass of the oxinate anion. A comparison of the oxinate complexes with ammine and pyridine *N*-oxide complexes led Kulkarni and Mudhedkar to report the M-L stretching vibrations in the narrow region 640 - 500 cm^{-1} [11]. The first and only use of isotopic labelling was published by Ohkaku and Nakamoto [12]. Metal isotopic labelling ($^{63,65}Cu$; $^{58,62}Ni$ and $^{64,68}Zn$) was used to assign the M-O and M-N stretching vibrations. These are quoted at about 300 and 200 cm^{-1}, respectively. Both νM-O and νM-N were found to vary according to the Irving-Williams stability sequence [35].

X-ray diffraction studies have been carried out on a series of complexes of the type $[M(ox)_2(H_2O)_2]$ (M = Ni, Cu, Zn, Cd or Pb) [13 - 15]. The results of these investigations have shown that the two chelating oxinate anions coordinate to the metal by forming a *trans*-planar structure[a]; the two water molecules occupy the axial positions to achieve octahedral stereochemistry about the metal atom. The bond length of 2.3 Å reported for $M-OH_2$ is longer than is usually found for a M-O bond. This is consistent with the fact that most of the above complexes are easily dehydrated to the anhydrous complex $[M(ox)_2]_n$ suggesting a fairly weak M-O bond.

---

[a]In this chapter, a *trans* complex refers to the structure in which the donor atoms of the ligand are in a *trans* configuration (and *vice versa* for the *cis* complex), *i.e.*, *trans*-$[M(ox)_2(H_2O)_2]$ ≡ *trans*(H_2O), *trans*(N), *trans*(O)-$[M(ox)_2(H_2O)_2]$ and *cis*-$[M(ox)_2(H_2O)_2]$ ≡ *trans*(H_2O), *cis*(N), *cis*(O)-$[M(ox)_2(H_2O)_2]$.

Fanning and Jonassen prepared two forms of anhydrous copper oxinate which were found to have unusual spectral properties [36]. The crystal structure of the α-form was determined by Hoy and Morriss [16] and that of the β-form by Palenik [17]. The copper atom in the α-form is six-coordinate. It is weakly bound in the axial positions by oxygen atoms from neighbouring molecules, the Cu-O out-of-plane distance being 3.32 Å and the in-plane distance 1.19 Å. The existence of four short and two long bonds in the distorted octahedral arrangement around the metal atom is an example of Jahn-Teller distortion in a Cu(II) complex. In the β-form, unlike the α-form, the copper atom has been shown to be five coordinate with the two nitrogen atoms at an average distance of 1.972 Å from the metal atom. The fifth ligand is an oxygen atom from a neighbouring molecule. This copper-oxygen distance is 2.83 Å, suggesting a rather weakly bound oxygen atom. From the difference in the structure of these two chelates, one would expect to observe a difference in the band pattern and positions of νM-L in their IR spectra. Crystal structures of anhydrous metal oxinates other than those of Cu(II) and Pd(II) have not been determined, although Mande and Chetal have reported that anhydrous Co(II) oxinate is tetrahedral from observations of the cobalt *K* X-ray absorption edge [37].

The crystal structure of the methanol adduct of $[Cr(ox)_3]$ and both the methanol and hexanol adducts of $[Mn(ox)_3]\cdot R\text{-}OH$ have been reported in the literature [18,19]. The chromium atom is octahedrally coordinated. The isomer is meridional and the alcohol does not coordinate to the metal. The octahedron

is distorted due to the strained configuration in the five-membered chelate rings. Both the Mn complexes are the meridional isomers with the manganese atoms also coordinated to the bidentate oxine ligands in a distorted octahedral configuration. As expected of octahedral high spin manganese(III) complexes, the octahedron shows Jahn-Teller distortion. There are two long metal-nitrogen bonds (the axial Mn-N(1) and Mn-N(2) bonds) and four M-L shorter bonds (see Fig. 3.1). Therefore, this complex will have two distinct Mn-N distances as has been found in acetylacetonato*bis*(*N*-phenylaminotroponiminato)manganese(III) by Bartlett and Palenik [20]. This should be verified by the IR spectrum of $[Mn(ox)_3]$ where one would expect two νMn-N bands.

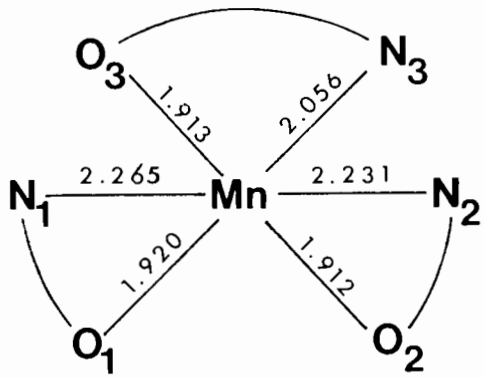

Fig. 3.1 Structure of $[Mn(ox)_3]\cdot$R-OH. Bond lengths (Å) refer to the mean values for the two structures.

In the course of this work, a series of 8-hydroxyquinoline complexes of the first row di- and trivalent transition metal ions and second row trivalent transition metal ions has been prepared.

The objective of this study is to firmly establish the ligand bands in their infrared spectra by deuteration of the ligand and, moreover, to assign the metal-ligand bands by means of a metal isotopic labelling study. The effect of metal ion substitution was also applied to the assignment of metal-ligand bands.

3.2 PREPARATION OF COMPLEXES

The isotopically-labelled compounds in this study together with their commercial sources and isotopic purities are listed in Table 3.1.

Table 3.1

Isotopic labelled compound	% purity	Commercial source
EtOD	99.8	Aldrich Chemical Company, Inc.
D_2O	99.0	Aldrich Chemical Company, Inc.
$^{64}Zn(SO_4)_2 \cdot 7H_2O$	98.56	BOC Prochem Ltd.
$^{68}Zn(SO_4)_2 \cdot 7H_2O$	97.62	BOC Prochem Ltd.
D_2SO_4	99.0	Merck, Sharp and Dohme (Canada) Ltd.[a]
o-aminophenol-d_7	99.7	Merck, Sharp and Dohme (Canada) Ltd.[a]
glycerol-d_8	98.6	Merck, Sharp and Dohme (Canada) Ltd.[a]

[a]Now Merck-Frosst Ltd.

3.2.1 *Preparation of deuterated 8-hydroxyquinoline by the Skraup synthesis*

The technique adopted for the preparation of the deuterated ligand is based upon the Skraup synthesis [38]. In this procedure a premix of amine, glycerol and sulphuric acid (mixture A) is maintained at a temperature which keeps it fluid (about 70°C). This is then added to the vessel containing the nitro compound (mixture B) and the mixture refluxed at about 150°C at which temperature the Skraup reaction begins to occur.

Mixture A contains 1.52 ml (2.76 g ≡ 0.276 mmol) D_2SO_4, 1.0 g (8.609 mmol) *o*-aminophenol-d_7, and 2.55 g (0.025 mol) glycerol-d_8. Mixture B contains 0.065 g (4.360 mmol) *o*-nitrophenol and 0.089 g (0.238 mmol) $Fe(SO_4)_2 \cdot 7D_2O$.

The thick liquid mixture A was added to the reaction vessel containing the nitro compound (mixture B). The dark brown mixture was then refluxed in a glycerol bath for about 3 hr (bath temperature ∿150°C). Care was taken not to overheat the mixture, the temperature over the liquid being maintained at 100 - 110°C. After cooling to room temperature, the black melt was neutralized carefully with NaOH (2.464 g ≡ 0.0616 mol) in 5 ml D_2O. The mixture was cooled in an ice bath so that the temperature did not rise above 40°C. Cold D_2O was then added until the final volume was about 25 ml. The mixture was allowed to stand for 0.5 hr, the pH of the resulting solution being about 7. Deuterated 8-hydroxyquinoline together with tarry by-products precipitated. Filtering of the black solid was difficult as the liquid was very viscous.

The crude product was well washed with excess cold D_2O and then dried over silica gel under reduced pressure for five days. Yield = 1.545 g dry black powder. The crude powder was sublimed under a slight positive pressure of nitrogen. The bath temperature was gradually increased from 65 to 95°C over 4.5 hr. Very light fluffy white needles appeared at a temperature of 80°C. The needles were carefully collected in a long tube and stored under nitrogen. M.p. 76 - 78°C, yield 0.041 g (3.21%). The yield is very low due to the tarry by-products which are a common feature of the Skraup synthesis. The deuteration is not 100% complete as shown by the mass spectrum in Fig. 3.2. Table 3.2 gives some assignments and the isotopic purity as estimated from the mass spectrum.

3.2.2 *Preparation of the complexes* $[M(ox)_2(H_2O)_2]$ *(M = Mn, Fe, Co, Ni, Cu, Zn).*

These complexes have been known for many years and have been widely used in the quantitative analysis of first row transition metal(II) ions [2].

The iron and copper complexes were prepared according to the method reported by Ohkaku and Nakamoto [12], the iron complex being prepared and isolated under nitrogen. The manganese, cobalt, nickel and zinc complexes were prepared by essentially the same general method. This involved mixing an aqueous solution of the appropriate metal chloride with an ethanolic solution of oxine in a 1 : 2.1 molar ratio. The complexes were filtered and washed with ethanol to remove excess ligand.

Table 3.2

Assignments and % deuteration of 8-hydroxyquinoline-d_n as estimated from Fig. 3.2.

m/e	d_n where n =	%
152	7	7
151	6	36
150	5	38
149	4	16
148	3	3

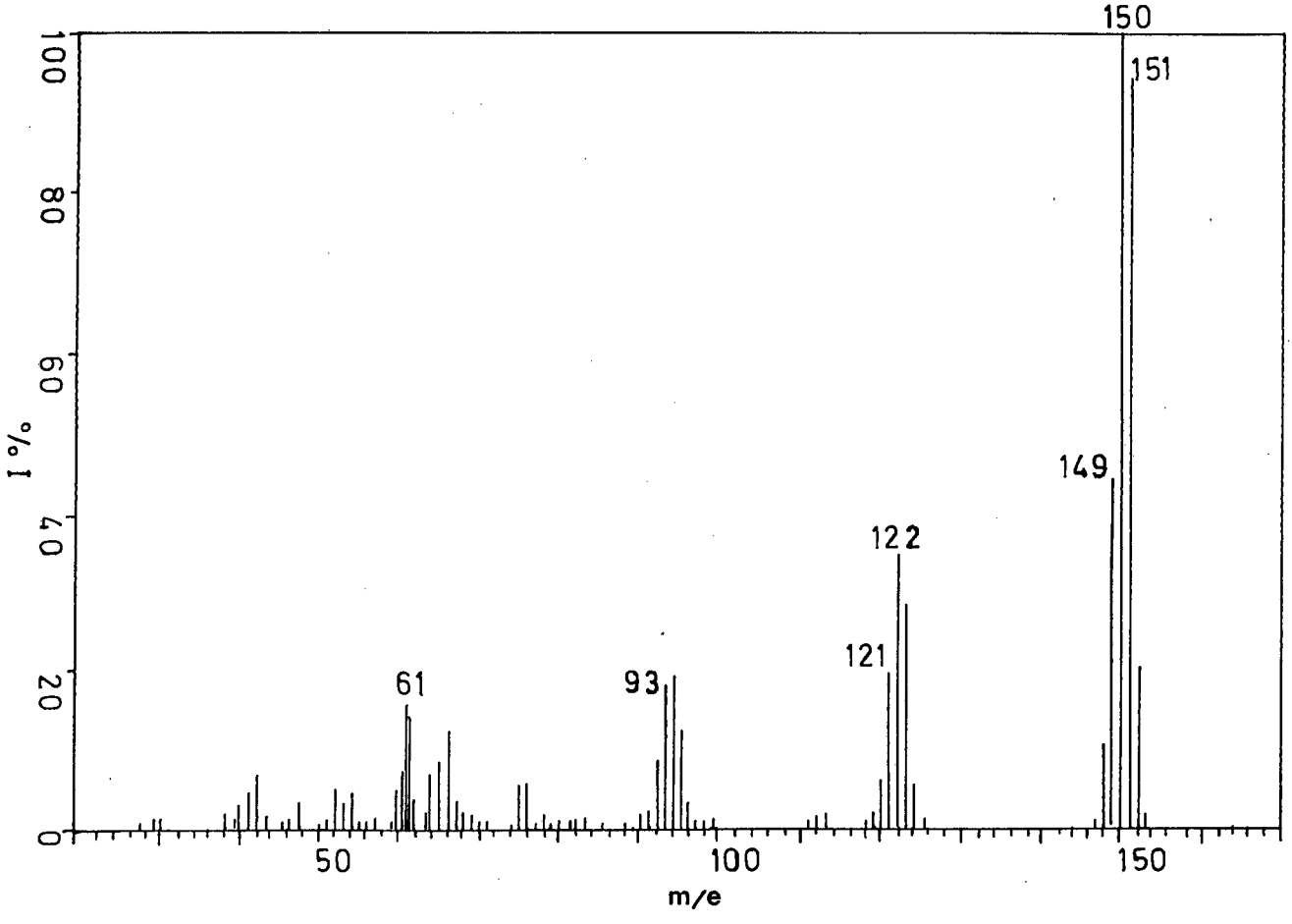

Fig. 3.2 Mass spectrum of deuterated 8-hydroxyquinoline.

The products were then dried overnight over silica gel under reduced pressure. $[Zn(ox)_2(D_2O)_2]$ and $[Ni(ox)_2(D_2O)_2]$ were prepared in a similar manner using EtOD and D_2O. $[^{64,68}Zn(ox)_2(H_2O)_2]$ was prepared in a similar manner to the unlabelled complex using $^{64,68}Zn(SO_4)_2 \cdot 7H_2O$. The deuterated oxine complexes were synthesized as described for the unlabelled compounds using the deuterated solvents previously mentioned and the deuterated ligand obtained from Section 3.2.1. The mass spectrum of the deuterated oxine complex of zinc is given in Fig. 3.3. Table 3.3 gives the percentage of deuteration of the deuterated oxine zinc complex as estimated from the mass spectrum. Similar results were obtained for the deuterated oxine complex of nickel.

All the deuterated complexes prepared above were stored under vacuum to prevent deuterium/hydrogen exchange.

3.2.3 *Preparation of the complexes* $[M(ox)_2] \cdot xH_2O$ *(M = Mn, Ni, α-Cu, β-Cu, Zn, x = 0; M = Co, x = 0.5).*

The anhydrous manganese, nickel and zinc complexes were prepared by the thermal dehydration of the appropriate metal dihydrate complex following the method of Hollingshead [2]. The loss of water which accompanies the structural change is indicated by a colour change. The process of dehydration was further controlled by weighing the sample after each period of heating. This procedure was continued until the calculated mass loss was achieved and the colour change was complete. The most favourable conditions applied to the dehydration of the dihydrate complexes are given in Table 3.4.

Table 3.3

Assignments and % deuteration for the complex $[Zn(ox\text{-}d_n)_2(D_2O)_2]$ as estimated from Fig. 3.3.

m/e	$[Zn(ox\text{-}d_n)_2]^+$ where n =	%
366	6	26
364	5	37
362	4	35
360	3	2

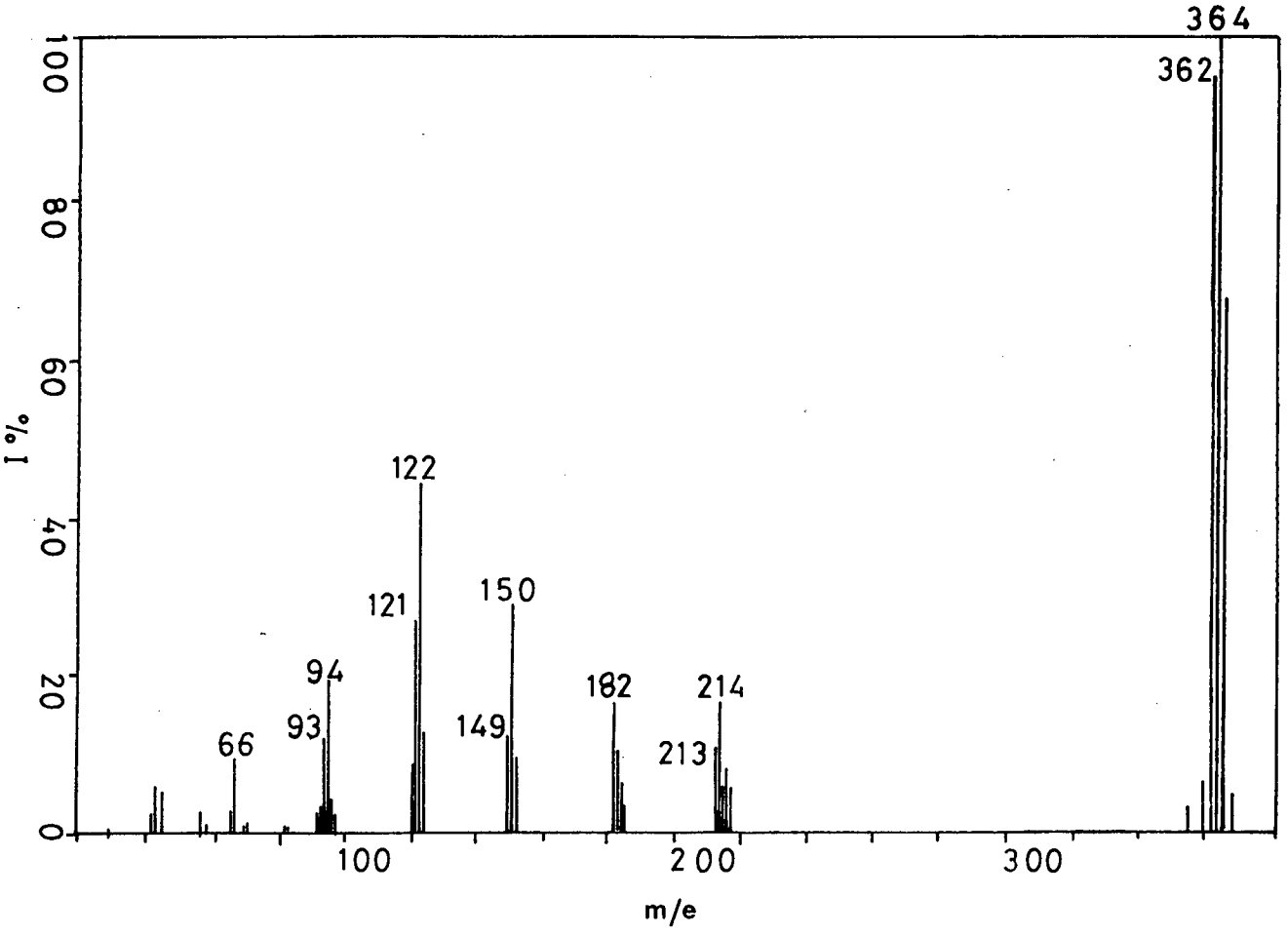

Fig. 3.3 Mass spectrum of $[Zn(ox\text{-}d_n)_2(D_2O)_2]$.

Table 3.4 Conditions for the dehydration of $[M(ox)_2(H_2O)_2]$

M	Temperature (°C)	Time (min)	Colour change
Mn	100	120	yellow → brown
Ni	130	100	green → yellow
Zn	170	100	green → yellow

The cobalt complex cannot be prepared by this technique and was therefore synthesized by refluxing $[Co(ox)_2(H_2O)_2]$ in benzene as described by Lenzer [39]. The β-copper oxinate was prepared as suggested by Fanning and Jonassen [36]. Attempts to prepare α-$[Cu(ox)_2]$ as reported by these workers yielded the β-form. The α-form was therefore produced as follows:

0.149 g (1.026 mmol) oxine was dissolved in 25 ml Analar methanol. Cu(II) acetate monohydrate (0.204 g ≡ 1.022 mmol) dissolved in 3 ml Analar methanol was added, yielding a green solution which was left to stand for about five minutes. A bronze precipitate formed. It was filtered off, well washed with Analar methanol and dried under reduced pressure over silica gel overnight. The product was then further dried in a drying pistol over KOH between 110 - 115°C for 1.5 hr.

3.2.4 *Preparation of the complexes* $[M(ox)_3]\cdot xH_2O$ *(M = Cr, Mn, Fe, Ga, x = 0; M = In, x = 0.5; M = Sc, V, Co, Rh, x = 1).*

The chromium, iron and gallium chelates were prepared in a similar manner to the procedure described in Section 3.2.2 for the metal(II)dihydrate complexes. An aqueous solution

of the metal(III) chloride was mixed with an ethanolic solution of oxine in a 1 : 3.15 molar ratio. The complex was filtered, washed with ethanol and dried under reduced pressure over silica gel overnight. The manganese complex was prepared from the corresponding acetylacetonate following the method of Ray and coworkers, using 2-propanol to prevent adduct formation [21]. The deuterated oxine complex of manganese was similarly prepared using the deuterated oxine from Section 3.2.1. The mass spectrum of the resulting complex gave similar results for the extent of deuteration as were obtained for the deuterated oxinate complex of zinc. The vanadium chelate was synthesized according to the method of Bayer and colleagues [40]. Preparation of the cobalt(III) oxinate complex was achieved by the initial hydrogen peroxide oxidation of Co(II) to Co(III) as described by Hollingshead [2]. Several attempts were made to prepare $[Ti(ox)_3]$ according to the method of Taylor and Wilkins [41]. It was found, however, that this complex was too air sensitive to isolate successfully.

It is well known that on the addition of an aqueous solution of scandium(III) chloride to an ethanolic solution of oxine in a 1 : 3.15 molar ratio the complex $Sc(ox)_3 \cdot Hox$ will form.[a] Heating of this complex does <u>not</u> produce $[Sc(ox)_3]$. We have synthesized the previously unreported $[Sc(ox)_3]$ from the corresponding acetylacetonate adapting the method of Ray and coworkers used for the preparation of $[Mn(ox)_3]$. 0.135 g

---

[a] A study of the infrared spectrum of $Sc(ox)_3 \cdot Hox$ is in progress.

(0.930 mmol) oxine, dissolved in 2-propanol (3 ml), was added to an aqueous solution of sodium acetate trihydrate (0.127 g ≡ 0.933 mmol in 7 ml water). This resulted in the formation of a pale yellow precipitate, presumably sodium oxinate. A further 2 ml 2-propanol was added to dissolve this precipitate. The yellow solution was then added to the metal solution (0.105 g (0.307 mmol) $Sc(acac)_3$ in 7 ml 2-propanol). This resulted in an instant colour change from fleshy-pink to yellow. The solution was gently heated for two hr and then cooled to room temperature. The resulting yellow precipitate was filtered off, washed with ether (as $[Sc(ox)_3]$ is fairly soluble in 2-propanol) and then dried overnight under reduced pressure over silica gel.

The indium complex was also prepared from the corresponding acetylacetonate as follows:

$In(acac)_3$ (0.106 g ≡ 0.257 mmol) was suspended in approximately 10 ml hot CH_2Cl_2. The ligand (0.131 g ≡ 0.902 mmol) was dissolved in a minimum of CH_2Cl_2 and then added to the metal suspension. This resulted in a yellow solution which was filtered through fine filter paper (Whatman 541 to remove any undissolved $In(acac)_3$) and the solution was then evaporated to dryness on a rotary evaporator. The resulting yellow complex of $[In(ox)_3]0.5H_2O$ was twice recrystallized from CH_2Cl_2/hexane.

Although $[Rh(ox)_3]$ has previously been reported in the literature [9], no reproducible method of preparation of this complex has been published. We synthesized the complex under nitrogen as follows:

A solution of oxine (0.272 g ≡ 1.874 mmol in 10 ml ethanol) was added to a solution of $RhCl_3 \cdot nH_2O$ (0.141 g ≡ 0.536 mmol[a] in 10 ml H_2O). No immediate colour change from the initial red hue occurred and the solution was therefore refluxed overnight. The resulting bright yellow complex was filtered off, washed with ethanol and dried under reduced pressure over silica gel overnight. It was necessary to recrystallize this chelate from CH_2Cl_2/hexane.

---

[a]Assuming $n = 3$.

3.3 ANALYSES OF COMPOUNDS

Table 3.5

Analytical data for the metal oxinate complexes.

Complex	Calculated			Found		
	%C	%H	%N	%C	%H	%N
$[Mn(ox)_2]$[a]	62.99	3.52	8.16	62.00	3.55	7.95
$[Co(ox)_2]$[b]	60.69	3.50	7.85	60.69	3.67	7.86
$[Ni(ox)_2]$	62.30	3.49	8.07	62.10	3.55	8.05
α-$[Cu(ox)_2]$	61.44	3.44	7.96	61.45	3.50	7.95
β-$[Cu(ox)_2]$	61.44	3.44	7.96	61.60	3.55	7.95
$[Zn(ox)_2]$	61.13	3.42	7.92	60.60	3.45	7.90
$[Mn(ox)_2(H_2O)_2]$	57.00	4.25	7.39	56.65	4.20	7.35
$[Fe(ox)_2(H_2O)_2]$	56.87	4.37	7.36	56.85	4.25	7.40
$[Co(ox)_2(H_2O)_2]$	56.41	4.21	7.31	56.00	3.95	7.30
$[Ni(ox)_2(H_2O)_2]$	56.44	4.21	7.31	56.35	4.25	7.25
$[Ni(ox)_2(D_2O)_2]$	55.85	4.17	7.24	55.30	4.20	7.05
$[Ni(ox\text{-}d_n)_2(D_2O)_2]$[c]	54.16	4.04	7.02	54.30	4.15	7.05
$[Cu(ox)_2(H_2O)_2]$	55.74	4.16	7.22	55.85	4.25	7.10
$[Zn(ox)_2(H_2O)_2]$	55.48	4.14	7.19	55.30	4.25	7.10
$[Zn(ox)_2(D_2O)_2]$	54.91	4.10	7.11	55.05	4.20	7.15
$[Zn(ox\text{-}d_n)_2(D_2O)_2]$[c]	53.28	3.97	6.90	53.15	4.00	6.90

Table 3.5 continued/

Complex	Calculated			Found		
	%C	%H	%N	%C	%H	%N
$[^{64}Zn(ox)_2(H_2O)_2]$	55.68	4.15	7.21	55.40	4.20	7.20
$[^{68}Zn(ox)_2(H_2O)_2]$	55.11	4.11	7.14	55.10	4.20	7.00
$[Sc(ox)_3]$[d]	65.46	4.07	8.48	65.40	4.10	8.45
$[V(ox)_3]$[d]	64.68	3.82	8.40	64.75	3.95	8.40
$[Cr(ox)_3]$	66.92	3.74	8.67	66.75	3.85	8.65
$[Mn(ox)_3]$	66.53	3.72	8.62	66.25	3.75	8.60
$[Mn(ox\text{-}d_n)_3]\cdot H_2O$[c]	61.95	3.85	8.03	62.30	3.80	7.55
$[Fe(ox)_3]$	66.40	3.72	8.60	66.20	3.70	8.65
$[Co(ox)_3]$[d]	63.67	3.95	8.25	63.60	4.05	8.05
$[Ga(ox)_3]$	64.58	3.62	8.37	64.60	3.80	8.10
$[Rh(ox)_3]$[d]	58.61	3.64	7.59	58.45	3.65	7.50
$[In(ox)_3]$[b]	58.30	3.44	7.55	58.05	3.70	7.45

[a]The microanalytical figures are the best results obtained from several attempts to prepare a pure complex.

[b]Hemihydrate

[c]The mass spectrum of this complex shows that it is a mixture of the d_6, d_5, d_4, d_3 deuterates. (See Sections 3.2.2 and 3.2.4 for details. The calculated figures are for the complex with n=6 or 7.

[d]Monohydrate.

3.4 RESULTS AND DISCUSSION

3.4.1 *General considerations*

At this stage, it is necessary to comment on the isotopic purity of the deuterated ligand. Mass spectroscopy was used to estimate the percentage deuteration of both the deuterated oxine as well as its metal chelates. In the mass spectrum of the deuterated ligand (Fig. 3.2), the presence of ions at *m/e* 152 (oxine-d_7), 151 (oxine-d_6), 150 (oxine-d_5), 149 (oxine-d_4) and 148 (oxine-d_3) indicates that either H/D exchange occurred during the synthesis of the ligand, or that the starting materials were not of the isotopic purity claimed by the suppliers. As to be expected, the metal chelates consisted of several isotopomers which were reflected in their mass spectra. The mass spectrum of $[Zn(ox\text{-}d_n)_2(D_2O)_2]$, one of the metal chelates prepared from the deuterated ligand, is shown in Fig. 3.3. The isotopic purity of both the ligand and the metal chelates was established by considering the relative ratios of the various isotopomers. This result is, however, only an approximation. In this way, the isotopic purity of 8-hydroxyquinoline-d_7 was found to be about 7% and that of $[Zn(ox\text{-}d_6)_2(D_2O)_2]$ 26% (Tables 3.2 and 3.3, respectively). A similar isotopic purity of 26% was found for both $[Mn(ox\text{-}d_6)_3]\cdot H_2O$ and $[Ni(ox\text{-}d_6)_2(D_2O)_2]$.

3.4.2 *The IR spectrum of 8-hydroxyquinoline*

The assignment of the fundamentals of this ligand is an extremely difficult task because of the substantial number

Table 3.6

A correlation between IR frequencies and band assignments for quinoline (column 1) and oxine (columns 2, 3, 4 and 5).

Column 5 gives the present assignments based upon references 34 and 42 for the oxine ligand.

Quinoline ν (cm^{-1})	Assignment [42]	oxine ν (cm^{-1})	Assignment [32]	oxine ν (cm^{-1})	Assignment [33]	oxine ν (cm^{-1})	Assignment [34]	Present work ν (cm^{-1})	Assignment
628	γ ring	572	γ ring	572	ν ring	637	γ ring	636(39)	γ ring
611	ν ring	634	ν ring	635(sh)	ν ring	575	ν ring	575(58)	ν ring
479	γ ring	460	γ ring	n.o.		543	γ ring	546(66)	γ ring
472	γ ring	n.o.		461	ν ring	491	γ ring	491(23)	γ ring
505	ν ring	488	ν ring	461	n.a.	470	n.a.	471(27)	ν ring?
						465	αC-O	464(21)	αC-O
392	γ ring	n.o.		n.o.		423	γ ring	423(87)	γ ring
						305	n.a.	304(8)	
						297	n.a.	298(sh)(10)	
						266	γC-O	266(17)	γC-O
193	γ ring	n.o.		n.o.		195	Γ_5	194(15)	γ ring
178	γ ring	n.o.		n.o.		*162*	γ ring	161(16)	γ ring

Values in parentheses are the shifts induced by deuteration of the ligand and are to lower frequencies.

Values in italics are estimated values only.

n.o. = not observed; n.a. = not assigned; sh = shoulder.

of vibrations present and the possibility of coupling between the modes with similar energies. Without normal coordinate analytical data for this ligand, a conclusive assignment of the vibrations is not possible. Assignments have therefore been made firstly, by considering oxine in terms of its similarity with quinoline [42]; secondly, by comparison with the partial assignments that have been reported for oxine [32-34]; and thirdly, by observing the effect of deuteration on the spectrum of the ligand.

Table 3.6 shows the correlation between the IR frequencies and assignments of quinoline and oxine from 700 to 150 cm^{-1}. Correlations between the spectra of the deuterated and undeuterated oxine are complicated by the fact that the ligand is not 100% isotopically pure. The identification of corresponding vibrations was therefore carried out in the following manner: Using previous assignments of oxine modes, together with ν^D/ν^H ratios calculated from data reported for quinoline and quinoline-d_7 [42,43] (*viz.*, 0.92 ± 0.08 for ring modes and 0.76 ± 0.08 for C-H modes), expected positions for bands in the spectrum of oxine-d_7 were deduced. Despite minor discrepencies, agreement between the calculated and observed values was found to be good. In this way, the majority of bands below 700 cm^{-1} were assigned as ring modes. The two bands at 465 and 266 cm^{-1} (which shift about 20 cm^{-1} to lower frequency on deuteration) were assigned as αC-O and γC-O, respectively. This is in agreement with Marchon *et al.* [34].

3.4.3 *The IR spectra of the metal(II) dihydrate complexes, $[M(ox)_2(H_2O)_2]$ (M = Mn, Fe, Co, Ni, Cu, Zn) from 700 to 50 cm^{-1})*

X-ray crystallographic studies have shown the structures of the Co, Ni, Cu and Zn chelates to have a *trans*-planar arrangement of the oxine molecules [13-15]. The water molecules are coordinated in the axial positions resulting in a six-coordinate octahedral stereochemistry. The band-for-band correspondence of the IR spectra of these chelates with those of Mn and Fe suggest that the latter two complexes are isostructural. The spectra of the complexes over the range 700 to 50 cm^{-1} are illustrated in Fig. 3.4. The actual tracings of the IR spectra of the pair of complexes $[^{64,68}Zn(ox)_2(H_2O)_2]$ are shown in Fig. 3.5.

The site symmetry of these complexes is C_{2h}. This requires three IR-active metal-ligand vibrations (one each for νM-O, νM-N and $\nu M-OH_2$). The M-L vibrations in a series of isostructural isovalent transition metal complexes are expected to follow the order of the CFSEs of the metal ions. Hence, those bands which show a metal ion dependence which mimics the CFSE order, will be assigned as νM-L. The reported magnetic moments (Table 3.7) indicate that a number of the chelates have a high-spin configuration, and hence for octahedral stereochemistry, we expect the order of νM-L to be metal ion dependent in the Irving-Williams stability sequence [35]. There are five main bands below 650 cm^{-1} which show this order, namely those within the ranges 520 - 500, 410 - 370, 320 - 250, 230 - 200 and 215 - 185 cm^{-1}.

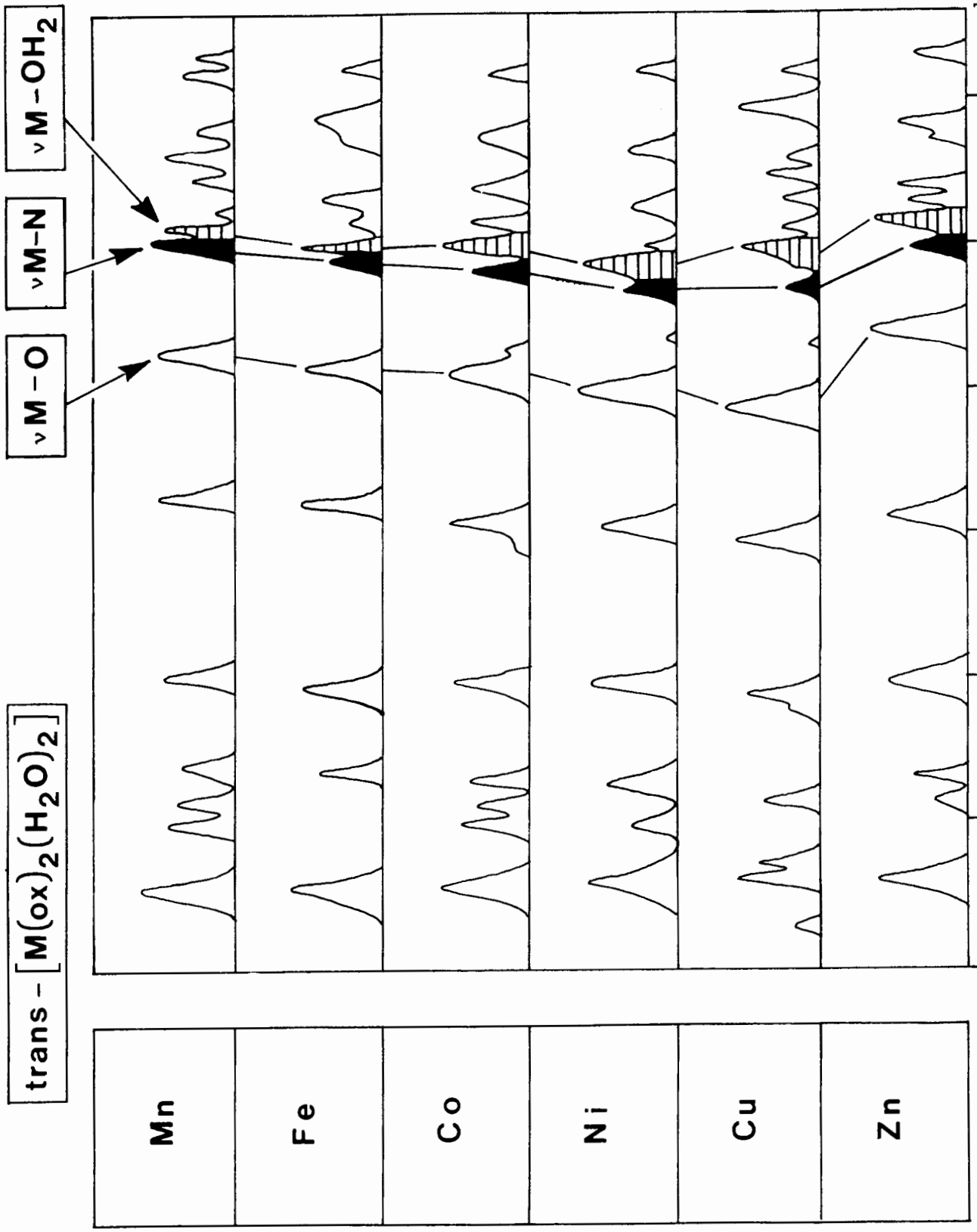

Fig. 3.4 Infrared spectra of the complexes *trans*-$[M(ox)_2(H_2O)_2]$ in the region 700 - 50 cm^{-1}.

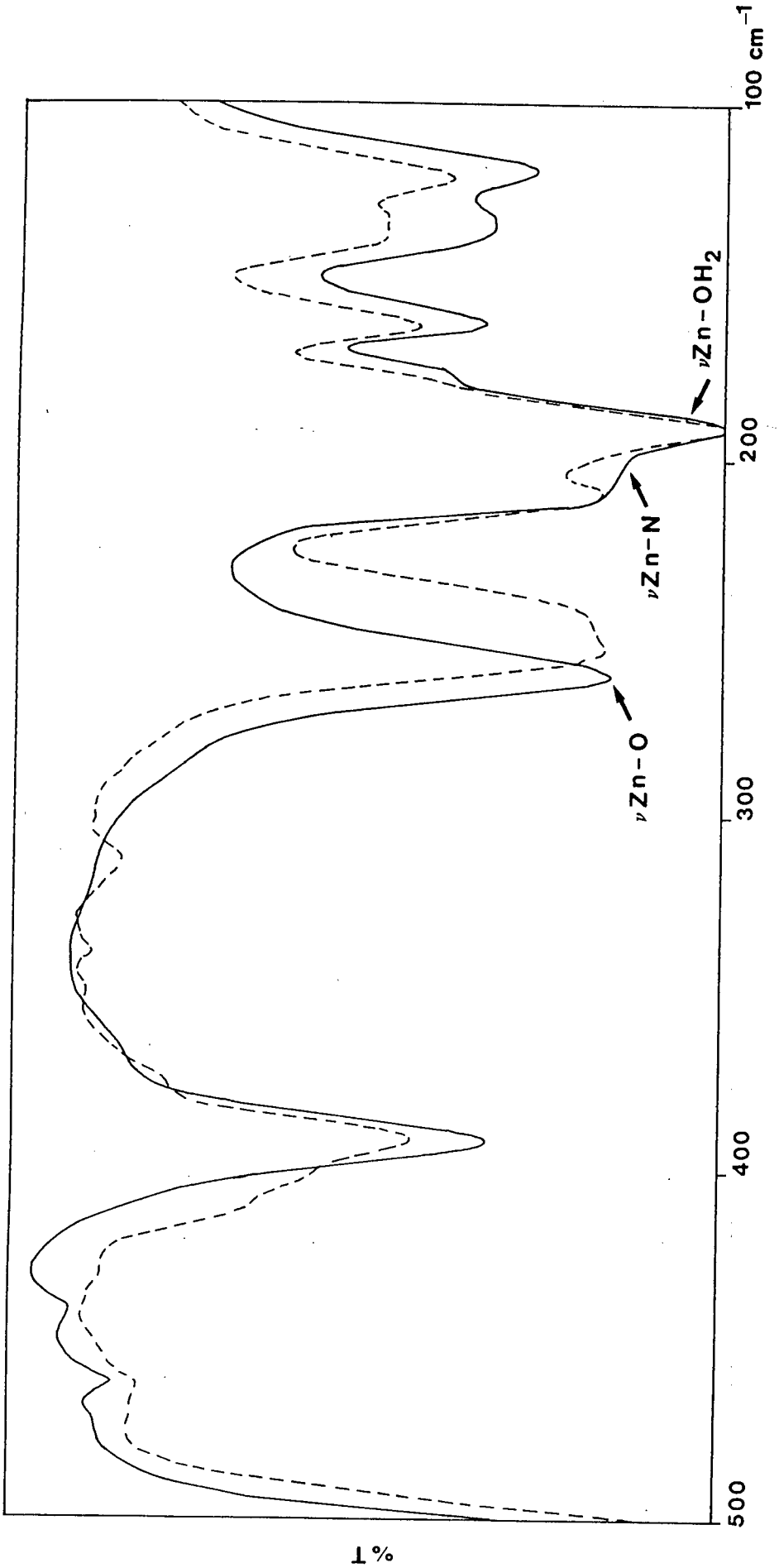

Fig. 3.5 IR spectrum of $[^{64}Zn(ox)_2(H_2O)_2]$ (——) and $[^{68}Zn(ox)_2(H_2O)_2]$ (---) in the region 500 ÷ 100 cm^{-1}.

Table 3.7

Magnetic moments for oxine complexes at 290 K

Complex	M	$\mu_{eff.}$ (B.M.)	Reference
$[M(ox)_2(H_2O)_2]$	Mn	4.5	44
	Co	4.6	39
$[M(ox)_2]_n$	Mn	4.5	44
	Co	4.6	39
	Ni	3.3	45
$[M(ox)_3]$	Mn	5.0	46
	Fe	4.4	44
	Co	diamagnetic	44

Combining the present work with that of Ohkaku and Nakamoto [12], yields the shift on deuteration, the shift on metal ion labelling and the low frequency shift on replacement of nickel by zinc in the nickel and zinc chelates (Table 3.8). Thus, the bands at 500 and 400 cm^{-1} are unaffected by metal isotopic labelling or by metal ion substitution, but shift significantly on ligand deuteration. This is in accord with their assignment to αC-O and chelate ring deformation modes, respectively, as has previously been reported [12].

The bands at 300 cm^{-1} (Ni) and 259 cm^{-1} (Zn) are strongly sensitive to metal isotopic labelling, significantly sensitive to the replacement of Ni by Zn and moderately sensitive to ligand deuteration. These factors suggest the assignment of these bands to metal-ligand stretches, undoubtedly νM-O.

Table 3.8 Frequency, shift and assignment data for *trans*-$[Ni(ox)_2(H_2O)_2]$ and $[Zn(ox)_2(H_2O)_2]$.

$[Ni(ox)_2(H_2O)_2]$				$[Zn(ox)_2(H_2O)_2]$			Assignment[a]
Band frequency[a] cm^{-1}	$\Delta\nu$ d_6[ab] cm^{-1}	$\Delta\nu$ i_M[c] cm^{-1}	$\Delta\nu$ Ni-Zn[ad] cm^{-1}	Band frequency[a] cm^{-1}	$\Delta\nu$ d_6[ab] cm^{-1}	$\Delta\nu$ i_M[e] cm^{-1}	
505	9	0	2	503	13	0(0)	αC-O
390	16	0	-1	391	17	0(0.5)	chelate ring def.
300	3	6.3	41	259	4	5(5)	νM-O
265	wb[f]	4.0					νM-N
226	∿5	0	21	205	10	sh[g](0)	
214	4	3.5	24	190	11	2(1)	$\nu M-OH_2$
200	sh[g]	0	23	177	sh[g]	sh[g](0)	γ ring
172	-	0	9	161	10	2(0.3)	δL-M-L
				123	2	1(n.r.)[h]	
133	-	n.r.[h]	10				
				119	2	0(n.r.)[h]	
80	-	n.r.[h]	13	73	-	1(n.r.)[h]	Lattice

[a] This work.

[b] Shift on ligand deuteration.

[c] Shift on substitution of ^{58}Ni by ^{62}Ni [12].

[d] Low frequency shift on substitution of Ni by Zn.

[e] Shift on substitution of ^{64}Zn by ^{68}Zn. The shift observed in this work is followed by the shift observed by Ohkaku and Nakamoto [12] in parentheses.

[f] wb = weak and broad; shift cannot be accurately determined.

[g] sh = shoulder; shift cannot be determined accurately.

[h] n.r. = not reported.

Wood and Jones [47] have calculated coordinate bond energies for several Ni(II) chelates, and found that Ni-N bond energies of a variety of nitrogen donor ligands were about 238 kJ mol^{-1}. They subsequently found the Ni-O bond energy in the oxine chelate to be 269 kJ mol^{-1}. The Ni-O is therefore the stronger bond and thus the band νNi-O would be expected to appear in the IR spectra at a higher frequency than νNi-N, as is observed here (and in general).

The band near 200 cm^{-1} is readily allocated to νM-N in the spectra of the zinc complex because of its relatively low intensity and shift of 10 cm^{-1} to lower frequency on ligand deuteration. The shift due to labelling of the zinc ion could not be detected because of its presence as a shoulder to the strong band at 190 cm^{-1}. The assignment of νNi-N is more complicated. Ohkaku and Nakamoto [12] proposed a weak band at 265 cm^{-1} for which a metal isotopic shift of 4 cm^{-1} was reported. In the present work, it was difficult to determine the sensitivity of this band towards ligand deuteration because it appears as a very weak and broad band. However, we observe a shoulder at 226 cm^{-1} which shifts by about 5 cm^{-1} on ligand deuteration and by 21 cm^{-1} on replacement of Ni by Zn, and this band is thus also assigned as νNi-N. This band does not shift on $^{58,62}Ni$ labelling [12].

The $\nu M-OH_2$ band is assigned unambiguously to the strong bands at 214 cm^{-1} (Ni) and 190 cm^{-1} (Zn). These bands are sensitive to metal ion substitution, ligand

deuteration and metal isotopic labelling. These bands, however, do not shift significantly to lower frequencies in the $[Ni(ox)_2(D_2O)_2]$ and $[Zn(ox)_2(D_2O)_2]$ complexes. The lower frequency bands in the region 170 - 100 cm^{-1} are tentatively assigned to ligand modes or L-M-L bending vibrations.

Extension of these results to the Mn, Fe, Co and Cu chelates yields the assignments given in Table 3.9. The assignments of the bands in the 650 - 500 cm^{-1} region are based on the assignments of the ligand vibrations given in Table 3.6 and are therefore tentative assignments. The assignment of the bands in the range 500 - 50 cm^{-1} are readily made on the basis of their band-for-band correspondence with the spectra of the nickel and zinc chelates.

The contribution to the observed frequency ν, provided by the CFSE, is the difference $(\nu-\nu_o)$ between the observed frequency and the frequency which would have been realized in the absence of crystal field stabilization, ν_o. The ν_o values are obtained by drawing an interpolation line through the observed frequencies with zero CFSE, *i.e.*, Mn and Zn (Fig. 3.6). Graphically-determined $(\nu-\nu_o)$ values are given in Table 3.9. These generally exhibit a qualitative parallel with the CFSE variation [48].

It is noteworthy that the observed metal-sensitivities of the νM-O and νM-N bands are without exception in the sequence Mn < Fe < Co < Ni < Cu > Zn, whilst the order of νM-OH_2 is Mn < Fe < Co < Ni > Cu > Zn. The latter sequence provides the most

Table 3.9

Frequency data (cm^{-1}) and assignments for the complexes *trans*-$[M(ox)_2(H_2O)_2]$.[a]

Mn	Fe	Co	Ni	Cu	Zn	Assignment
643	641	642	641	638	641	γ ring
601		602	606	629	603	ν ring
584	587	587	587	587	586	γ ring
560	563	568	570		567	γ ring
499	505(7)	505(6)	505(5)	517(16)	503	αC-O
374	379(0)	386(6)	390	405(17)	391	chelate ring def.
277	285(14)	290(21)	300(35)	312(51)	259	νM-O
		271	265(vw)	269(66)		νM-N
198	210(10)	217(17)	226(25)	229(27)	205	
189	200(11)	202(12)	214(24)	205(15)	190	$\nu M-OH_2$
178	181(3)	183(5)	200(22)	191(14)	177	γ ring
155	168(13)	162(5)	172(13)	171	161	δL-M-L
142					123	
121	126(5)	129(8)	133(11)	153(30)	119	
	112			107		
83	79(0)	81(2)	80(1)	81(4)	73	Lattice

[a]Figures in parentheses give the sensitivity of the band to metal ion substitution, *i.e.*, $(\nu - \nu_o)$. For a full explanation of the significance of this value see text or reference 48.

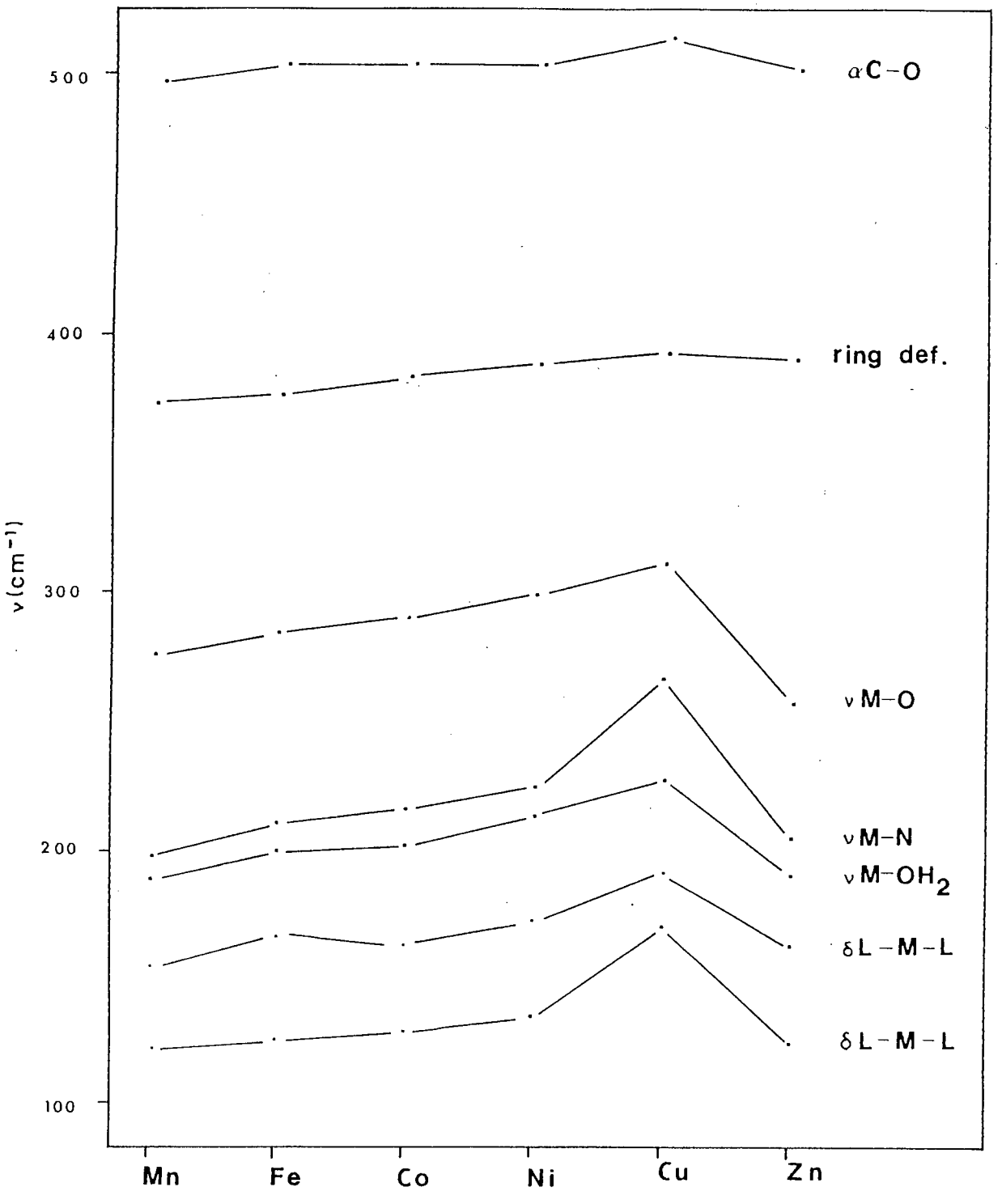

Fig. 3.6 Metal-sensitivity of certain bands of the *trans*-$[M(ox)_2(H_2O)_2]$ complexes in the region 550 - 100 cm^{-1}.

convincing evidence for the correctness of the assignment of $\nu M\text{-}OH_2$, since the Cu(II) chelate exhibits Jahn-Teller distortion which results in elongation of the $Cu\text{-}OH_2$ bonds. Such a situation leads to a decrease of the $Cu\text{-}OH_2$ bond strengths and hence a decrease of $\nu Cu\text{-}OH_2$ [49].

3.4.4 *The IR spectra of the bis(oxinate) complexes,* $[M(ox)_2]_n$ *(M = Mn, Co, Ni, α-Cu, β-Cu, Zn) from 700 to 50* cm^{-1}.

The spectra of these complexes have also been examined by Ohkaku and Nakamoto [12]. Metal isotopic labelling ($^{58,62}Ni$, $^{63,65}Cu$ and $^{64,68}Zn$) was employed for the assignment of the metal-ligand stretching frequencies and the structural implications of the spectra were discussed. There are three possible structures for these complexes : *trans*-planar (C_{2h}), *cis*-planar (C_{2v}) and tetrahedral (C_{2v}). According to group theory, the required number of infrared-active metal-ligand stretching bands are two for C_{2h} symmetry ($2B_u$) and four for C_{2v} symmetry ($2A_1 + 2B_1$ for *cis*-planar and $2A_1 + B_1 + B_2$ for tetrahedral).

Tetrahedral coordination has been proposed for the Ni(II) chelate on the basis of its magnetic moment (Table 3.7) and IR spectrum [12,44]. Mande and Chetal [37] have proposed that the Co(II) oxinate complex is tetrahedral from observations of the cobalt *K* X-ray absorption edge. The zinc chelate is considered to be tetrahedral by Ohkaku and Nakamoto [12]. Depending on the preparative conditions employed, the copper compound may be isolated in the α- or β-form [36]. The α-complex consists of units of six-

coordinate Cu(II) with a *trans*-planar arrangement of the two oxinate anions [16]. The chain of planar chelates formed in this way is weakly bound in the perpendicular direction by Cu-O bonds of length 3.32 Å. The β-form exists as dimers of essentially five-coordinate Cu(II) with only one bonded oxygen atom above the plane of the square. The out-of-plane Cu-O distance is 2.83 Å [17].

Our results (Table 3.10) are generally in good agreement with those of Ohkaku and Nakamoto [12]. The relative complexity of the IR spectra of the Ni(II) and Zn(II) complexes, is consistent with the proposed tetrahedral structure, there being two νM-O and two νM-N bands. However, since we only observe one νCo-O and one νCo-N band, we tend to disagree with the proposed tetrahedral structure of the Co(II) chelate. A polymeric octahedral structure seems to be the more likely alternative as this structure has been found for the analogous Co(II) acetylacetonate chelate [50]. Moreover, a polymeric octahedral structure has also been proposed by Lenzer [39] for the Co(II) oxinate complex on the basis of its magnetic moment (Table 3.7).

If we assume that the Co(II) and Ni(II) complexes are both tetrahedral as has been suggested by others [12,37, 44], we would expect, on CFSE grounds, that νCo-L would exceed νNi-L. However, the reverse situation is observed. This is consistent with our proposal that the Co(II) complex is polymeric octahedral since the higher coordination number of the cobalt complex would ensure that νCo-L < νNi-L.

Table 3.10

Frequency data (cm^{-1}) and assignments for the complexes $[M(ox)_2]_n$[a].

Mn	Co	Ni	α-Cu	β-Cu	Zn	Assignment
647	646	647	641	641	649	γ ring
623	612	624	629	629		ν ring
598	600	609			600	γ ring
		602				
		595			588	
577	568	572	582	582	560	γ ring
533	531					
491	503	519	520	520	496	αC-O
	490	504				
433	441	454	467	467	439	γ ring
		435				
393	409	408	406	404	411	chelate ring def.
	382	388			403	
					389	
					374	
340	338	332			313	ν ring?
324	320				301	
284	266	311(6)	326(3)	322(3.5)	241(5)	νM-O
235		279(5)			209(4)	
218	229	243(4)	291(3)	288(3)	193(2.5)	νM-N
201		230(3)	278(n.r.)[b]	276(n.r.)[b]	179(3)	
			218	217		lig.[c]
			210			

Table 3.10 continued/

Mn	Co	Ni	α-Cu	β-Cu	Zn	Assignment
		174	182	182		
			167	166		
			162			
135	138	129	138	135	137	lig.[c] +
129			132		133	δL-M-L
			109	109		
82			74	72	79	
66						

[a]Values in parentheses give the sensitivity of the band to metal isotopic labelling [12].

[b]n.r. = not reported.

[c]lig. = ligand vibration.

Fig. 3.7 shows the spectra of these chelates from 700 to 50 cm^{-1}. It is interesting to note that the α- and β-Cu(II) chelates exhibit spectra which are fairly similar to each other. The essential difference lies in the splitting of the bands near 215, 165 and 135 cm^{-1} which occurs in the α-chelate. Both chelates exhibit two bands in the region 350 - 250 cm^{-1} (326 and 291 cm^{-1} for the α-form and 322 and 288 cm^{-1} for the β-form) which according to Ohkaku and Nakamoto [12] are significantly metal isotope sensitive ($\Delta\nu \sim 3$ cm^{-1}). This observation is in accord with the *trans*-planar (C_{2h}) symmetry found by the X-ray studies [16,17]. In general, νM-O is more intense than νM-N and hence we assign the stronger bands at higher frequencies to νCu-O. The less intense bands at lower frequencies are assigned to νCu-N. The relatively weak band observed at about 276 cm^{-1} in the present work was not observed by Ohkaku and Nakamoto and its sensitivity to metal isotopic labelling is therefore not known. This band is most probably an additional νCu-N mode. One might expect an additional Cu-O stretching band due to the weak bond between the central copper atom and the oxygen atom of the adjacent molecule. However, this Cu-O stretching band could not be distinguished with certainty in the present work, probably because its frequency is very low. This seems reasonable because the out-of-plane oxygen atom is only weakly bound in the α- and β-Cu(II) chelates. The Cu-O bond lengths (3.32 Å and 2.83 Å, respectively) are much longer than those within the chelate rings (1.93 Å). It is also interesting to note that the Cu-O stretching frequency decreases as the in-plane Cu-O distance increases. Thus the

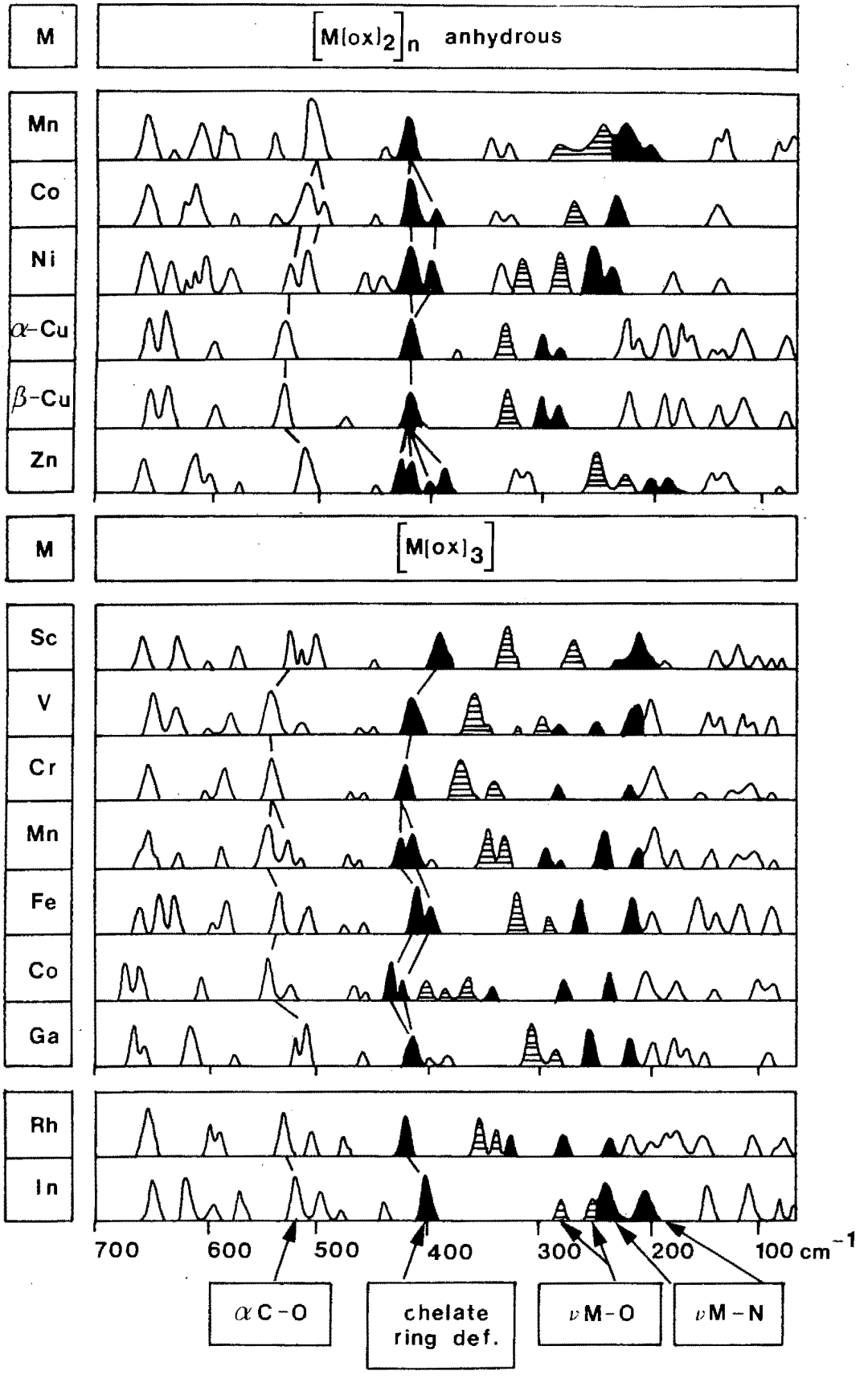

Fig. 3.7 IR spectra of the $[M(ox)_2]_n$ and $[M(ox)_3]$ chelates in the region 700 - 50 cm^{-1}. Linked bands: αC-O; solid linked bands: chelate ring deformation; shaded unlinked bands: νM-O; solid unlinked bands: νM-N.

νCu-O values of α- and β-$[Cu(ox)_2]$ (average in-plane Cu-O bond length 1.93 Å) and $[Cu(ox)_2(H_2O)_2]$ (Cu-O bond length 2.0 Å) are 326, 322 and 312 cm^{-1}, respectively. The $Cu-OH_2$ stretching frequency of $[Cu(ox)_2(H_2O)_2]$ (Cu-O bond length 2.3 Å) is 205 cm^{-1}.

3.4.5 *The IR spectra of the metal(III) oxinates, $[M(ox)_3]$ (M = Sc, V, Cr, Mn, Fe, Co and Ga) from 700 to 50 cm^{-1}.*

There are two probable structures for these chelates. The symmetries are facial (C_3) and meridional (C_1). Group theory predicts four νM-L bands ($2A + 2E$), *i.e.*, two νM-O and two νM-N bands for C_3 localized point symmetry and six νM-L bands, *i.e.*, three νM-O and three νM-N bands for C_1 symmetry.

Fig. 3.7 depicts the spectra of these complexes over the range 700 to 50 cm^{-1}. The Fe(III) chelate is the only complex for which a previous isotopic labelling study has been reported [12]. Ohkaku and Nakamoto found four bands significantly sensitive to metal isotopic labelling, *viz.*, the bands at 315 ($\Delta\nu$ = 5.1), 280 ($\Delta\nu$ = 2.5), 259 ($\Delta\nu$ = 3.4) and 201 ($\Delta\nu$ = 1.3) cm^{-1}. No other bands were found to shift more than 1 cm^{-1}. Examination of the spectra of the remaining complexes shows four bands (except for additional bands in the spectra of the vanadium, manganese and cobalt complexes) in the region 390 - 200 cm^{-1} which correspond to the metal isotope sensitive bands found for the iron complex. These bands occur in a similar region to the νM-L bands found for the divalent metal chelates (Table 3.9). The bands are also metal-sensitive in the sequence Sc < V < Cr > Mn > Fe < Co > Ga which is in the same order as their crystal

field stabilization energies. Since such an observation is a general characteristic of νM-L (Section 1.2), these bands may logically be assigned to νM-L (Table 3.11). Outside the range 390 - 200 cm^{-1}, several bands are found over the entire range 700 - 50 cm^{-1} which are not appreciably metal-sensitive and are therefore assigned as ligand bands. The assignments of the bands in the region 700 - 450 cm^{-1} and 200 - 50 cm^{-1} are tentative and are based on the assignments given in Table 3.6 for the vibrations of 8-hydroxyquinoline. Our assignment of the four metal-sensitive bands in the far-IR region of the *tris*(oxinates) includes the four bands previously assigned as νM-L on the basis of the metal isotopic labelling study and therefore fully supports their assignments and also the proposal that this chelate has facial symmetry.

X-ray crystallographic studies [18,19] of the manganese and chromium chelates have shown that these compounds crystallize as the meridional isomers and one should therefore observe six metal-ligand bands in their IR spectra. It is highly unlikely that in a series of isovalent chelates of the same general formula, two chelates should have different symmetries, *i.e.*, the iron chelate is facial but the chromium and manganese chelates have meridional symmetries. The discrepancy apparent between our results and the crystal structure determinations may be explained by the possibility of the masking of a weak band by a strong band or by two bands being accidentally degenerate. This is indeed supported by the spectra of the vanadium and cobalt complexes where six bands

Table 3.11

Frequency data (cm^{-1}) and assignments for the $[M(ox)_3]$ complexes[a].

Sc	V	Cr	Mn	Fe	Co	Ga	Assignment
646	638	639	639(10)	643	655	649	γ ring
					644		
			626(14)	625			lig.[b]
614	618		613(12)	616			ν ring
590	590	590		595	591	593	γ ring
561	563	571	574(22)	569		575	γ ring
516	531	529	532(18)	523	532	525	αC-O
			515(14)				
507						513	γ ring
493	500		502	495	509	502	ν ring
455	468	466	465(26)	466	457		γ ring
441	442	446	436(34)	439	443	444	
382	402	406	410(25)	399	421	406	chelate
			401(30)	392	411		ring def.
376	373		385(15)			390	lig.[b]
						374	
322	352	360	339(4)	311	388	301	νM-O
	316						νV-O
260	293	330	325(4)	279	376	290	νM-O
					356		νCo-O
	273						νV-N
223	241	278	285(21)	257	334	242	νM-N
			271				

Table 3.11 continued/

Sc	V	Cr	Mn	Fe	Co	Ga	Assignment
					268		νCo-N
203	208	214	234(5) 202(4)	207	231	211	νM-N
194	196	184	190(13)	187	197	189	γ ring
138	143	151	166[c]	156	167	167 161	δL-M-L
119	135	120	141[c]	135	134	143	δL-M-L
98	108	100	116[c]	113	92	85	Lattice

[a]Values given in parentheses are shifts to lower frequencies induced by deuteration of the ligand.

[b]lig. = ligand vibration.

[c]Below ∿170 cm^{-1}, the IR spectrum of the manganese deuterated complex is too poor for accurate shifts to be determined.

in the region 390 - 200 cm^{-1} can be assigned to νM-L.

The appearance of extra bands in the spectrum of the Mn(III) complex is symptomatic of Jahn-Teller distortion expected on theoretical grounds for a high-spin d^4 system. Distortion of this complex has been verified by the crystal structure determination [19] which reveals two significantly different Mn-N distances of 2.056 Å and 2.248 Å. Only a minor difference in the Mn-O bond lengths was observed (mean Mn-O bond distance 1.915 Å). Previous work in this laboratory has shown that IR spectroscopy can be used as a sensitive probe for detecting small differences in bond lengths caused by Jahn-Teller distortion [48]. We may therefore expect significant splitting of νMn-N, but minor splitting of νMn-O. This is reflected in Table 3.11 and Fig. 3.7 where the expected splitting of νMn-N is observed for the Mn(III) complex.

It was extremely difficult to study the effects of deuteration on the spectra of the Mn(III) complex because of the small quantity of deuterated ligand which was available for its preparation. The far-IR spectrum was extremely poor in the region 150 - 50 cm^{-1}. Below 500 cm^{-1}, bands sensitive to deuteration were found at 410 ($\Delta\nu$ = 25), 401 ($\Delta\nu$ = 30), 339 ($\Delta\nu$ = 4), 325 ($\Delta\nu$ = 4), 285 ($\Delta\nu$ = 21), 234 ($\Delta\nu$ = 5), 202 ($\Delta\nu$ = 4) and 190 ($\Delta\nu$ = 13) cm^{-1}. In agreement with our results for the divalent metal chelates, we assigned the bands at 410 and 401 cm^{-1} to chelate ring deformation modes. The bands at 339 and 325 cm^{-1} were assigned to νMn-O and those at 285, 271, 234 and 202 cm^{-1} to νMn-N bands. The

remaining band at 190 cm^{-1} is probably a γ ring ligand band. The metal-ligand bands have been found to be significantly less deuteration-sensitive ($\Delta\nu$ < 10 cm^{-1}) than the ligand bands ($\Delta\nu$ > 10 cm^{-1}).

The cobalt(III) complex is unique amongst the metal(III) oxinates due to its low-spin configuration (Table 3.7). This implies a particularly high CFSE which is undoubtedly responsible for the big shift in νM-L which occurs on replacing Fe(III) by Co(III).

We have established above that metal-sensitive bands (νM-O and νM-N) show a correlation with d-orbital population, which is consistent with the relative CFSEs of the metal ions. A knowledge of the spin states, especially for the chelates with d^4 to d^7 configurations, is necessary for calculating the CFSEs. Table 3.7 indicates that the Mn(III) and Fe(III) chelates are high-spin, whereas the cobalt chelate, in common with the large majority of Co(III) chelates, is spin-paired. Hence the CFSEs of these metals can be calculated from

$$CFSE = -(0.4n_{t_{2g}} - 0.6n_{e_g})fg$$

The pairing energy of the cobalt complex is ignored in this calculation, as it does not upset the CFSE order.

It is interesting to note that if νM-L is plotted against $3d$-orbital population of the metal ion (Fig. 3.8), the interpolation line joining the points of Sc(III) ($3d^0$) and Ga(III) ($3d^{10}$) passes through the point for Fe(III) ($3d^5$) for three

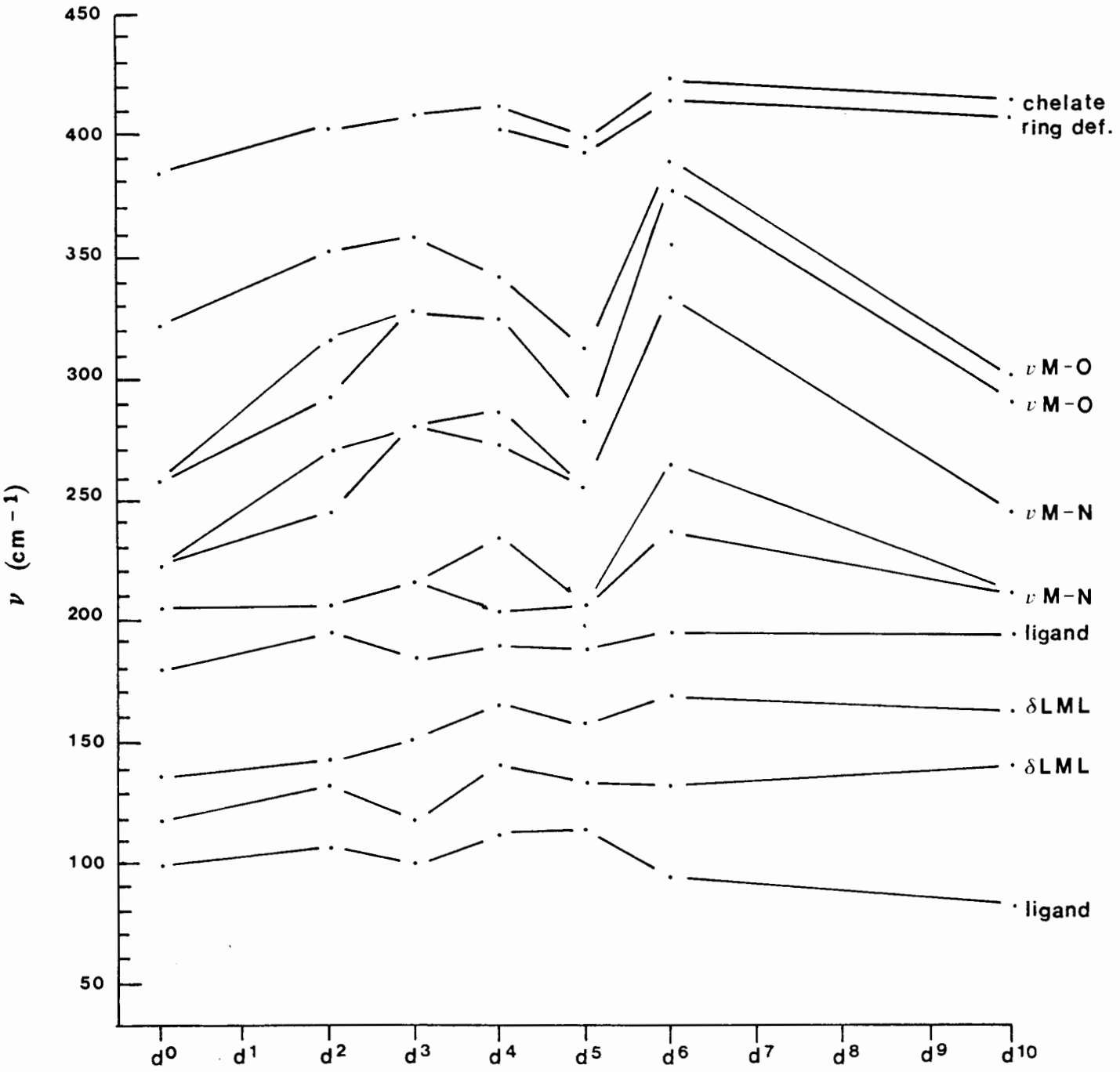

Fig. 3.8 Metal-sensitive bands of the first transition metal(III) oxinate complexes.

of the four metal-ligand bands. This interpolation line represents the frequencies realized for the complexes which are not stabilized by the crystal field (CFSE = 0). For the remaining chelates, the CFSE effect is superimposed on effects such as the increase in ionic mass and decrease in ionic radius across the transition series. If the observed frequencies are designated ν and the interpolated 'CFSE-free' frequencies ν_o, then $(\nu - \nu_o)$ represents a direct measure of the crystal field contribution to νM-L in spectroscopic terms. Such graphically determined values are given in Table 3.12. The values of $(\nu - \nu_o)$ are almost invariably in the order Sc < V < Cr > Mn < Fe < Co > Ga which is in the same order as the CFSEs of the complexes (the CFSE values in Table 3.12 have been calculated (in units of f) from the g values of the metal ions given by Figgis [51]). The particularly high value of $(\nu - \nu_o)$ for the cobalt complex originates in the spin-paired nature of this chelate.

3.4.6 *The IR spectra of the complexes, $[M(ox)_3]$ (M = Rh, In) from 700 to 50 cm^{-1}*

We had originally hoped to compare the spectra of the oxinate complexes of the second transition series trivalent ions of Y(III) ($4d^0$), Ru(III) ($4d^5$), Rh(III) ($4d^6$) and In(III) ($4d^{10}$) with their first transition series analogues, since the effect of changing the spin state from high-spin (as in Fe(III)) to low-spin (as in Ru(III)) can be of considerable assistance in assigning metal-ligand bands. However, only the rhodium and indium chelates could be successfully prepared.

Table 3.12

CFSE data for the metal(III) oxinates, $[M(ox)_3]$.

M	Config.	g	-CFSE		$(\nu-\nu_o)$ cm^{-1}			
		kK	Dq	f	νM-O	νM-O	νM-N	νM-N
Sc	$3d^0$	-	0	-	0	0	0	0
V	$3d^2$	18.6	8	14.9	34	29	16	4
Cr	$3d^3$	17.0	12	20.4	50	60	51	8
Mn	$3d^4$	21.0	6[a]	12.6[a]	24	54	48[b]	12[c]
Fe	$3d^5$	14.0	0	-	0	0	0	0
Co	$3d^6$	19.0	24[d]	5.6[d]	78	96	102	22
Ga	$3d^{10}$	-	0	-	0	0	0	0

[a] Omitting extra stabilization due to Jahn-Teller effect.

[b] Mean of doublet : 285 and 271 cm^{-1}.

[c] Mean of doublet : 234 and 202 cm^{-1}.

[d] Excluding the pairing energy.

It was noted in the previous section that the Co(III) complex has a low-spin configuration. The high values of νM-L for this chelate are associated with this configuration, all the other ions of the trivalent complexes being high-spin. Two factors account for the low-spin states of Rh(III). \ Firstly, $10Dq$ in the complexes of second transition series ions is known to be about 50% higher than in those of the analogous first transition series ions [52]. Jørgensen [53] reports the ratio

$$\frac{10Dq \text{ (Second Period)}}{10Dq \text{ (First Period)}} = 1.54.$$

The second factor is the much lower spin pairing energies of the second transition series ions compared with their first transition series analogues [52]. The order for the CFSE of low-spin trivalent ions is $d^0 < d^1 < d^2 < d^3 < d^4 < d^5 < d^6 > d^{10}$ [54].

The vibrational spectra of the second transition series trivalent metal oxinates are represented in Fig. 3.7 and the band assignments given in Table 3.13. Comparison of the IR data for the isoelectronic $3d^6$ and $4d^6$ complexes (Co(III) and Rh(III), respectively) show that where there is no change in spin state, the change in νM-L is small. Similarly, the values of νM-L for the Ga(III) and In(III) complexes, where the crystal field stabilization is zero, are similar. If the ruthenium complex could have been prepared, one would have expected a significant increase in νM-L when the electron

configuration changed from high-spin in $3d^5$ [$Fe(ox)_3$] to low-spin in $4d^5$ [$Ru(ox)_3$]. Secondly, the νM-L bands for the Ru(III) and Rh(III) chelates would be of comparable frequencies since both these chelates have low-spin configurations.

Table 3.13

Frequencies (cm^{-1}) and band assignments for the second transition series trivalent metal oxinates from 700 to 50 cm^{-1}

Rh	In	Assignment
648	642	γ ring
	617	ν ring
593	591	γ ring
584		
	566	γ ring
525	516	αC-O
504		γ ring
	492	ν ring
473	470	γ ring
	437	
413	395	chelate ring deformation
348	275	νM-O
335	248(sh)[a]	
321	241	νM-N
274	202	
252		νRh-N
218		lig.[a]
199		γ ring
186		
162	144	δL-M-L
112	106	δL-M-L
65	79	Lattice
	66	

[a] sh = shoulder lig. = ligand vibration.

REFERENCES

1. R.C. Elderfield, *Heterocyclic Compounds* [Wiley, Chapman and Hall] New York and London 4 (1952) 146.

2. R.G.W. Hollingshead, *Oxine and Its Derivatives* [Butterworths] London Volumes I to IV (1954).

3. K.G. Stone, *J. Amer. Chem. Soc.*, 76 (1954) 4997.

4. R.G. Charles, H. Freiser, R. Friedel, L.E. Hilliard and W.D. Johnston, *Spectrochim. Acta*, 8 (1956) 1.

5. J.P. Phillips and J.F. Deye, *Anal. Chem. Acta*, 17 (1957) 231.

6. R.J. Magee and L. Gordon, *Talanta*, 10 (1963) 851.

7. R.J. Magee and L. Gordon, *Talanta*, 10 (1963) 961.

8. R.J. Magee and L. Gordon, *Talanta*, 10 (1963) 967.

9. J.E. Tackett and D.T. Sawyer, *Inorg. Chem.*, 3 (1964) 962.

10. R. Larsson and O. Eskilsson, *Acta Chem. Scand.*, 22 (1968) 1067.

11. A. Kulkarni and A.J. Mudhedkar, *Poona University Journal of Science and Technology*, 36 (1969) 21.

12. N. Ohkaku and K. Nakamoto, *Inorg. Chem.*, 10 (1971) 798.

13. L.L. Merritt, *Anal. Chem.*, 25 (1953) 718.

14. G.J. Palenik, *Acta Cryst.*, 17 (1964) 696.

15. L.L. Merritt, R.T. Cady and B.W. Mundy, *Acta Cryst.*, 7 (1954) 473.

16. R.C. Hoy and R.H. Morriss, *Acta Cryst.*, 22 (1967) 476.

17. G.J. Palenik, *Acta Cryst.*, 17 (1964) 687.

18. K. Folting, M.M. Cox, J.W. Moore and L.L. Merritt, *Chem. Communs.*, (1968) 1170.

19. R. Hems and M.F. Mackay, *J. Cryst. Mol. Structure*, 5 (1975) 227.

20. M. Bartlett and G.J. Palenik, *Chem. Communs.*, 7 (1970) 416.

21. M.M. Ray, J.N. Adhya, D. Biswas and S.N. Poddar, *Aust. J. Chem.*, 19 (1966) 1737.

22. B.C. Baker and D.T. Sawyer, *Anal. Chem.*, 40 (1968) 1945.

23. G.E. Jackson and L.G. Scott, *S. Afr. J. Chem.*, 36 (1983) 120.

24. A.E. Jenkins, J.R. Majer and M.J.A. Reade, *Talanta*, 14 (1967) 1213.

25. J.R. Majer, M.J.A. Reade and W.I. Stephen, *Talanta*, 15 (1968) 373.

26. I. Ichishima, *J. Chem. Soc.*, (1950) 442.

27. K.K. Deb, *Indian J. Phys.*, 35 (1961) 535.

28. R. Ammini Amma, K.P.R. Nair and S.N. Singh, *Indian J. Pure Appl. Phys.*, 7 (1969) 7.

29. K. Jatkar, *Indian J. Phys.*, 10 (1937) 23.

30. M.A. Shashidkar, *Indian J. Pure Appl. Phys.*, 8 (1970) 762.

31. A.R. Katritzky and R. Alan-Jones, *J. Chem. Soc.*, (1960) 2942.

32. S.N. Sharma, R.B. Gupta and P.L. Gupta, *Acta Ciencia Indica*, 6 (1980) 58.

33. S.L. Srivastava, M. Prasad and Rohitashava, *Spectrochim. Acta*, 40A (1984) 681.

34. B. Marchon, L. Bokobza and G. Cote, *Spectrochim. Acta*, 42A (1986) 537.

35. H. Irving and R.J.P. Williams, *J. Chem. Soc.*, (1953) 3192.

36. J.C. Fanning and H.B. Jonassen, *J. Inorg. Nucl. Chem.*, 25 (1963) 29.

37. C. Mande and A.R. Chetal, *Curr. Sci.*, 23 (1964) 707.

38. A. Vogel, *A Textbook of Practical Organic Chemistry*, 3rd edition [Longman] London and New York (1967) p. 870.

39. S. Lenzer, *J. Chem. Soc.*, Suppl. 1 (1964) 5768.

40. E. Bayer, H.J. Bielig and K.H. Hausser, *Ann. Chem.*, 584 (1953) 116.

41. F.B. Taylor and T.A. Wilkins, *J. Chem. Soc. Dalton Trans.*, 6 (1973) 87.

42. G.M. Watkins, *Ph.D. Thesis*, University of Cape Town (1988).

43. M.L. Niven, *Ph.D. Thesis*, University of Cape Town (1980).

44. G.S. Shephard, *Ph.D. Thesis*, University of Cape Town (1973).

45. F. Basolo and W.R. Matoush, *J. Amer. Chem. Soc.*, 75 (1953) 5663.

46. A.R. Burns, T.J. Cardwell and R.W. Cattrall, *Aust. J. Chem.*, 24 (1971) 661.

47. J.L. Wood and M.M. Jones, *J. Phys. Chem.*, 67 (1963) 1049.

48. D.A. Thornton, *Coord. Chem. Rev.*, 55 (1984) 113.

49. L.G. Hulett and D.A. Thornton, *Spectrochim. Acta*, 29A (1973) 757.

50. F.A. Cotton and R.C. Elder, *Inorg. Chem.*, 4 (1965) 1145.

51. B.N. Figgis, *Introduction to Ligand Fields* [Interscience] New York (1966).

52. P. George and D.S. McClure, *Progr. Inorg. Chem.*, 1 (1959) 381.

53. C.K. Jørgensen, *Absorption Spectra and Chemical Bonding in Complexes* [Pergamon] London (1962).

54. R.D. Hancock and D.A. Thornton, *J. Mol. Structure*, 6 (1970) 441.

Chapter Four

CHAPTER FOUR

4 INFRARED STUDIES OF THE METAL(II) COMPLEXES OF 8-AMINOQUINOLINE : BAND ASSIGNMENTS AND STRUCTURAL ASPECTS OF THE SPECTRA

4.1 INTRODUCTION

8-Aminoquinoline or 8-quinolylamine is a chelating agent which is a structural composite of pyridine and aniline in that coordination to a metal ion can occur through a heterocyclic nitrogen atom and an amino group. Undoubtedly, the initial interest in this ligand came from its association with these more common ligands. Stable five-membered chelate rings are formed with many metal cations.

There is considerable compositional and structural diversity amongst the metal(II) complexes formed by 8-aminoquinoline. Species formulated $[M(aq)_3]^{2+}$, $[M(aq)_2]^{2+}$, $M(aq)_2(H_2O)_2X_2$ and $[M(aq)X_2]$ where X = Cl^- or Br^- have been described [1-10]. None of these chelates has received crystallographic attention and conductance measurements are difficult because the majority of the chelates are insoluble in water or organic solvents [1-3]. This study shows that infrared spectroscopy can be of considerable assistance in elucidating the molecular structures of these complexes.

To date, no vibrational assignments of the fundamental frequencies of this ligand have been reported in the literature. Only limited attention has been given to the IR spectra of the 8-aminoquinoline chelates [2-9] as compared with metal(II)

complexes of quinoline and aniline. As may be expected, the spectra of these complexes are relatively rich in bands, many of which originate in the internal vibrations of the amino group. Early reports [2,4] have been restricted to tentative assignments for these ligand vibrations by comparison with known vibrational assignments for aniline [11]. Coakley [5] and Jensen and Nielsen [6] attempted to assign the internal vibrations of the amino group by deuteration. Deuteration of the amino group involved refluxing the ligand in acidified D_2O for 2.5 hr, but only partial D/H exchange was achieved.

The assignments of the metal-ligand stretching frequencies have been sketchy [4, 7-9], and there has been no application of far-IR spectroscopy to the structure and bonding of 8-aminoquinoline chelates. Casabó and colleagues [4] studied a series of complexes of general formula $[M(aq)_2(NCS)_2]$ (M = Cu, Zn) and $[M(aq)_3]I_2$ (M = Ni, Zn) and reported the metal-amine stretching frequencies to be in the narrow region 510 - 495 cm^{-1}. Izquierdo and coworkers [7,8] have reported the synthesis of several nickel and copper chelates with derivatives of 8-aminoquinoline, *viz.*, 5,7-dibromo-, 5,7-dichloro- and 5,7-diiodo-8-aminoquinoline (dbaq, dcaq and diaq, respectively). The complexes prepared were of the type NiL_2X_2 (L = dbaq; X = Cl^-, Br^-, I^- and NCS^-), $NiLX_2 \cdot H_2O$ (L = dbaq, dcaq and diaq; X = Cl^-) and $CuLX_2$ (L = dbaq, dcaq and diaq; X = Cl^-, Br^-, I^- and SCN^-). On the basis of electronic spectral and magnetic moment measurements, a monomeric octahedral structure was proposed for the chelates NiL_2X_2 and a polymeric structure with bridging halogens for

the complexes $NiLX_2 \cdot H_2O$. The electronic spectra of the copper chelates were similar to those of their ethylenediamine and bipyridyl analogues and hence a polymeric structure with bridging and terminal halogen atoms was proposed for these complexes. Copper-halogen stretching frequencies corresponding to terminal and bridging halogens were observed in the regions 300 - 290 cm^{-1} and 260 - 250 cm^{-1}, respectively. The metal-amine stretching vibrations in both the nickel and copper complexes were assigned in the region 600 - 500 cm^{-1}. Durig and coworkers [9] prepared a palladium complex $[Pd(aq)Cl_2]$. In agreement with the symmetry requirements for square-planar *cis*-configuration (C_{2v}), two palladium-amine bands were found in the range 530 - 505 cm^{-1}, and two palladium-chlorine bands were assigned in the region 340 - 330 cm^{-1}.

There has been no conclusive evidence in the literature as to whether water molecules or halogen ions complete the octahedral stereochemistry in the chelates $M(aq)_2X_2(H_2O)_2$ (X = halogen). Nast and colleagues [3] have described the preparation of two *bis*(8-aminoquinoline)cobalt(II) complexes formulated as $[Co(aq)_2X_2]$ ($X = Cl^-, NO_3^-$). On the basis of magnetic moments and conductance measurements, a *trans,trans,trans*-octahedral structure was proposed for these complexes. This, however, is contrary to Nielsen and Dahl [10]. From ultraviolet absorption results, these workers suggested that water molecules occupy the axial positions about the nickel atom in the complex $Ni(aq)_2(H_2O)_2X_2$.

From the above literature survey, it can be seen that there has been no systematic study of the IR spectra of the *mono*, *bis* and *tris*(8-aminoquinoline) complexes of the first transition metal(II) ions. There is also controversy as to the structure of the chelates $M(aq)_2(H_2O)_2X_2$ ($X = Cl^-, Br^-$). Moreover, no definite assignments of the metal-nitrogen stretching frequencies have been published for any of the 8-aminoquinoline chelates. This work therefore represents the first study of the IR spectra of a series of complexes $[M(aq)_3](ClO_4)_2$ (M = Fe, Co, Ni); $M(aq)_2(H_2O)_2Cl_2$ (M = Fe, Co, Ni, Cu); $M(aq)_2(H_2O)_2Br_2$ (M = Co, Ni, Cu) and $[M(aq)X_2]$ (M = Cu, Zn; X = Cl, Br). The objective of this study is to assign the metal-ligand stretching frequencies and hence to establish the structures of the above complexes. Since an empirical approach to the assignment problem would be subject to conjecture in view of the presence of two metal-nitrogen bonds (distinguished in this study as $\nu M\text{-}NH_2$ and $\nu M\text{-}N(py)$), we have approached this problem by deuteration of the amino group in some of the chelates. The effects of metal ion substitution in relation to the structures of the complexes have also been discussed. These results facilitate a more definite assignment of the metal-ligand stretching frequencies. In addition, the internal vibrations of the amino group in the mid-IR region can be more firmly assigned.

4.2 PREPARATION OF COMPLEXES

4.2.1 *General*

All the iron and cobalt complexes in this section were

prepared and isolated using Schlenk tube techniques and stored under nitrogen. The isotopically-labelled substances used in this study, together with their isotopic purities and commercial sources, are given in Table 4.1.

Table 4.1

Isotopically-labelled substance	Isotopic purity (atom %)	Commercial source
EtOD	99.8	Aldrich Chemical Company, Inc.
D_2O	99.7	Merck, Sharp & Dohme (Canada) Ltd.[a]
MeOD	99.0	Merck, Sharp & Dohme (Canada) Ltd.[a]
$^{18}OH_2$	90.0	Alfa Inorganics, Inc

[a]Now Merck-Frosst Ltd.

4.2.2 *Preparation of 8-aminoquinoline-d_2*

Partial deuteration of 8-aminoquinoline was accomplished by refluxing the ligand for 3 hr in EtOD. The solution was cooled to room temperature and the solvent removed under vacuum. The process was repeated twice in order to successively deuterate the amino group. The deuterated ligand was stored over silica gel under reduced pressure to prevent H/D exchange. The 8-aminoquinoline-d_2 prepared in this manner was used in the preparation of all the deuterated ligand complexes. These complexes were all prepared and

isolated using Schlenk tube techniques and stored under nitrogen in order to prevent H/D exchange.

4.2.3 *Preparation of the complexes* $[M(aq)_3](ClO_4)_2 \cdot xH_2O$ *(M = Fe, x = 0.5; M = Co, x = 2; M = Ni, x = 1)*

Only the cobalt complex has previously been prepared [3]. The iron and nickel chelates were made by an adaptation of this method. In general, an ethanolic solution of the appropriate hydrated metal perchlorate was added dropwise to an ethanolic solution of the ligand in a molar ratio 1 : 3.5. This resulted in the formation of a precipitate. After 5 min, the complex was filtered, washed with ethanol and dried over silica gel overnight under reduced pressure. The nickel complex was subsequently found to be hygroscopic and was therefore stored in a desiccator. The analogous copper and zinc chelates could not be prepared by this route, even if a sixfold excess of ligand was used.

4.2.4 *Preparation of the complexes* $M(aq)_2(H_2O)_2X_2$ *(M = Fe, Co, Ni, Cu; X =* Cl^- *and M = Co, Ni, Cu; X =* Br^-*)*

The cobalt, nickel and copper compounds were prepared from the corresponding metal halide by previously reported methods [1,2]. The iron complex was synthesized by the addition of an aqueous solution of hydrated ferrous halide to an ethanolic solution of 8-aminoquinoline in a 1 : 2.5 molar ratio. This resulted in the formation of a red precipitate which was stirred for 0.5 hr, filtered, well washed with ethanol and dried over silica gel overnight under

reduced pressure. The corresponding iron bromide complex could not be successfully prepared.

The deuterated 8-aminoquinoline nickel and copper chelates were prepared in an identical manner to the unlabelled complex, except that EtOD and D_2O were used instead of EtOH and H_2O. The complex $Ni(aq)_2(^{18}OH_2)_2Br_2$ was prepared in a similar manner to the unlabelled chelate, except that $^{18}OH_2$ was used instead of H_2O.

4.2.5 *Preparation of the complexes* $[M(aq)X_2]$ *(M = Cu, Zn; X =* Cl^-, Br^-*).*

The chloro complexes were prepared from the appropriate metal chloride by previously reported methods [5,10]. The bromo complexes were prepared as follows:

A methanolic solution of 8-aminoquinoline was added to an aqueous solution of the anhydrous metal bromide in a 1 : 1 molar ratio. A precipitate, which formed after a few minutes, was stirred for 0.5 hr, filtered, well washed with methanol and dried over silica gel overnight under reduced pressure.

The deuterated 8-aminoquinoline zinc chelate was similarly prepared using the appropriate deuterated solvents.

4.3 ANALYSES OF COMPOUNDS

Table 4.2

Analytical data for the metal(II) 8-aminoquinoline chelates.

Complex	Calculated			Found		
	%C	%H	%N	%C	%H	%N
$[Fe(aq)_3](ClO_4)_2$ [a]	46.58	3.62	12.07	46.70	3.80	12.20
$[Co(aq)_3](ClO_4)_2$ [b]	44.65	3.89	11.57	44.90	3.95	11.35
$[Ni(aq)_3](ClO_4)_2$ [c]	45.80	3.70	11.87	45.40	3.70	11.65
$[Ni(aq\text{-}d_2)_3](ClO_4)_2(D_2O)_2$	45.03	3.92	11.67	45.00	3.85	11.45
$Fe(aq)_2(H_2O)_2Cl_2$	47.92	4.47	12.42	47.60	4.47	12.30
$Co(aq)_2(H_2O)_2Cl_2$	47.59	4.43	12.33	47.40	4.25	12.20
$Ni(aq)_2(H_2O)_2Cl_2$	47.62	4.44	12.34	47.45	4.20	12.25
$Cu(aq)_2(H_2O)_2Cl_2$	47.12	4.39	12.21	47.05	4.25	12.15
$Cu(aq\text{-}d_2)_2(D_2O)_2Cl_2$	46.31	4.32	12.00	47.00	4.40	12.15
$Co(aq)_2(H_2O)_2Br_2$	39.80	3.71	10.31	39.80	3.80	10.30
$Ni(aq)_2(H_2O)_2Br_2$	39.82	3.71	10.32	39.80	3.60	10.30
$Ni(aq)_2(^{18}OH_2)_2Br_2$	39.46	3.68	10.23	39.50	3.80	10.10
$Ni(aq\text{-}d_2)_2(D_2O)_2Br_2$	39.24	3.65	10.17	39.50	3.80	10.10
$Cu(aq)_2(H_2O)_2Br_2$	39.47	3.68	10.23	39.60	3.65	10.10
$Cu(aq\text{-}d_2)_2(D_2O)_2Br_2$	38.07	3.55	9.87	38.30	3.40	9.75
$[Cu(aq)Cl_2]$	38.80	2.89	10.05	38.80	2.85	10.05
$[Zn(aq)Cl_2]$	38.54	2.88	9.99	38.85	3.00	9.80
$[Zn(aq\text{-}d_2)Cl_2]$	38.27	2.85	9.92	37.80	2.95	9.80
$[Cu(aq)Br_2]$	29.41	2.19	7.62	29.25	2.20	7.45
$[Zn(aq)Br_2]$	29.27	2.18	7.58	28.90	2.20	7.40

[a] Hemihydrate [b] Dihydrate [c] Monohydrate

4.4 RESULTS AND DISCUSSION

4.4.1 *General*

As mentioned in the Introduction (Section 4.1), studies of the 8-aminoquinoline system have been minimal and there has been no complete vibrational assignment of either the ligand or its metal complexes. This is undoubtedly due to the diversity of their composition and structure, the complexity of the IR spectra due to vibrational coupling and the difficulty and cost of applying reliable assignment techniques such as deuteration of the ring protons of the ligand. This work represents the first assignment of the metal-ligand stretching frequencies for the metal complexes based on isotopic labelling. It will be shown that deuteration of the amino group enables firm assignments for certain ligand and metal-ligand modes to be made. In the ensuing discussion, bands shifted by deuteration are termed *d*-sensitive, whilst the term M-sensitive has been used to describe those bands which shift on metal ion substitution.

4.4.2 *The IR spectrum of the ligand, 8-aminoquinoline, in the regions 3500 - 3000 and 1700 - 50 cm^{-1}.*

8-Aminoquinoline may be regarded as structurally similar to aniline and quinoline. Its spectrum may therefore, to a first approximation, be thought of as consisting of bands originating from the vibrations of aniline and quinoline. An initial attempt to assign the vibrations of 8-aminoquinoline was therefore made by examining the spectrum of the free ligand in conjunction with the spectra of aniline

and quinoline. It is, however, appreciated that the greater complexity of the spectrum of *mono*-substituted fused ring systems, such as 8-aminoquinoline, as compared with those of aniline and quinoline may complicate such an approach. Relatively comprehensive vibrational studies of aniline [11] and quinoline [12] have reported assignments for the ligand bands of these two molecules, making a comparison of this nature easier. A comparison of the fundamental frequencies and the assignments of aniline, quinoline, 8-aminoquinoline and 8-aminoquinoline-d_2 is given in Table 4.3.

Bands associated with the internal vibrations of the N-H group are expected and observed in the mid-IR region. In agreement with previous workers [4,6], the two N-H stretching frequencies are discernible in the region 3500 - 3000 cm^{-1}. Even after three successive attempts at deuteration of the ligand, very weak residual bands within this region indicated that D/H exchange was not quite complete. It is known that νN-H bands are so strong as to give residual absorption bands even at high levels of deuterium exchange. It was not possible to estimate the percentage deuteration from mass spectrometry because 8-aminoquinoline and its complexes decomposed within the ionization chamber of the mass spectrometer. The νN-D bands occurred, as expected, within the region 2590 - 2440 cm^{-1}. These bands are relatively pure, the observed shifts being approximately those calculated for isolated N-H(D) species from the ν^D/ν^H ratio = 0.73 [13].

In the 1700 - 1500 cm^{-1} region, 8-aminoquinoline exhibits

Table 4.3 A comparison of the fundamental frequencies and band assignments (3500 - 3000, 1700 - 50 cm^{-1}) of aniline, quinoline, 8-aminoquinoline and 8-aminoquinoline-d_2.

Aniline	Assignment [11]	Quinoline	Assignment [12]	8-Amino-quinoline	8-Amino-quinoline-d_2	Assignment	Previously reported frequencies and assignments for 8-aminoquinoline
3440	νN-H asym.			3450	2583	νN-H asym.	3440 νN-H sym. [4]; 3450 νN-H [5]
3360	νN-H sym.			3349	2445	νN-H sym.	3340 νN-H asym. [4]; 3345 νN-H [5]; 3340 νN-H [6]
1618	NH_2 scissor	1619	ν ring	1615	1610	ν ring + NH_2 scissor	1619 NH_2 scissor [6]
1600	ν ring	1593		1599	1573		
1586	ν ring			1590(sh)[a]	1588	ν ring	
		1571		1566	1152	ν ring + NH_2 scissor	
1500	ν ring	1500		1505	1502	ν ring	
1468	ν ring	1469	ν ring	1470	1469	ν ring	
		1431		1426	1424		
1382	comb. band[b]	1392		1394	1390	ν ring	
		1371		1368	1372		
1330	ν ring			1335	1336	ν ring	1336 νC-N [2]; 1330 νC-N [4]; 1339 νC-N [6]
1278	ν ring + νC-N			1279	1309	ν ring + νC-N	
		1256		1239	1234		
		1216	αC-H	1207	1204	αC-H	
1175	αC-H	1192		1183	1190		
1118	αC-H	1118		1125	1132	αC-H + τNH_2	
					1106		
		1095	αC-H	1094	1092	αC-H	
					1086		
1028	αC-H	1031	αC-H	1037	1030	αC-H	
		1013	ν ring	1021		ν ring	

Table 4.3 continued/

Aniline	Assignment [11]	Quinoline	Assignment [12]	8-Amino-quinoline	8-Amino-quinoline-d_2	Assignment	Previously reported frequencies and assignments for 8-aminoquinoline
984	$^{13}C^{12}C_5H_5 \cdot NH_2$	980		985	985		
970	γC-H	970	γC-H	962	962	γC-H	
960	γC-H	939		942	942		
880	γC-H			889	886	γC-H	
		867	γ ring	863	863	γ ring + ωNH$_2$	
					851		
832	γC-H			819	819	γC-H	
		786	γC-H	789	789	γC-H/ν ring	
		785	ν ring				
		760		760	759	ν ring	760 ρNH$_2$ [4]
761	γC-H	741	γC-H	751	748	γC-H	
691	γ ring			703	702	γ ring + ρNH$_2$	704 ρNH$_2$ [6]
					694		
618	γ ring	628	γ ring	641	641	γ ring	
				577	581	ρNH$_2$	
					568		
527	ρNH$_2$	521	ν ring	545	538	ν ring + ρNH$_2$	
501		(505)[c]		509	517		
490	2 x NH$_2$ torsion	479	γ ring	484	484	γ ring	
		415	γ ring	436	436(sh)[a]	γ ring	
390	γ ring	392		400	398		
					314		
				297			
				267	258	γC-N?	

Table 4.3 continued/

Aniline	Assignment [11]	Quinoline	Assignment [12]	8-Amino-quinoline	8-Amino-quinoline-d_2	Assignment	Previously reported frequencies and assignments for 8-aminoquinoline
		193	γ ring	186	185	γ ring	
		178		163	158		
				113	112	NH_2 torsion	
				77	77		
				68	68		

[a] sh = shoulder

[b] comb. band = combination band

[c] Estimated values only.

several bands attributable to coupled ν ring and NH_2 scissor vibrations. This is in accordance with Casabó and colleagues [4] and Jensen *et al.* [6]. The intense absorption at 1566 cm^{-1} is by far the most *d*-sensitive; the magnitude of the d_2-shift (∿414 cm^{-1}) is of the order expected for a NH_2 scissor vibration on the basis of the diatomic oscillator analogy. This band is therefore probably the most vibrationally pure NH_2 scissor vibration.

Previous workers [2,4,6] have assigned the band at about 1330 cm^{-1} to νC-N. We, however, assign this band to ν ring because (i) the band at 1330 cm^{-1} in aniline has been unambiguously assigned as ν ring and (ii) this band is *d*-insensitive. We have assigned the *d*-sensitive band at 1279 cm^{-1} to νC-N coupled, possibly, with ν ring. The unexpected upward shift of this vibration to 1309 cm^{-1} in 8-aminoquinoline-d_2 is in agreement with that found in aniline and aniline-d_2 [11]. The NH_2 twisting mode yields a *d*-sensitive band near 1125 cm^{-1}. The possibility of this band being coupled to an αC-H vibration cannot be ignored, since the band at 1118 cm^{-1} in quinoline is due to an αC-H vibration [12]. Similarly, the band at 863 cm^{-1} is assigned to NH_2 wag coupled with γ ring.

It is noteworthy that the band at 760 cm^{-1}, previously assigned to a NH_2 rocking mode [4], is *d*-insensitive. We have therefore assigned this band to ν ring. In agreement with Jensen *et al.* [6], we have assigned the *d*-sensitive band at 703 cm^{-1} to ρNH_2 coupled with a γ ring vibration. Several bands in the 500 cm^{-1} region were also significantly

d-sensitive and were attributed (at least in part) to ρNH_2 vibrations. The previously unassigned peak at 267 cm^{-1}, shifting 9 cm^{-1} towards lower frequency on deuteration, has been assigned to γC-N. This is supported by the assignment of γC-O in 8-hydroxyquinoline to a band at 266 cm^{-1} by Marchon *et al.* [14].

4.4.3 *The IR spectra of the tris(8-aminoquinoline) metal(II) perchlorates in the regions 3500 - 3000 and 1700 - 50 cm^{-1}*

4.4.3.1 *The regions 3500 - 3000 and 1700 - 500 cm^{-1}*

The IR spectra (1700 - 500 cm^{-1}) of the *tris* complexes are depicted in Fig. 4.1. The frequencies in the regions 3500 - 3000 and 1700 - 50 cm^{-1}, the frequencies induced by deuteration of the amino group in the complex $[Ni(aq\text{-}d_2)_3](ClO_4)_2 \cdot (D_2O)_2$, and assignments are reported in Table 4.4.

Ligand modes are observed at remarkably similar frequencies in all the complexes, in the ranges 3500 - 3000 and 1700 - 500 cm^{-1}. The nine vibrational degrees of freedom of the tetrahedral point group for the free perchlorate ion are distributed over the four fundamental vibrational modes: $A_1(\nu_1) + E(\nu_2) + 2T_2(\nu_3,\nu_4)$ [15]. The triply degenerate modes are IR-active, ν_3 occurring as a broad and intense peak near 1090 cm^{-1}, spanning $\sim$150 cm^{-1}. A number of ligand modes are partially or totally obscured by this band, and hence their assignment is somewhat tentative. The non-degenerate ν_1 band, theoretically

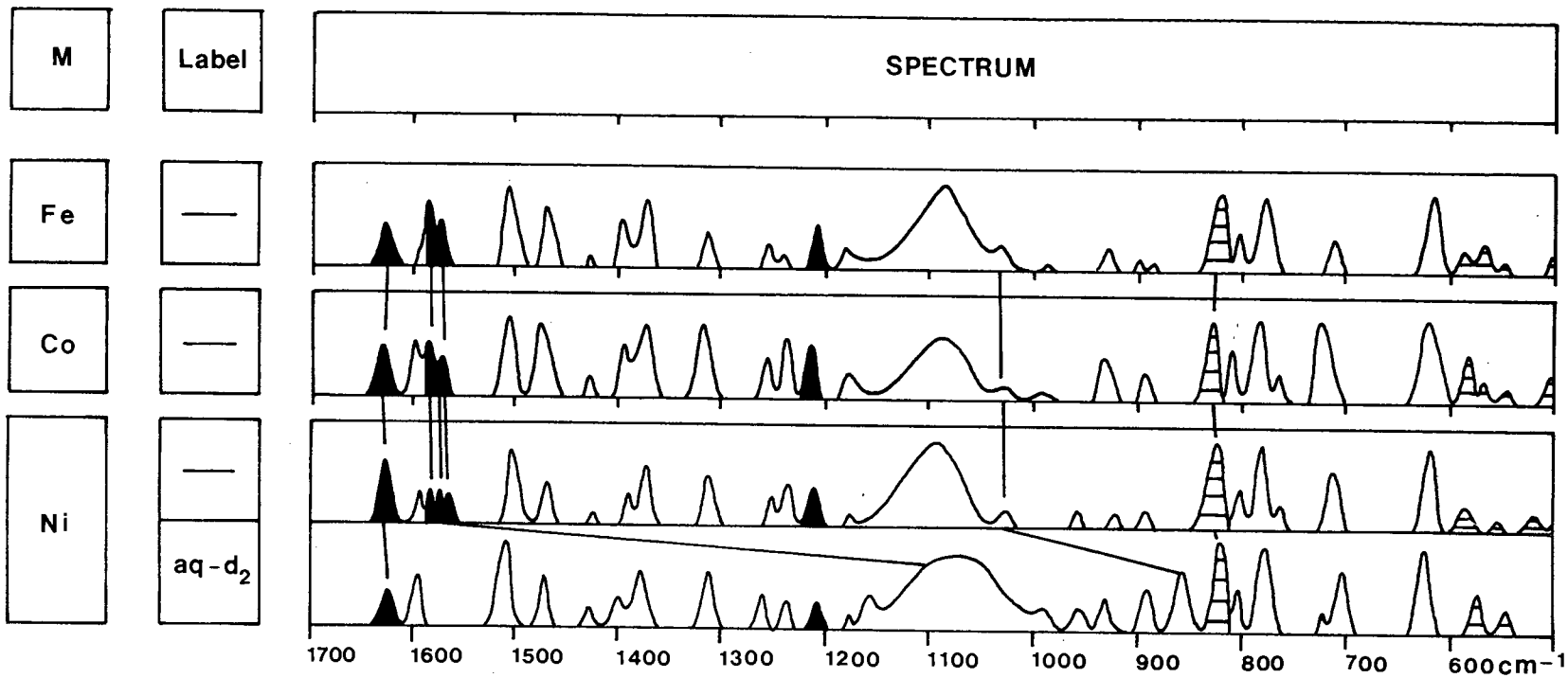

Fig. 4.1 IR spectra of the complexes $[M(aq)_3](ClO_4)_2$ from 1700 - 500 cm^{-1}. Solid linked bands: coupled NH_2 scissor; solid unlinked bands: coupled νC-N; linked bands: τNH_2; shaded linked bands: coupled ωNH_2; shaded unlinked bands: coupled ρNH_2.

Table 4.4

Frequencies and band assignments of the complexes $[M(aq)_3](ClO_4)_2$ (M = Fe, Co, Ni) in the regions 3500 - 3000 and 1700 - 50 cm^{-1}.

M: Label:	Fe[a]	Co[b]	Ni[c]	Ni aq-d_2	Assignment
	3260	3299	3299	2467, 2420	νN-H asym.
	3230	3244	3248	2388, 2335	νN-H sym.
	1626	1625	1627	1620	ν ring + NH_2 scissor
	1595(sh)[d]	1593	1594	1593	ν ring
	1582	1585	1586	1157	ν ring + NH_2 scissor
			1582		
	1565(sh)[d]	1569	1568	1093[e]	NH_2 scissor
	1505	1504	1506	1507	ring + C-H modes
	1470	1472	1472	1473	
	1426	1426	1426	1428	
	1396	1390	1392	1397	
	1374	1375	1375	1379	
	1314	1315	1316	1316	
	1257	1259	1259	1261	
	1239	1239	1239	1239	
	1209	1212	1214	1207	αC-H + νC-N
				1157	
	1179	1176	1177	1178	αC-H
	1091	1086	1091	1093[f]	ν_3 ClO_4
	1033	1028	1029	859	τNH_2
	986	989	989	989	γC-H
			959	959	
	928	930	930	930	ν_1 ClO_4
	901				γC-H
	892	892	894	890	γC-H

Table 4.4 continued/

M: Label:	Fe[a]	Co[b]	Ni[c]	Ni aq-d_2	Assignment
	825	826	826	821	γC-H + ωNH_2
	808	808	808	808	γC-H/ν ring
	779	782	782	777	ν ring + ωNH_2
		771	771	765(sh)[d]	γC-H
	715	715	717	718	γ ring + ρNH_2
				707	
	621	621	621	621	γ ring
	589	585	587	573	γ ring + ρNH_2
	567	570			
	550	553	560	546	ν ring + ρNH_2
	505(sh)[d]	510(sh)[d]	520	447	ρNH_2
	497	499	499	496	γ ring
	466	468	467	468	γ ring
	446				
	414	418	424	401	νM-NH_2
	345	369	381	370	νM-NH_2
	269	264	261	257	ligand
	235	229			
	196	198	209	203	νM-N(py)
	143(w)[d]	148(w)[d]	156(w,br)[d]	158(w,br)[d]	
	134	139			δL-M-L + lattice
	91				
	69	72	72	72	
	65	65	65		

[a]Hemihydrate [b]Monohydrate [c]Dihydrate

[d](sh) = shoulder (w,br) = weak, broad [e]Masked by ν_3 ClO_4

[f]Coupled with ND_2 scissor

IR-forbidden, occurs as a weak band near 930 cm^{-1}. This is due to relaxation of the tetrahedral symmetry criteria in a field of lower symmetry [16,17]. The ν_1 and ν_3 perchlorate bands are *d*-insensitive. Possible activation of ν_2 (near 460 cm^{-1}) and ν_4 (near 620 cm^{-1}) cannot be ruled out because of masking by 8-aminoquinoline bands which occur in these regions.

A comparison of the bands in the spectra of the complexes with those of the free ligand indicates that some of the ligand vibrations become IR-active on complexation. Bands occurring in the free ligand spectrum are generally shifted slightly toward higher frequencies in the complexes. The assignment of the N-H stretching and bending modes is assisted by NH_2 - deuteration of the Ni(II) complex (Table 4.4). The ND_2-shifts of the NH_2 stretching modes exceed 800 cm^{-1} as has been observed in aniline complexes [18-20]. The aromatic stretching modes are found near 1600 cm^{-1}. The principal NH_2 scissoring mode is observed near 1570 cm^{-1}, where it is distinguished from the ν ring modes by its significant sensitivity to deuteration ($\Delta\nu$ = 475 cm^{-1}). The νC-N band is observed at 1214 cm^{-1} ($\Delta\nu$ = 57 cm^{-1}) and the NH_2 twisting (τNH_2) at 1029 cm^{-1} ($\Delta\nu$ = 170 cm^{-1}) for the nickel chelate. The bands at 826 and 782 cm^{-1} are NH_2 wagging modes (ωNH_2), evidently coupled with ring modes in view of their relatively small sensitivities to deuteration. The variously coupled NH_2 rocking modes (ρNH_2) occur at 717, 587 and 560 cm^{-1}. The most vibrationally pure ρNH_2

band is at 520 cm^{-1} ($\Delta\nu$ = 73 cm^{-1}). No further discussion of this region is given, since it is only below 500 cm^{-1} that νM-L bands occur and subsequent structural information is expected to arise.

4.4.3.2 *The region 500 - 50 cm^{-1}.*

Since uncoordinated 8-aminoquinoline exhibits no fewer than eleven bands in this region, the possibility of vibrational coupling between ligand and metal-ligand bands cannot be overlooked. However, without IR spectral data for fully deuterated 8-aminoquinoline or its metal chelates, it is difficult to comment on any vibrational coupling which may occur. Furthermore, it is not possible to unambiguously assign the metal-ligand bending frequencies. The spectral region 500 - 50 cm^{-1} is represented in Fig. 4.2 and the frequencies and assignments are listed in Table 4.4.

Only the Co(II) complex of this series has previously received any IR attention. The IR spectrum above 600 cm^{-1} was reported, but no assignments were made [3]. The magnetic moment of this complex ($\mu_{eff.}$ = 5.10 B.M.) is typical of spin-free octahedral Co(II) chelates. The complexes $[M(aq)_3](ClO_4)_2$ are undoubtedly therefore octahedral monomers with either facial (C_3) or meridional (C_1) symmetry. The former configuration requires four νM-L and the latter six νM-L bands. Since we only observe four such bands, facial symmetry is proposed for these chelates.

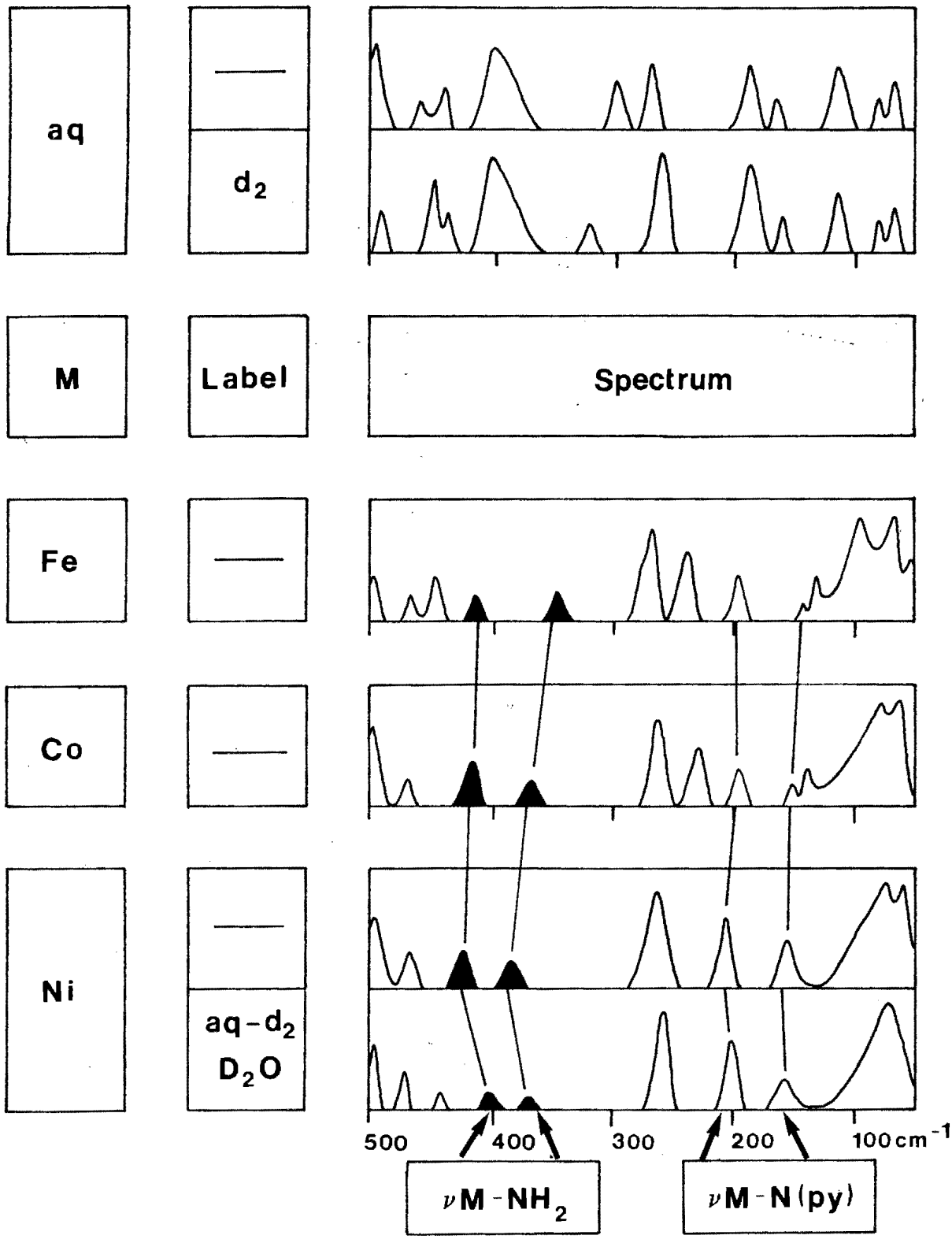

Fig. 4.2 Far-IR spectra of the complexes $[M(aq)_3](ClO_4)_2$ in the region 500 - 50 cm^{-1}.

There are five or six bands in the 430 - 140 cm^{-1} region where νM-L bands are expected to occur. Of these bands, two (near 420 and 380 cm^{-1}) are significantly sensitive to both metal ion substitution and ND_2-deuteration ($\Delta\nu$ = 23 and 11 cm^{-1}, respectively). The bands near 210 and 160 cm^{-1} are M-sensitive but relatively *d*-insensitive. On the basis of the shifts observed, it is clear that the bands near 420 and 380 cm^{-1} are $\nu M-NH_2$ bands, whilst those near 200 and 160 cm^{-1} are νM-N(py) bands. The remaining bands down to 50 cm^{-1} are L-M-L bends and lattice modes. The position of the νM-N(py) bands agree well with those observed for the complexes $[M(ox)_3]$ (Section 3.4.4). The ρNH_2, $\nu M-NH_2$ and νM-N(py) bands exhibit significant M-sensitivity and are in the sequence of their crystal field stabilization energies, *viz.*, Fe < Co < Ni. This feature further supports the proposed assignments and octahedral structures.

4.4.4 *The bis(8-aminoquinoline) complexes of the metal(II) halides: assignments and structural aspects of the spectra.*

4.4.4.1 *The regions 3500 - 3000 and 1700 - 500 cm^{-1}*

There has been some controversy as to whether these complexes are correctly formulated $[M(aq)_2(H_2O)_2]X_2$ or $[M(aq)_2X_2](H_2O)_2$. The IR spectral investigation undertaken in this work, represents an excellent method for determining whether the halides are coordinated or not. Fig. 4.3 depicts the IR spectra of these complexes in the region 1700 - 500 cm^{-1}. A comparison of the

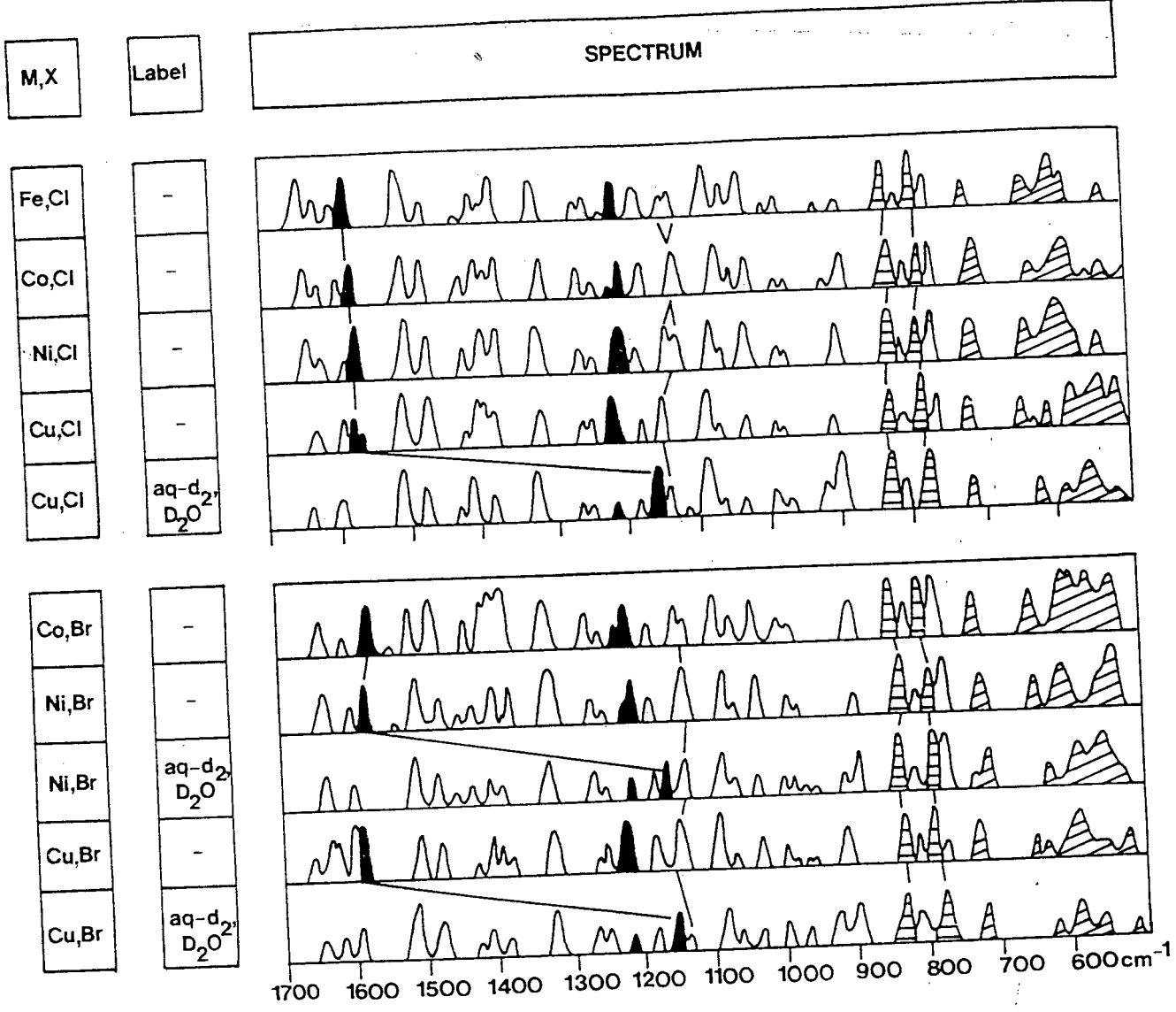

Fig. 4.3 IR spectra of the complexes $[M(aq)_2(H_2O)_2]X_2$ in the region 1700 - 500 cm^{-1}. Solid linked bands: NH_2 scissor; solid unlinked bands: coupled νC-N; linked bands: coupled τNH_2; shaded linked bands: coupled ωNH_2; shaded unlinked bands: coupled ρNH_2.

frequencies together with possible assignments is given in Table 4.5. Similarities in the band patterns of the spectra for both series of chelates indicate that the complexes are isostructural. Owing to the greater ligand field strength of water, the water molecules rather than halide ions are considered to be coordinated to the metal ion. A similar conclusion has been reached with the *N*-methyl-2-aminopyridine (a ligand which is similar in structure to 8-aminoquinoline) complex of NiI_2 [21]. The complex with coordinated water precipitated for solubility reasons.

Three of the complexes (M = Ni, X = Br; M = Cu, X = Cl, Br) were deuterated at the amino group in order to assign the NH_2 stretching and bending modes and to distinguish between the νM-NH_2 and νM-N(py) bands. Furthermore, ^{18}O-labelling of the complex with M = Ni and X = Br also assisted in the assignment of νO-H and δO-H.

The νO-H mode was readily assigned to the band near 3300 cm^{-1}. It is sensitive to both ^{18}O-labelling ($\Delta\nu$ = 7 cm^{-1}) and D_2O deuteration ($\Delta\nu \simeq 850$ cm^{-1}). The relative sharpness of this band is a clear indication that the water is actually coordinated to the metal and not present as lattice water. The O-H bend occurs at 1533 cm^{-1} in the nickel bromide chelate. The shifts on ^{18}O- and D_2O-labelling are 12 and 379 cm^{-1}, respectively.

Table 4.5 Frequencies and band assignments of the complexes $[M(aq)_2(H_2O)_2]X_2$ in the regions 3500 - 3000 and 1700 - 50 cm^{-1}

M = Fe	M = Co		M = Ni		M = Cu[b]		Assignment
X = Cl	X = Cl	X = Br	X = Cl	X = Br[a]	X = Cl	X = Br	
n.d.[c]	3295	3289	3305	3323(7;831,864)	3409(901)	3414(890)	νO-H
3202	3199	3197	3208	3197(0;802)	3109(768)	3146(787)	νN-H asym.
		3151		3152(0;787)			
3098	3104	3102	3100	3104(8;747)			
3078	3082	3078	3080	3078(0;709)	3062(803)	3051(787)	νN-H sym.
1646	1647		1651			1651(2)	
1623	1626	1632	1627	1633(0;0)	1630(+8)	1631	ν ring
						1621(5)	
1591	1592	1591	1593	1592(0;0)	1592(0)	1593(0)	
1576	1579	1573	1580	1574(0;420)	1577(425)	1581(427)	NH_2 scissor
					1569		
		1527		1533(12;379)			δO-H
1505	1504	1502	1505	1504(0;0)	1508(0)	1503(+6)	
1472	1474	1472	1474	1473(0;0)	1475(0)	1476(0)	
				1443(0;+4)			
1423	1424	1421	1424	1424(2;0)	1423(0)	1425(2)	
1397	1400	1401	1401	1401(sh)[c]	1405(+2)	1402(+5)	
					1400	1393	
1385	1389	1392	1400(sh)[c]	1395(0;+5)	1382(0)	1382(0)	ring + C-H modes
				1382(0)			
1376	1375	1373	1376	1374(0;0)			
1316	1318	1316	1320	1318(0;0)	1318(0)	1319(0)	
1260	1262	1258	1262	1258(0;0)	1257(+2)	1255(+4)	
1244	1245	1243	1245	1244(0;0)	1246(0)	1247(0)	

Table 4.5 continued/

M = Fe	M = Co		M = Ni		M = Cu[b]		Assignment
X = Cl	X = Cl	X = Br	X = Cl	X = Br[a]	X = Cl	X = Br	
1215	1216	1213	1216(sh)[c]	1215(sh)[c](0;+10)	1216(6)	1218(7)	νC-N + αC-H
1203	1207	1204	1209	1207(0;2)	1206	1209	
1174	1175	1174	1177	1175(0;+2)	1174(+4)	1176(+2)	αC-H
1131	1132	1130	1141	1133(0;3)	1145(8)	1153(15)	τNH$_2$ + αC-H
1125	1120(sh)[c]	1125	1133				
1076	1070	1078	1080	1078(0;0)	1084(4)	1085(5)	αC-H
1056	1059	1058	1062	1061(0;0)	1065(0)	1065(0)	
1028	1029	1028	1030	1030(0;+4)	1030(+3)	1030(+1)	
990	991	990	990	989(0;0)	989(0)	992(0)	γC-H
975	979	975	980	976(0;+2)	976(6)	979	
						958(+5)	
						952	
921	915						
894	898	897	900	899(0;2)	905(7)	906(7)	ωNH$_2$
829	829	828	829	827(0;4)	827(3)	828(0)	ωNH$_2$ + γC-H
807	808	807	808	808(0;0)	809(0)	810(0)	γC-H
789	788	787	788	786(3;8)	780(6)	782(7)	ωNH$_2$ + ν ring
775	775	771	775	771(0;0)	767(n.d.)[c]	772(n.d.)[c]	γC-H
718	718	718	719	718(0;+2,10)	723(9)	725(10)	ρNH$_2$ + γ ring
633	641	632	647	636(0;12)	643	647	
					628(9)	632(12)	
					608(26)	589(3)	ρNH$_2$
589	592	589	592	600(0;24)			
577		581	577	590(sh)[c](0)	575		ρNH$_2$ + γ ring
	557	556		560(sh)[c](0;13)			

Table 4.5 continued/

M = Fe	M = Co		M = Ni		M = Cu[b]		Assignment
X = Cl	X = Cl	X = Br	X = Cl	X = Br[a]	X = Cl	X = Br	
528	537	528	542	531(0;0)	539	546	ρNH_2
496	501	494	506	496(0;10)	494(3)		ρNH_2 + γ ring
464	470	465	463	470(0;0)	463(+2)	462(+2)	
					425(0)	427(0)	
419	428	425	433	431(0;15)			
370	381	381	390	390(0;9)	412(2)	408(4)	$\nu M-NH_2$
	314	322	315	324(0;0)			
266	272	267	285	284(0;0)	299(2)	297(0)	
216	235	231	252	249(0;0)	279(0)	271(0)	$\nu M-N(py)$
216	220	213	234	229(0;2)	183(5)	158(5)	
180	189	198	219	206(0;2)	169(2)	193(sh)[c]	$\nu M-OH_2$
160	175	175	191	185(0;10)	216(0)	211(0)	$\nu M-N(py)$
138	135	130	139	138(0;0)	154(0)	155(7)	
103	110	100(sh)[c]	115	117(+5;9)	96(0)	83(0)	$\delta L-M-L$
88	99	86	104	95(0;0)	96(0)	83(0)	
	77	62	81	69(0;0)	77(0)	74(4)	
55	55	-	-	55(0;0)	55(0)	69(0)	Lattice

[a] Values in parentheses are the shifts induced by ^{18}O-labelling, followed by the shifts induced by ND_2^- and D_2O-labelling of the complex $[Ni(aq)_2(H_2O)_2]Br_2$. Shifts $\leq$ 1 cm^{-1} are not reported.

[b] The value in parentheses is the shift induced by ND_2^- and D_2O-labelling of the complexes $[Cu(aq)_2(H_2O)_2]X_2$ ($X = Cl^-, Br^-$). Shifts $\leq$ 1 cm^{-1} are not reported.

[c] n.d. = not detected sh = shoulder.

Note: A shift preceded by a positive sign indicates a shift towards higher frequency.

The intense absorption at ∿ 1570 cm^{-1} clearly splits into two components in one of the chelates. Only the lower frequency component shows appreciable *d*- and M-sensitivity. This is consistent with the interpretation that coordination to a metal may restrict vibrational coupling. In addition, the magnitude of the ND_2-shift (∿414 cm^{-1}) is of the order expected for an NH_2 scissor vibration [13]. Band assignments for the remaining internal vibrations of the amino group in the mid-IR region were based on their M-sensitivity and the fact that deuteration of the amino group in the nickel bromide, copper chloride and copper bromide chelates shifts the bands towards lower frequencies by several wavenumbers.

4.4.4.2 *The region 500 - 50 cm^{-1}.*

In an investigation of the bonding of the ligands around the metal ions, it is the metal-ligand modes which are of the greatest interest. From symmetry considerations, the number of ν M-NH_2 bands is most likely the same as the number of ν M-N(py) bands in a given chelate. The assignment of the number of ν M-N(py) bands has therefore been based upon the more easily discernible ν M-NH_2 bands. Assignments have also been confirmed by the deuteration of the amino group in three of the chelates. Fig. 4.4 depicts the IR spectra of the complexes in the region 500 - 50 cm^{-1}. Fig. 4.5 is an actual tracing of the far-IR spectra of the nickel bromide complex and its deuterated analogue. Table 4.5 gives the list of the frequencies and band assignments. It is noteworthy that

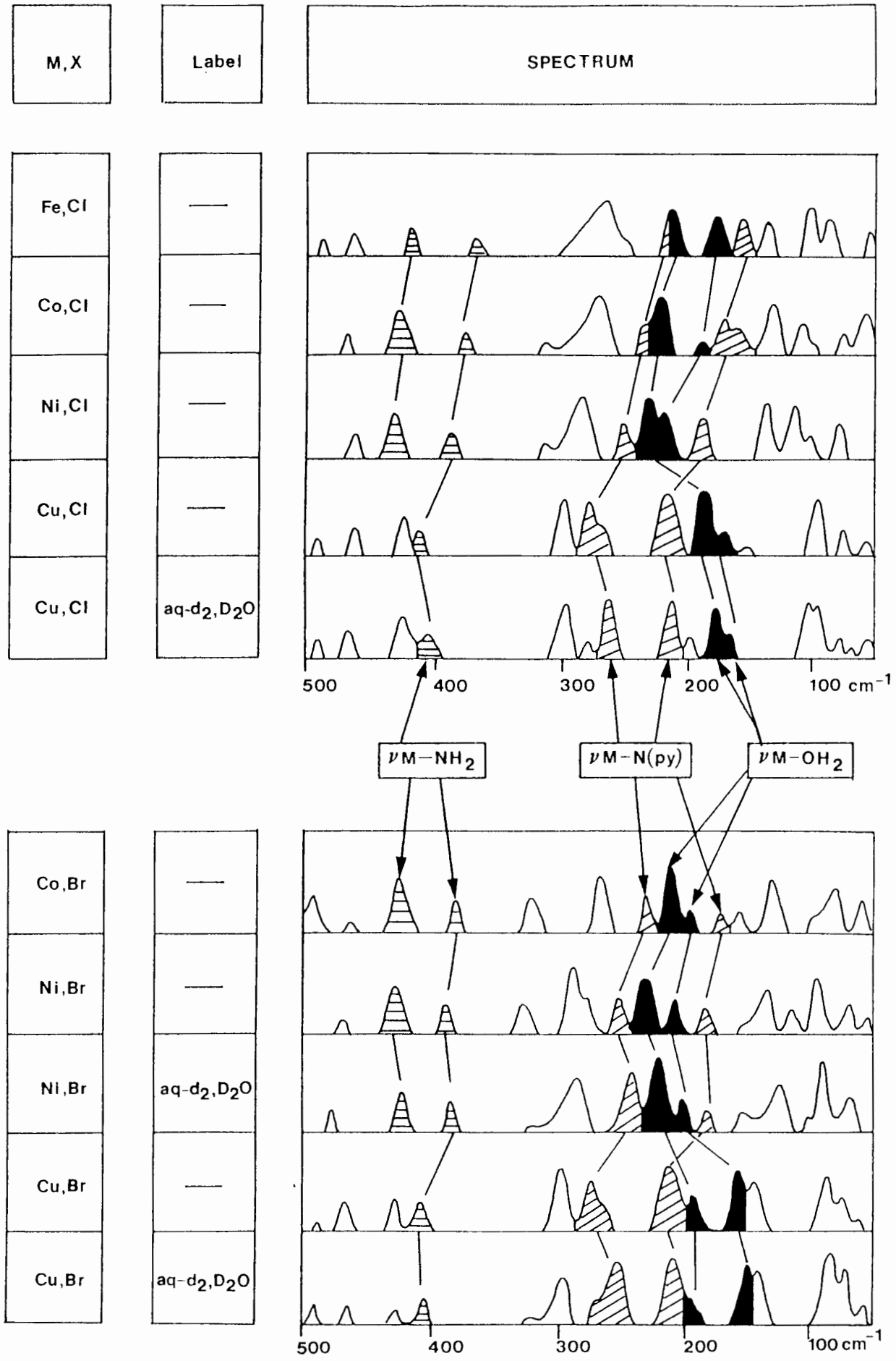

Fig. 4.4 IR spectra of the complexes $[M(aq)_2(H_2O)_2]X_2$ in the region 500 - 50 cm^{-1}

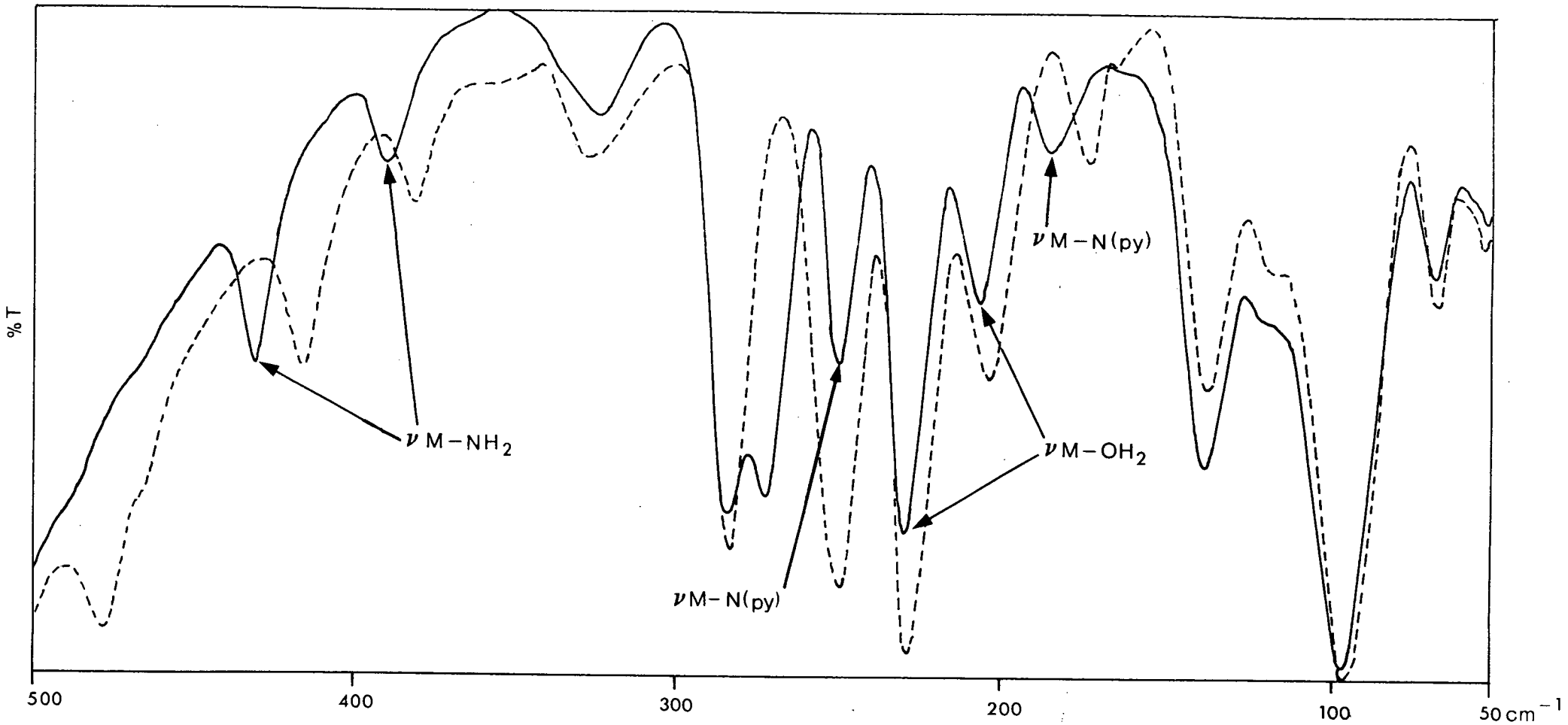

Fig. 4.5 IR spectra of $[Ni(aq)_2(H_2O)_2]Br_2$(——) and $[Ni(aq\text{-}d_2)_2(D_2O)_2]Br_2$(----) in the region 500 - 50 cm^{-1}.

there is no evidence of a strong νM-X band which would be significantly shifted by the substitution of Br for Cl. Hence, we may again conclude that the halides are outside the coordination sphere.

Deuteration of the amino group in the nickel bromide chelate shifts the bands at 430 and 390 cm^{-1} to lower frequencies, by 10 or more cm^{-1}. This implies that there are two $\nu M-NH_2$ bands. Furthermore, extending this result to the iron and cobalt chelates ($X = Cl^-$, Br^-) shows that these bands, exhibit a metal-sensitivity which mimics the change in CFSE. In the copper complexes there are two bands at approximately 420 and 410 cm^{-1} which could possibly be assigned to the corresponding $\nu Cu-NH_2$ modes. However, only the lower frequency component is significantly *d*-sensitive and thus only this band is firmly assigned to a $\nu Cu-NH_2$ mode.

The M-sensitive bands in the region 250 - 150 cm^{-1} are considered to arise from νM-N(py) and $\nu M-OH_2$ vibrations. The νM-N(py) bands are observed at 249 and 185 cm^{-1} in the nickel bromide chelate since these bands occur at similar frequencies in the $[M(ox)_2(H_2O)_2]$ complexes (Section 3.4.3). The bands at 229 and 206 cm^{-1} in the nickel bromide complex may be assigned to $\nu M-OH_2$ modes. Both bands are sensitive to metal ion substitution and D_2O deuteration ($\Delta\nu$ = 2 cm^{-1} for both bands). It is interesting to note that the νCu-N(py) bands in the chloro and bromo series of complexes are observed at nearly

30 cm^{-1} higher than the νNi-N(py) bands. Moreover, the νCu-OH_2 bands are observed at several wavenumbers lower than the νNi-OH_2 bands. This may be explained by the fact that the Cu(II) chelate, in common with the $[Cu(ox)_2(H_2O)_2]$ chelate, is tetragonally distorted. Such a situation leads to an increase of the Cu-OH_2 bond length and hence a decrease in νCu-OH_2.

Of the two types of metal-nitrogen vibrations, the νM-NH_2 modes occur at higher frequencies than the νM-N(py) modes. This is in agreement with previous, related work [18,22]. The observation of six νM-L bands is consistent with the group theoretical requirements for C_{2v} point symmetry, which is therefore assigned (Fig. 4.6).

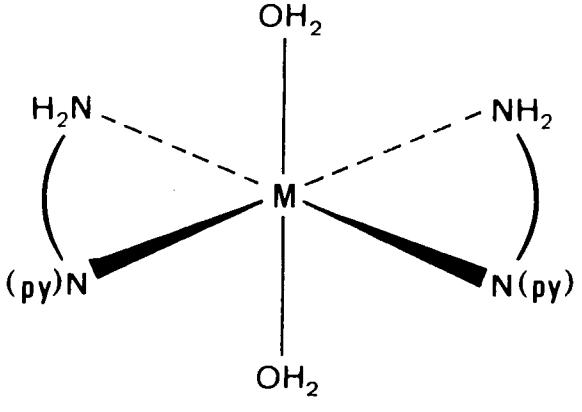

Fig. 4.6 Diagrammatic representation of $[M(aq)_2(H_2O)_2]^{2+}$

4.4.5 *The mono(8-aminoquinoline) complexes of metal(II) halides: assignments and structural aspects of the spectra.*

Complexes of the formula $[M(R_2\text{-aq})X_2]$ (M = Ni, Cu; X = Cl^-, Br^-; R = Cl, Br, I) have been reported by Izquierdo *et al.* [7,8]. On the basis of their electronic spectra, the compounds were assigned polymeric octahedral structures with terminal and bridging halides. As will be seen, the IR spectra are consistent with this proposal.

Since it is below 500 cm^{-1} that metal-ligand bands occur, a detailed discussion of the region 500 - 50 cm^{-1} only will be given. Table 4.6 reports the frequencies and assignments of these complexes in the range 3500 - 3000 cm^{-1} and 1700 - 50 cm^{-1}. Figs. 4.7 and 4.8 depict the IR spectra of the complexes in the regions 1700 - 500 cm^{-1} and 500 - 50 cm^{-1}, respectively. The tracings of the far-IR spectra of the complexes $[Cu(aq)Cl_2]$ and $[Cu(aq)Br_2]$ are shown in Fig. 4.9.

ND_2-labelling was applied to the complex $[Zn(aq)Cl_2]$. Below 470 cm^{-1} eleven bands occur. Apart from the lattice mode at 69 cm^{-1}, four of the eleven bands (at 277, 230, 137 and 121 cm^{-1}) are unaffected by ND_2-labelling and are therefore assigned to Zn-Cl modes. This is confirmed by the substantial shifts which occur on bromide substitution. It is proposed that the first two bands are assigned to $\nu Zn\text{-}Cl_t$ (terminal) and $\nu Zn\text{-}Cl_{br}$ (bridging) modes, and the last two to Cl-Zn-Cl bending vibrations. Of the remaining six bands, the group of three at 417, 395 and 321 cm^{-1}, which shift between 8 and 10 cm^{-1} on ND_2-labelling, are firmly assigned

to νZn-NH_2 bands, and the bands at 203 and 191 cm^{-1} to νZn-N(py) modes. These occur within the region reported for 8-hydroxyquinoline complexes (Chapter 3). Their sensitivity to ND_2-labelling is probably a result of vibrational coupling of νZn-N(py) with νZn-NH_2, or a ligand mode incorporating the NH_2 group. The assignment of the δL-M-X and δL-M-L bands is difficult because these bands are generally much weaker than the δX-M-X bands and could be masked by the latter. This was indeed confirmed by the substitution of Cl by Br which causes the δX-M-X bending modes to shift to much lower frequencies ($\Delta\nu \simeq 50$ cm^{-1}), exposing the underlying δN-Zn-N and/or δN-Zn-Br bands at 135 and 113 cm^{-1}.

The assignments for the [Cu(aq)X_2] spectra are readily made by comparison with the analogous zinc complexes. The doubling of the νCu-X stretching modes is undoubtedly associated with the tetragonal distortion (Jahn-Teller effect) which is known to occur in the copper complexes but not in the zinc chelates. The finding of three νM-NH_2 bands and two νM-N(py) bands is not surprising when the low symmetry of these polymeric molecules is considered.

Table 4.6 Frequency data (cm^{-1}) and assignments of the complexes $[M(aq)X_2]$ from 1700 to 50 cm^{-1}

M = Cu		M = Zn		Assignment
X = Cl	X = Br	X = Cl[a]	X = Br	
1617	1625	1626(7)	1626	ν ring
1588	1588	1595(5)	1593	
1561	1558	1571(429)	1571	NH_2 scissor
		1523	1521	
1505	1505	1502(+2)	1503	
1471	1471	1470(+2)	1469	
1424	1421	1423(0)	1423	
1406(sh)[b]	1406			ring + C-H
1394	1392	1398(0)	1398	modes
	1385	1387(3)	1386	
1378	1375	1375	1370	
1312	1317	1320(0)	1319	
1260		1271		
1250	1255	1252(+6,6)	1250	νC-N + ν ring
1231	1237	1239	1238	
1213	1215	1213(3)	1212	
1198		1198	1198	αC-H
1165	1166	1170(+6)	1167	
1137	1142	1131(+4)	1131	
1109	1099	1110(19)	1110	τNH_2 + αC-H
1083	1070	1076(4)	1073	τNH_2
1060	1053	1057(+8)	1054	αC-H
1029	1029	1029(+5)	1027	
	1008			

Table 4.6 continued/

M = Cu		M = Zn		Assignment
X = Cl	X = Br	X = Cl[a]	X = Br	
985	983	989(+5)	989	γC-H
980		979(0)	977	
		958(25)		τNH_2
921		911		
899	901	899(9,23)	899	ωNH_2 + γC-H
829	830	829(10)	827	
810	806	806(+4)	806	γC-H
782	779	780(8)	779	ωNH_2 + ν ring
775		766	766	γC-H
726	725	721(14)	719	ρNH_2 + γ ring
636	631	623(+2)	621	γ ring
611	604			
593	595	589(14)	588	ρNH_2
	577		573	
570	568			
		558(8)	557	ρNH_2 + ν ring
535	531	525(sh)[b]		
513	510	510(32,40)	508	ρNH_2
501	500			
493	493	493(+4)	493	γ ring
462	463	463	461	
423	421	417(11)	415	ν M-NH_2
405	400	395(10)	400	
335	338	321(8)	320	
306	275	277(0)	254	ν M-X_t[c]
282	253		241(sh)[b]	

Table 4.6 continued/

M = Cu		M = Zn		Assignment
X = Cl	X = Br	X = Cl[a]	X = Br	
230	174	230(1)	172	$\nu M-X_{br}$ [c]
205	209	203(10)	207	$\nu M-N(py)$
192	192	191(10)	191	
162	149	137(0)	86	$\delta X-M-X$
123	112	121(0)	75	
			135	$\delta X-M-L$
	99		113	+ $\delta L-M-L$
61	78	69(0)	59	Lattice

[a] Values in parentheses are the ND_2-induced shifts. Shifts $\lesssim$ 1 are not reported.

[b] sh = shoulder

[c] X_t = $X_{terminal}$ X_{br} = $X_{bridging}$

Note: A shift preceded by a positive sign indicates a shift towards higher frequency.

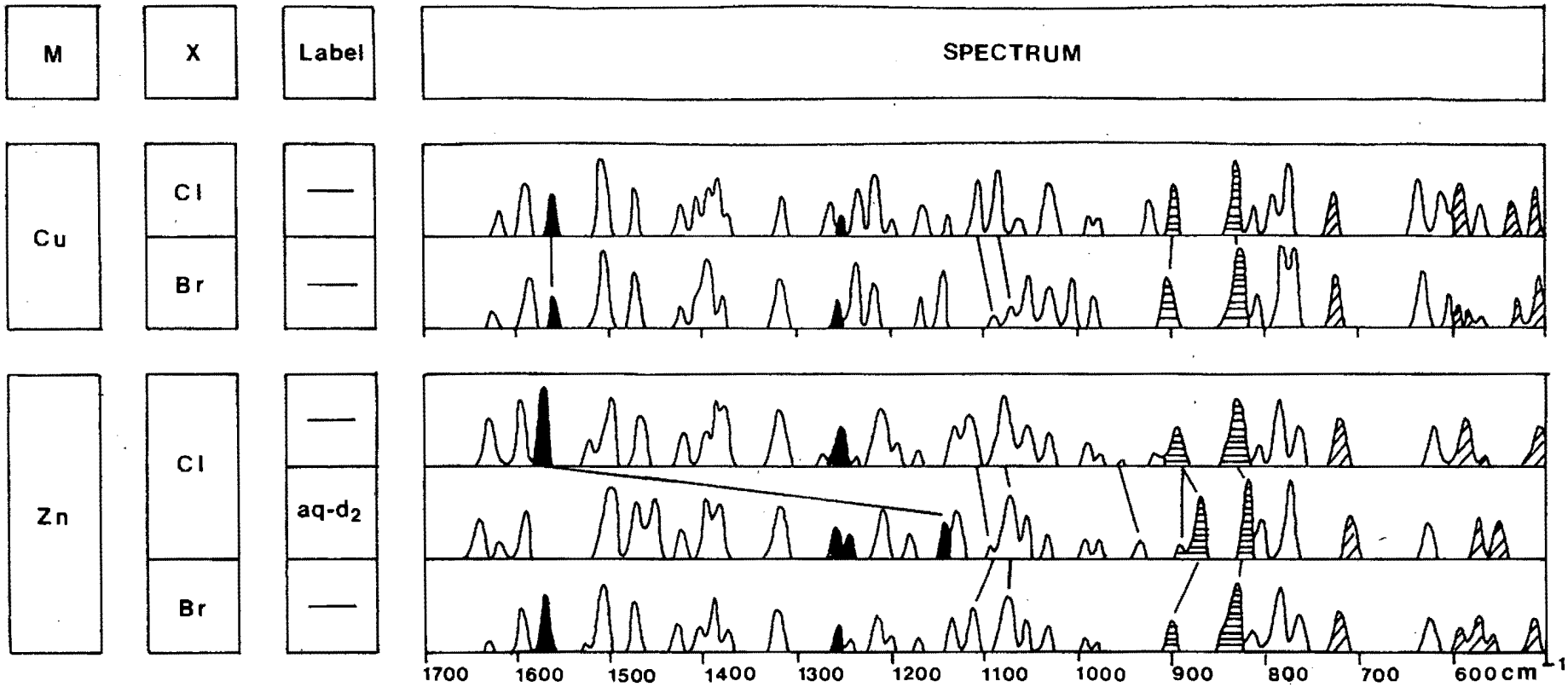

Fig. 4.7 IR spectra of the complexes $[M(aq)X_2]$ in the region 1700 - 500 cm^{-1}.
Solid linked bands: NH_2 scissor; solid unlinked bands: coupled νC-N; linked bands: coupled τNH_2; shaded linked bands: coupled ωNH_2; shaded unlinked bands: coupled ρNH_2.

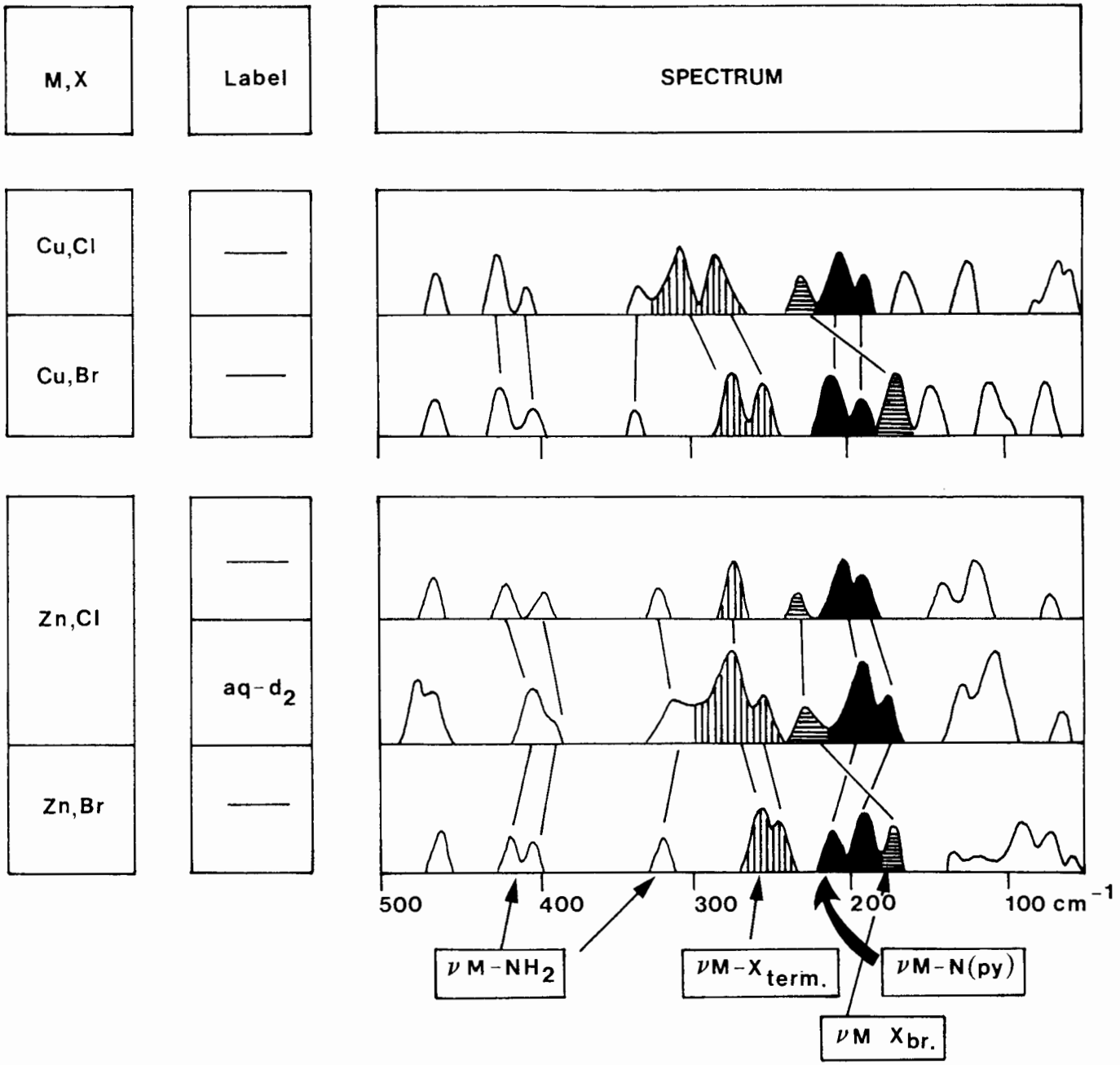

Fig. 4.8 Far-IR spectra of the complexes $[M(aq)X_2]$ in the region 500 - 50 cm^{-1}

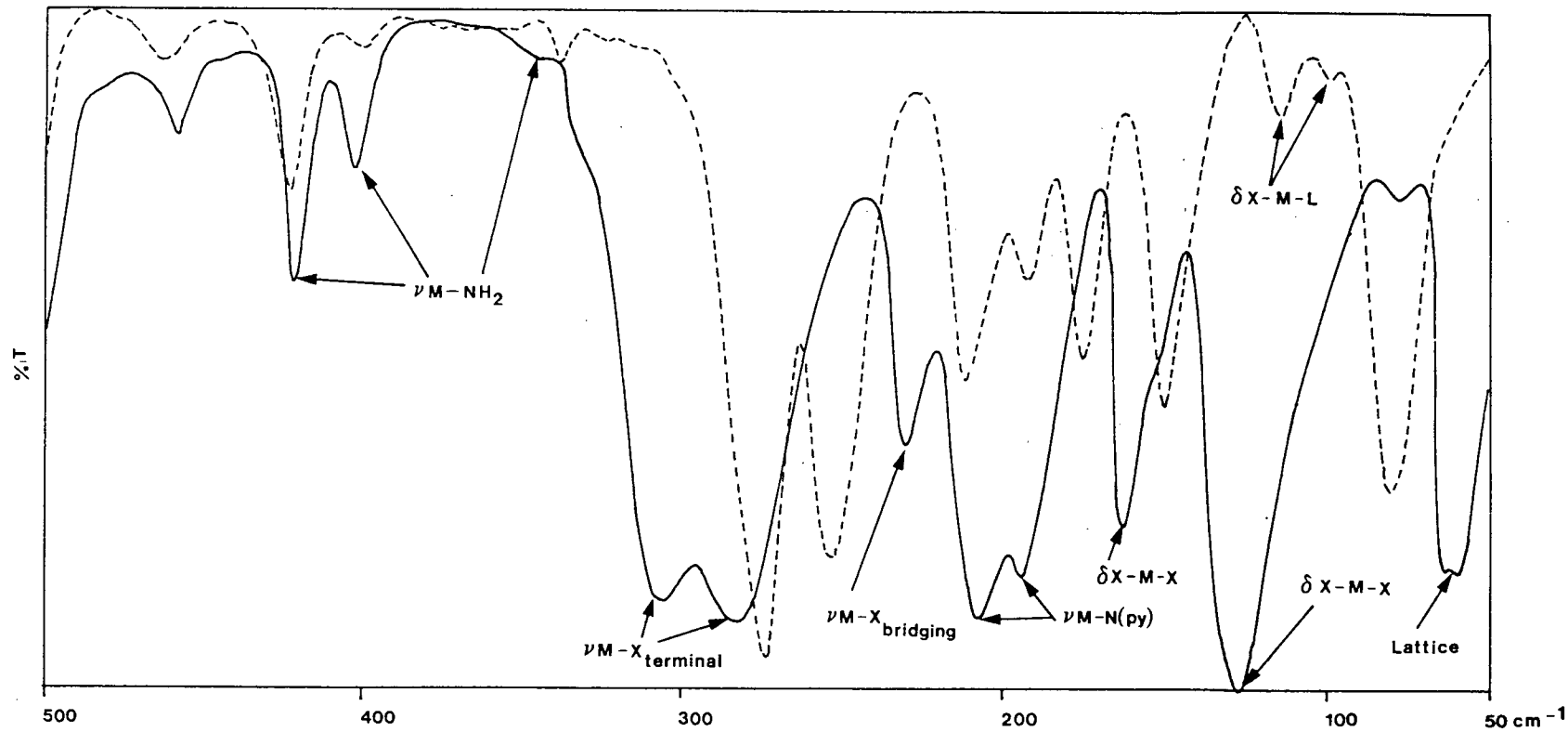

Fig. 4.9 IR spectra of the complexes $[Cu(aq)Cl_2]$ (——) and $[Cu(aq)Br_2]$ (---) in the region 500 - 50 cm^{-1}

REFERENCES

1. C.M. Harris and E.D. McKenzie, *J. Inorg. Nucl. Chem.*, 29 (1967) 1047.

2. J.C. Fanning and L.T. Taylor, *J. Inorg. Nucl. Chem.*, 27 (1965) 2217.

3. R. Nast, H. Bier and J. Gremm, *Z. anorg. allg. Chemie*, 309 (1961) 289.

4. J. Casabó, J. Ribas and J. Bartroli, *Rev. Chem. Min.*, 13 (1976) 149.

5. M.P. Coakley, *Appl. Spectrosc.*, 18 (1964) 149.

6. K.A. Jensen and P.H. Nielsen, *Acta Chem. Scand.*, 18 (1964) 1.

7. M. Izquierdo, J. Casabó, C. Díaz and J. Ribas, *Polyhedron*, 2 (1983) 529.

8. J. Casabó, M. Izquierdo, J. Ribas and C. Díaz, *Transition Met. Chem.*, 8 (1983) 110.

9. J.R. Durig, R. Layton, D.W. Sink and B.R. Mitchell, *Spectrochim. Acta*, 21 (1965) 1367.

10. P.H. Nielsen and O. Dahl, *Acta Chem. Scand.*, 20 (1966) 1113.

11. J.C. Evans, *Spectrochim. Acta*, 16 (1960) 428.

12. G.M. Watkins, *Ph.D. Thesis*, University of Cape Town, 1988.

13. S. Pinchas and I. Laulicht, *Infrared Spectra of Labelled Compounds* [Academic Press] London and New York (1971).

14. B. Marchon, L. Bokobza and G. Cote, *Spectrochim. Acta*, 42A (1986) 537.

15. K. Nakamoto, *Infrared Spectra of Inorganic and Coordination Compounds* [Wiley-Interscience] New York (1963) p. 156.

16. S.D. Ross, *Spectrochim. Acta*, 18 (1962) 225.

17. B.J. Hathaway and A.E. Underhill, *J. Chem. Soc.*, (1961) 3091.

18. A.T. Hutton and D.A. Thornton, *Spectrochim. Acta*, 34A (1978) 645.

19. T.P.E. Auf der Heyde, G.A. Foulds, D.A. Thornton and G.M. Watkins, *J. Mol. Structure*, 77 (1981) 19.

20. G.A. Foulds and D.A. Thornton, *J. Mol. Structure*, 98 (1983) 309.

21. A.R. Nicholson and G.J. Sutton, *Aust. J. Chem.*, 22 (1969) 59, 373, 1543.

22. J.E. Rüede and D.A. Thornton, *J. Mol. Structure*, 34 (1976) 75.

Chapter Five

CHAPTER FIVE

5. NUCLEAR MAGNETIC RESONANCE SPECTRAL ANALYSIS OF PARAMAGNETIC NICKEL(II) OXINE COMPLEXES

5.1 INTRODUCTION

The NMR study of paramagnetic molecules has arisen from a spectroscopic search for a powerful and promising new research method with wide applications in the chemical and biological sciences. This field originated in solid-state physics in the middle 1950s with the study of bonding in transition metal fluoride crystals [1]. By the 1960s, the technique had been introduced to chemistry with the investigation of metallocenes [2,3] and solvated transition metal ions [4,5]. Since then, the NMR of paramagnetic molecules has had a profound effect on several areas of chemistry.

It has been shown that NMR is a sensitive probe for spin delocalization in a paramagnetic system [6], the unpaired spin density giving rise to substantial isotropic shifts in the NMR spectrum. These chemical shifts can arise from either a dipolar mechanism if the complex is anisotropic, or *via* a contact mechanism, which reflects spin delocalization into the ligand system.

In the interpretation of the spectra, the contact shifts are of interest, since they may be related to the transfer of spin either from or to the ligand (σ or π), whereby the unpaired electrons are delocalized from the paramagnetic metal into the ligand system. In the Introduction (see Section 1.5.2), it

was shown that the contact shift, $\Delta\nu^{con}$, is related to the spin density by the hyperfine coupling constant A_N, which is directly proportional to the spin density at the nucleus (N) by

$$(\Delta\nu^{con}/\nu) = -[A_N g_{av.}{}^2 \beta^2 S(S+1)]/[g_N \beta_N 3kT]$$

where $A_N = (k|\phi_{sN}(r_N)|^2)\rho_{sN}$ and the remaining symbols have their usual significance [7]. Experimentally, the magnitude of A_N can be determined from the hyperfine splitting of the ESR spectra of radicals. Both the magnitude and sign of A_N can be determined from the contact shifts in the NMR spectra of paramagnetic transition metal complexes. In the present work, we have attempted to correlate theory and experiment by calculating the spin density distribution on the oxine ligand by the method of Intermediate Neglect of Differential Overlap (INDO) developed by Pople and Beveridge [8]. In this method, molecular orbitals are determined for all the valence electrons of a molecule by the linear combination of atomic orbitals. The intermediate neglect of differential overlap is the neglect of electron interaction between all atomic orbitals except those involving one electron and different atomic orbitals on the same atom. This allows for electron exchange between orbitals on the same atom which allows for the delocalization of spin density in a σ-orbital. The INDO method is the least complex, semi-empirical method available which can account for the general observed features of ESR spectra of radicals and contact shifts in the NMR spectra of transition metal complexes. It is a valence electron method capable of calculating spin densities arising from electron correlation

because it uses unrestricted wavefunctions.

In the INDO study of a paramagnetic metal complex, the metal atomic orbitals are completely neglected in forming the molecular orbitals. The metal atom is considered simply as an electron source or sink for the ligand. The calculations are therefore based upon considering the ligand as either the anionic or cationic radical. This is equivalent to assuming that the order of the orbitals calculated for the ligand radical ion would be retained if they were combined with metal orbitals to form molecular orbitals for the complex [9]. If this were not the case, the calculated spin densities would be incorrect.

Since its introduction, the INDO method has been used extensively for the interpretation of ^{1}H-NMR contact shifts [9-12]. The nickel(II) complexes of aminotroponeimines and salicylaldimine [10,11] have been investigated. The experimental data agreed very well with valence bond calculations. Several workers [12,13] have investigated the spin delocalization in pyridine and substituted pyridines, and have predicted a combined σ-π type delocalization mechanism.

The present work has been undertaken in order to extend the recently reported NMR spectral analysis of paramagnetic nickel oxine complexes [Ni(R-ox)$_2$(H$_2$O)$_2$] (from here on referred to as Ni(R-oxine)) [14,15]. In our work, an initial attempt to interpret the ^{1}H-NMR spectrum of the Ni(oxine) complex by chemical substitution failed because several isomers of this complex were found to co-exist at room temperature. This, however, is contrary to the results previously reported at

90 MHz where relatively simple spectra albeit with broad peaks were found. The fluxionality of the above-mentioned complex (as well as that of the Ni(5-Cl-oxine) analogue) is observed in the present work because the spectra were recorded at 200 MHz. Thus, although the chemical shift difference in ppm between the different environments is the same in both studies, the frequency difference (in Hz) in the present work is much larger (by a factor of 2). Hence, the coalescence temperature is raised. The broadness of the peaks in the previous study indicates that their system was just below the coalescence temperature. Variable temperature studies of both the unsubstituted and 5-chloro-substituted complexes were undertaken. The free energy of activation, $\Delta G^{\ddagger}$, between the initial and transition state for the unsubstituted nickel(II) complex was calculated using computer simulation. The assignment of the ^{1}H-NMR spectrum of the Ni(oxine) complex (and hence determination of contact shifts of the ligand resonances) by chemical substitution was performed at 393.1 K at which temperature the complex is undergoing rapid chemical exchange and only an average environment is observed. Two mechanisms have been proposed to account for the fluxional process. INDO calculations of spin density were performed and an attempt has been made to interpret the shifts in terms of spin delocalization mechanisms into the ligand.

5.2 EXPERIMENTAL

Substituted *bis*(8-quinolinol)nickel(II) dihydrate complexes were prepared as previously described in Section 3.2.2. The elemental analyses of the resulting compounds are given in Table 5.1. The ^{1}H-NMR spectrum of each of these compounds was obtained on a VXR-200 MHz Fourier Transform Spectrometer in the region -20 ppm to 160 ppm. The spectra were recorded at both ambient temperature (297.5 K) as well as 393.1 K. Since the Ni(oxine) and Ni(5-Cl-oxine) complexes were not fluxional at ambient temperatures, variable temperature ^{1}H-NMR spectra were recorded over the range 297.5 K to 393.1 K.

INDO OPEN shell computations were performed on a Univac 1100/81 computer using the INDO program written by P.A. Dobosh. This program required as initial input geometrical parameters which were obtained from X-ray crystallographic data [16]. Additional bond lengths and bond angles were taken as follows: C-H (aromatic) 1.08 Å; O-H 0.96 Å; $\hat{COH}$ 109°47'; N-H 0.99 Å; $\hat{CNH}$ 120°. The standard geometry of benzene was used for benzene derivatives: C-C (aromatic) 1.40 Å; C-H 1.08 Å; $\hat{CCC}$ and $\hat{HCC}$ 120° for comparison. In all cases, the geometry of the free ligand was retained and in general planarity was assumed. Methyl groups were considered to rotate freely leading to an average spin density for the three protons.

5.3 ANALYSES OF COMPOUNDS

Table 5.1

Analytical data for the complexes *trans*-$[Ni(R\text{-}ox)_2(H_2O)_2]$.

R	Calculated			Found		
	%C	%H	%N	%C	%H	%N
H	56.44	4.21	7.32	56.20	4.20	7.30
5-Cl	47.84	3.12	6.20	47.50	3.15	6.15
5,7-diCl[a]	40.14	2.62	5.20	39.90	2.75	5.15
5,7-diBr-2-Me	32.00	2.14	3.73	32.45	2.30	3.70

[a]Monohydrate

5.4 RESULTS AND DISCUSSION

5.4.1 *The analysis of the ^{1}H-NMR spectrum of the Ni(oxine) complex.*

The assignment of the ^{1}H-NMR spectrum of the Ni(oxine) compound is complex because the compound is not fluxional at room temperature. For this reason initial assignments were made at 393.1 K (fast exchange conditions) using chemical substitution. The room temperature assignments then followed from a variable temperature study. The ^{1}H-NMR spectra for the complexes $[Ni(R\text{-}ox)_2(H_2O)_2]$ at 393.1 K are shown in Fig. 5.1 and the ^{1}H-NMR chemical shifts for these compounds are given in Table 5.2. As dmso coordinates readily with nickel, it is expected to replace the water molecules which occupy the axial positions in the above complexes. Octahedral nickel(II) species are magnetically isotropic and hence pure contact shifts are expected. Five peaks shifted from the diamagnetic positions are observed in the Ni(oxine) complex (Fig. 5.1). The sharp singlet at δ 17.8 can be assigned unambiguously to the H-5 as it is absent in the spectrum of the 5-Cl-; 5,7-diCl- and 5,7-diBr-2-Me-substituted complexes. The broad peak at δ 7.4 is readily assigned to H-7 as it is present in the 5-chloro-substituted complex, but disappears in the spectra of both the 5,7-diCl- and 5,7-diBr-2-Me-substituted analogues. A peak, shifted substantially downfield of the dmso peak, is expected for H-2, since this proton would be most directly affected by spin delocalization through the nitrogen atom of the ligand. However, no such peak was observed for any of the complexes at 393.1 K. A peak at δ 168 was observed in the spectrum of the

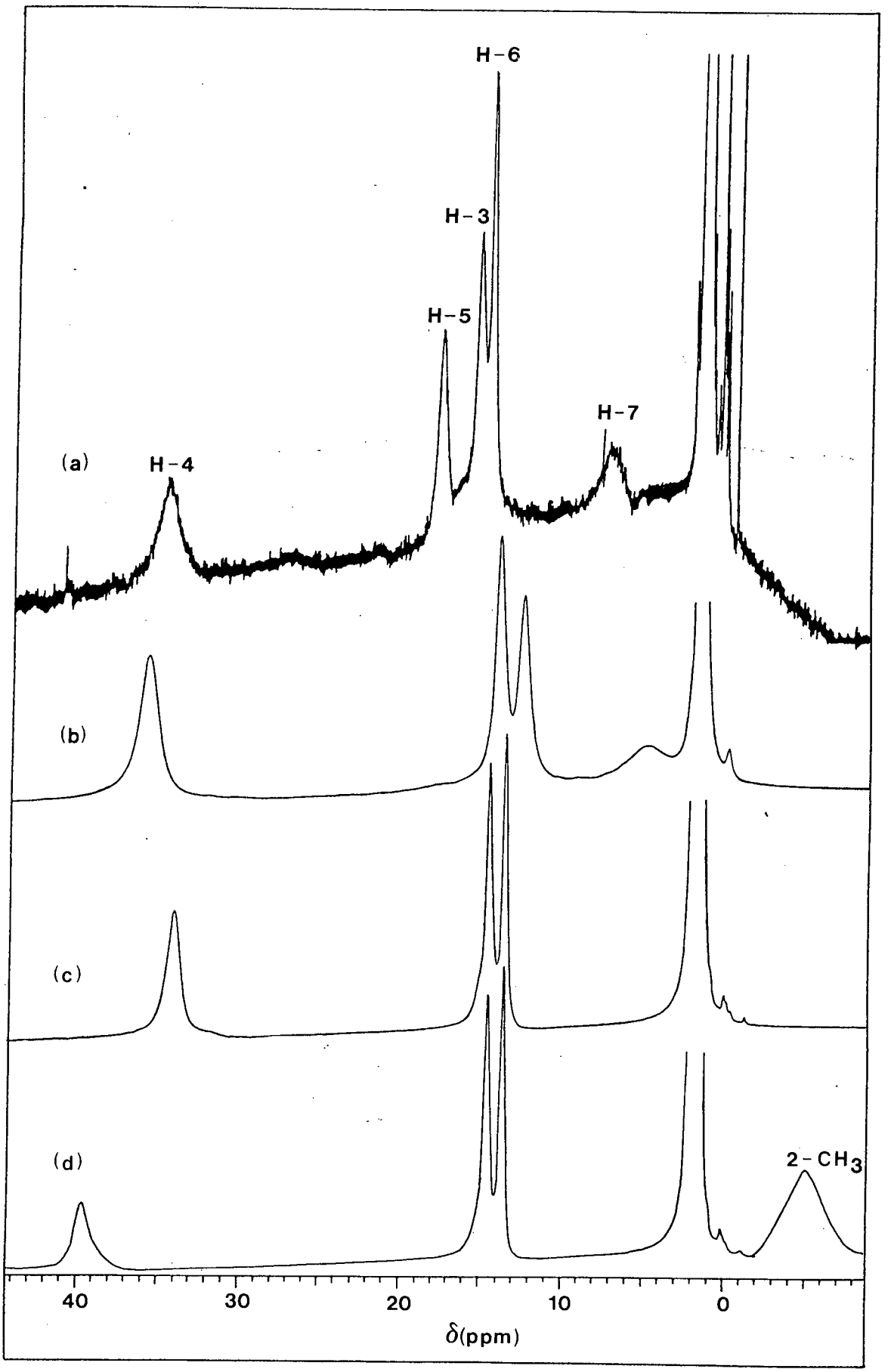

Fig. 5.1 ^{1}H-NMR spectra of the complexes $[Ni(R\text{-}ox)_2(H_2O)_2]$ in dmso-d_6 at 393.1 K (a) R = H (b) R = 5-Cl (c) R = 5,7-diCl (d) R = 5,7-diBr-2-Me.

Table 5.2

^{1}H-NMR chemical shifts for $[Ni(R\text{-}ox)_2(H_2O)_2]$ in dmso-d_6 at 393.1 K.

R	Chemical shift[a] 2-H	3-H	4-H	5-H	6-H	7-H	2-CH_3
H	n.o.[b]	15.5	34.6	17.8	14.6	7.4	-
5-Cl	n.o.[c]	14.2	36.0	-	12.7	5.1	-
5,7-diCl	n.o.[d]	14.8	34.2	-	13.6	-	-
5,7-diBr-2-Me	-	13.7	39.8	-	13.5	-	-5.1
$\Delta\nu^{con}$	-160[e]	-8.1	-26.4	-10.5	-7.2	-0.3	-

[a] Relative to dmso-d_6 (ppm)

[b] n.o. = Not observed

[c] Two broad peaks at δ 153 and δ 176 were observed at T = 297.5 K

[d] Broad peak at δ 168.0 was observed at T = 297.5 K

[e] Estimated to be approximately -160 ppm from superscript d above. Negative sign indicates a downfield shift relative to the diamagnetic position.

Ni(5,7-diCl-oxine) complex at 297.5 K, whilst two peaks were observed at δ 153 and δ 176 in the spectrum of the Ni(5-Cl-oxine) complex. These peaks are assigned to H-2. The fact that two peaks are observed for the Ni(5-Cl-oxine) complex where only one peak is expected, can be explained by the non-fluxional behaviour of this complex at 297.5 K. The NMR spectra give evidence for there being at least two isomers in solution. Comparison with the results of Ni(II) pyridine [9] suggests the assignment of H-4 to the peak at δ 34.6. The two remaining peaks at δ 15.5 and δ 14.6 are attributable to H-3 and H-6. As no 3- or 6-substituted complexes could be prepared, the actual assignment of these protons is tentative. However, since the chemical shift difference between these two resonances is small (∿ 1 ppm), it can be anticipated that any subsequent experimentally determined results (*e.g.* hyperfine coupling constants) should be fairly similar.

The ^{1}H-NMR spectra of the Ni(oxine) and Ni(5-Cl-oxine) complexes in the range 297.5 K to 393.1 K are shown in Figs. 5.2 and 5.3 respectively. Isotropic shifts often exhibit a Curie temperature dependence and this fact can be used in making assignments. Thus, a plot of chemical shift against $1/T$ should give the diamagnetic position when extrapolated to zero. Such a plot is shown for Ni(oxine) in Fig. 5.4. Attempts to obtain unambiguous assignments using this plot failed because the diamagnetic chemical shift range was so small. However, a linear (Curie) behaviour was shown by all the observed protons. In the case of protons 3, 4 and

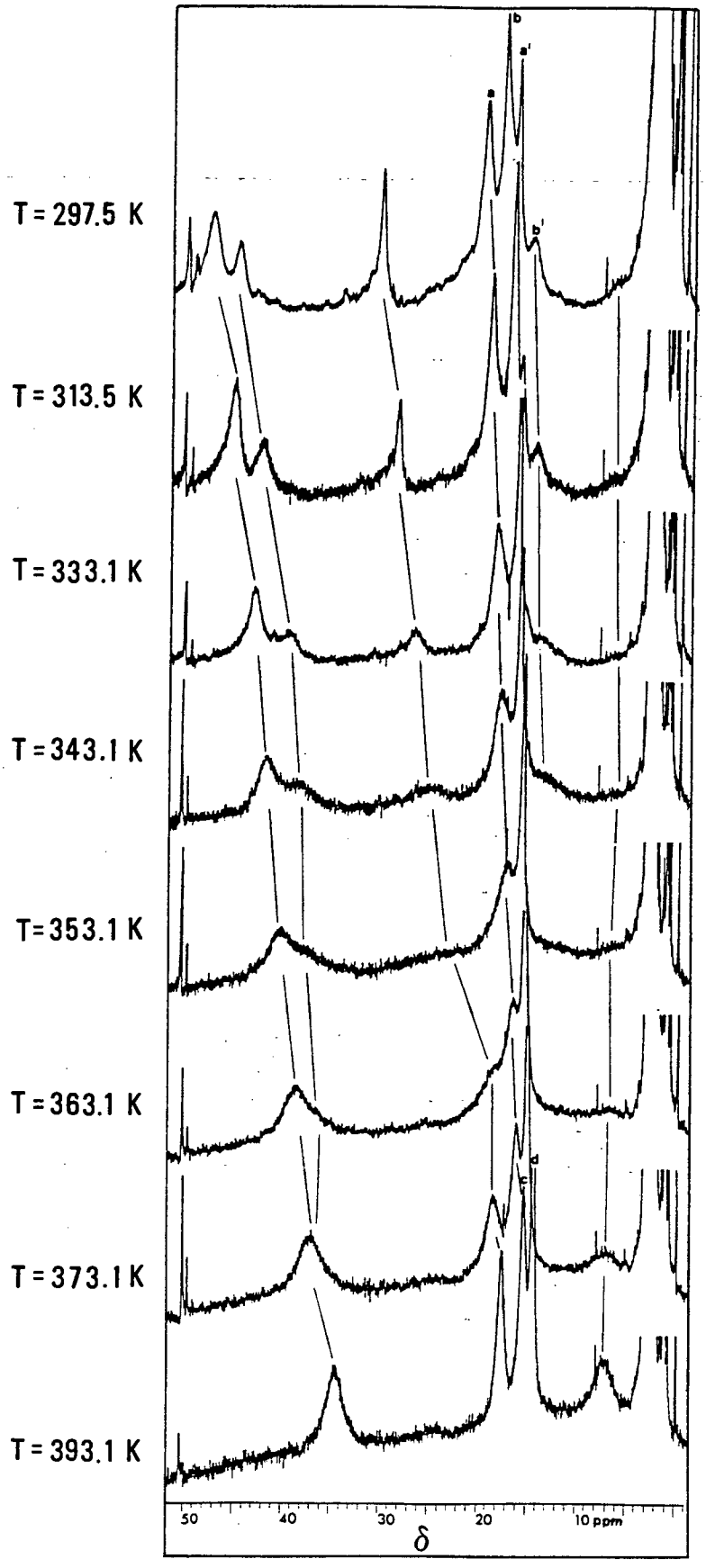

Fig. 5.2 ^{1}H-NMR spectra of $[Ni(ox)_2(H_2O)_2]$ in dmso-d_6. Note the peaks a and a' converge to c and peaks b and b' converge to d at high T.

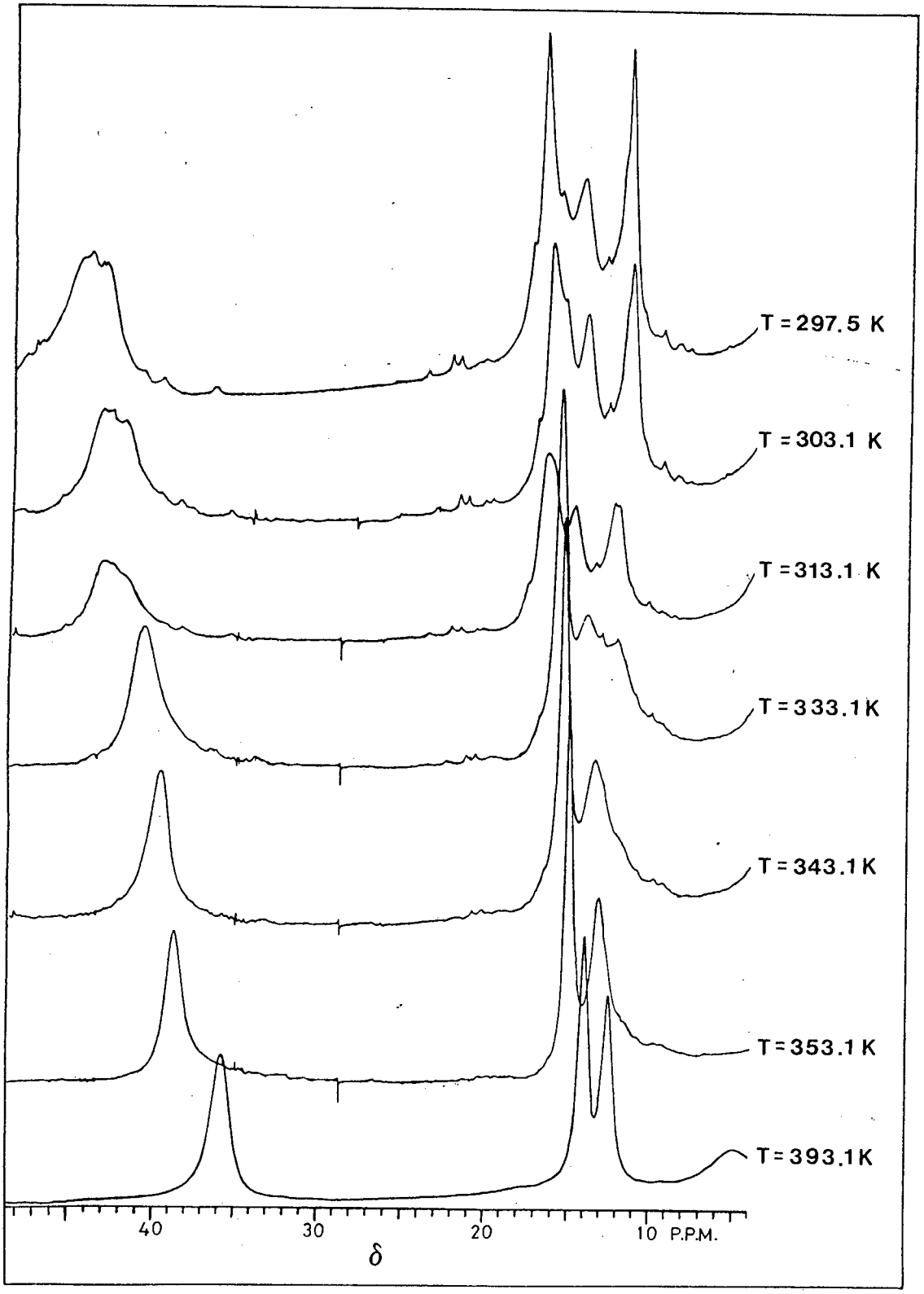

Fig. 5.3 ^{1}H-NMR spectra of Ni(5-Cl-oxine) in dmso-d_6.

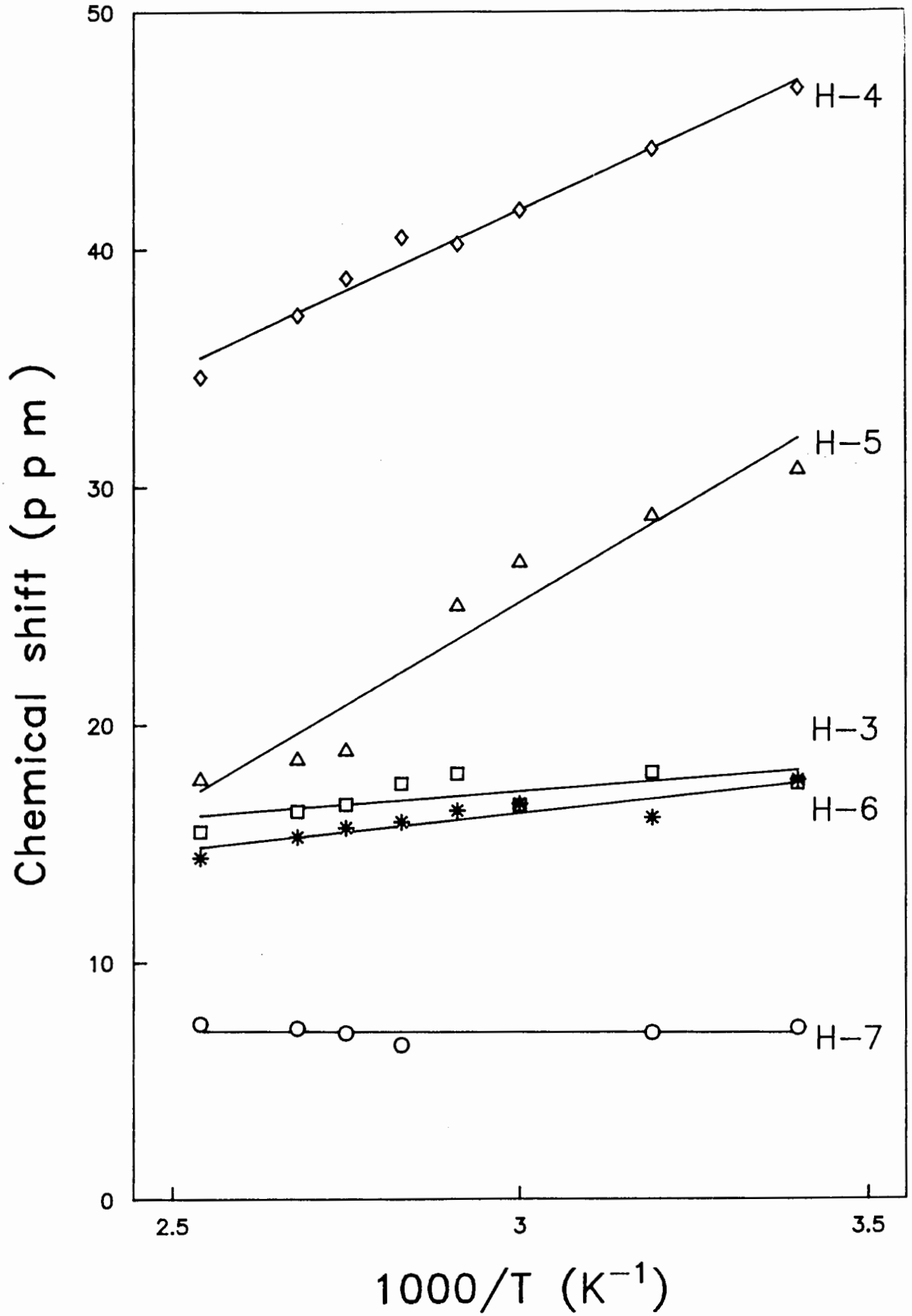

Fig. 5.4 Temperature dependence of the isotropic chemical shifts for Ni(oxine) in dmso-d_6.

6, which were found to exist in several different environments, only when the average chemical shifts for these different environments were plotted, was a linear relationship obtained.

5.4.2 *The fluxional behaviour of Ni(R-oxine) complexes (R = H, 5-Cl).*

Inorganic and organometallic chemistry comprise a plethora of stereochemically nonrigid molecules. In particular, many octahedral metal chelate compounds are stereochemically labile (or fluxional) due to the flexibility of the bonding framework about the metal atom. This situation was not recognized until the 1960s, when NMR studies uncovered spectral features for many molecules which were explicable only in terms of rapid molecular rearrangements [18-20]. By the late 1960s, NMR studies of stereochemically nonrigid molecules became quite common. Computer aided NMR studies have been used extensively in the study of rapid equilibria. This application of NMR depends on the fact that the observed signals (line shapes) are dependent on the rate at which the resonating nuclei exchange. If exchange processes are slow, signals are observed for each environmentally distinct magnetic nucleus. However, when rate constants for exchange processes are similar in magnitude to the total spread of the NMR spectrum, profound changes in the total spectrum may occur. Analysis of these line shapes can provide rate constants for dynamic processes and insight into exchange mechanisms.

The ^{1}H-NMR spectrum of Ni(oxine) (Fig. 5.2) reveals that there are two signals for H-4 at ambient temperature. These two

signals are not resolved and there may in fact be hyperfine structure of the two peaks. Clearly, at this temperature, the complex is not fluxional on the NMR time scale and there may be several isomers present in solution. The five possible isomers which can exist in solution are shown in Fig. 5.5.

The crystal structure of $[Zn(ox)_2(H_2O)_2]$ has shown that the two oxinate anions coordinate to the metal by forming a *trans*-(H_2O), *trans*(N), *trans*(O) structure (represented by Fig. 5.5e) of C_{2v} symmetry. The two water molecules complete the octahedral stereochemistry by occupying the axial positions. Hence, it is most likely that this isomer is converting in solution to any of the remaining four isomers at room temperature. Evidence for this stems from the fact that the percentage population of the isomers are unequal. This can be expected for the type of isomerization where the *trans*(X), *trans*(N), *trans*(O) isomer is the sterically most favoured isomer. The 5,7-dichloro- and 5,7-dibromo-2-methyl-substituted complexes are either in fast exchange or are sterically rigid at ambient temperature. It is most likely that the latter is the case with the *trans*(X), *trans*(N), *trans*(O) isomer being thermodynamically more stable at ambient temperature because of the steric implication of the bulky halogen and methyl groups.

Bandshape analysis was confined to the region of maximum exchange broadening (near the coalescence temperature at 353.1 K), since it has been established that the rate constant

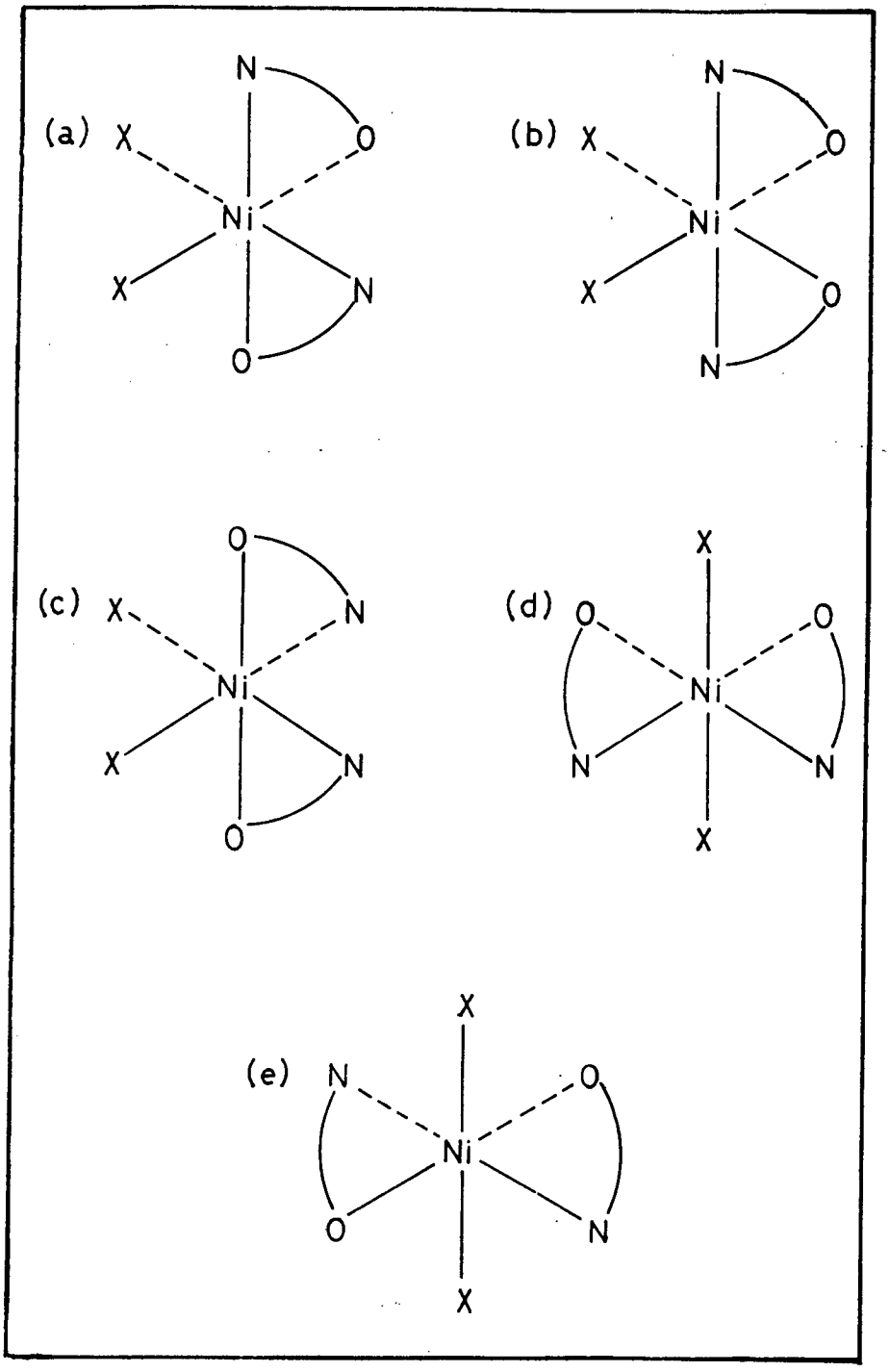

Fig. 5.5 The five geometrical isomers for $[Ni(ox_2)_2X_2]$ (X = dmso): (a) = *cis*(X), *cis*(N), *cis*(O); (b) = *cis*(X), *trans*(N), *cis*(O); (c) = *cis*(X), *cis*(N), *trans*(O); (d) = *trans*(X), *cis*(N), *cis*(O); (e) = *trans*(X), *trans*(N), *trans*(O).

can be determined more accurately near coalescence [21]. A relaxation time of 6.5×10^{-3} s (or $K = 77\ s^{-1}$) was estimated in this way by a computer simulation study. The free energy of activation can be calculated from a single rate constant at a single temperature by means of the Eyring equation [22].

$$K = (kT/h)[\exp(-\Delta G^{\ddagger}/RT)]$$

where k, h, R = Boltzmann, Planck and Gas constants respectively

T = temperature

$\Delta G^{\ddagger}$ = free energy of activation difference between the initial and the transition state.

The free energy of activation was estimated to be 74 kJ mol^{-1}. Table 5.3 gives typical $\Delta G^{\ddagger}$ values measured for the isomerization processes of several metal complexes. A comparison of our observed value indicates that the observed value is significantly higher than the $\Delta G^{\ddagger}$ value found for the square planar to tetrahedral conversion of Ni(II) complexes, and within the range for the free energy of activation required for the *trans* to *cis* isomerization of various complexes. $\Delta G^{\ddagger}$ values for *trans* to *cis* isomerization range from about 70 kJ mol^{-1} to 115 kJ mol^{-1}. This can be regarded as support for the rapid isomerization of the *trans*(dmso), *trans*-(N), *trans*(O) Ni(R-oxine) complexes (R=H, 5-Cl) to any one of the remaining four isomers at temperatures greater than 353.1 K. Unfortunately, we do not have kinetic data for *trans/cis* isomerization of Ni complexes of the type $[Ni(AB)_2X_2]$ which would be more relevant to our study.

Table 5.3

Typical $\Delta G^{\ddagger}$ values for the *trans/cis* isomerization process.[a]

Complex	$\Delta G^{\ddagger}$ kJ mol^{-1}	Reference
$[Co(en)_2(OH_2)Br]^{2+}$	94.7	23
$[Co(en)_2(OH_2)N_3]^{2+}$	68.6	
$[Co(en)_2(OH_2)Cl]^{2+}$	68.2	
$[Co(en)_2(OH_2)_2]^{3+}$	101.8	24
$[Co(en)_2(OAc)(OH_2)]^{2+}$	98.8	
$[Cr(CO)_2(dpm)_2]$	76.8	25
$[W(CO)_2(dpm)_2]$	72.5	
$[Mo(CO)_2(dpm)_2]$	80.2	
$[W(CO)_2(dpe)_2]$	78.7	
$[Co(en)_2(dmso)Cl]^{2+}$	88.6	26
$[Cr(mal)_2(H_2O)_2]^{-}$	103.5	27
$[Ni(R_2\text{-ati})_2]$[b] (R = Et)	-12.2	28
(R = Ph)	- 4.1	
(R = Bz)	- 3.4	
$[Mo(CO)_4(PPh_3)_2]$	112.1	29
$[Mo(CO)_4(P\text{-}n\text{-}Bu_3)_2]$	109.4	30
$[Co(diars)_2Cl_2]^{+}$	100.0[c]	31
$[Cr(ox)_2(OH_2)_2]^{-}$	92.1	32
$[Co(acac)_2(NO_2)py]$	98.3	33

Table 5.3 cont/d

[a]Where en = 1,2-diaminoethane; dpm = *bis*(diphenylphosphino)-methane; dpe = 1,2-*bis*(diphenylphosphino)ethane; mal = malonato; R_2-ati = *bis*(*N*-alkylbenzoylacetoneiminato); Et = ethyl; Ph = phenyl; Bz = benzoyl; P-*n*-Bu_3 = *tris*-(*n*-butylphosphine); ox = oxalato; acac = acetylacetonato; py = pyridine; *n*-Pr = *n*-propyl; diars = Nyholm's diarsine; dmso = dimethylsulphoxide; OAc = $CH_3CO_2^-$.

[b]Planar to tetrahedral isomerization.

[c]In methanol.

At this stage, it is necessary to comment on possible mechanisms for the isomerization process. A non-bond rupture mechanism provides a low-energy path for the stereochemical rearrangement. On the basis of the low $\Delta G^{\ddagger}$ value, we therefore propose that the *trans/cis* isomerization process proceeds *via* this pathway. This "Bailar twist" mechanism [30,34] (illustrated in Fig. 5.6 for the rearrangement of the *trans,trans,trans*-isomer to the *cis,cis,cis*-isomer) can be pictured as the rotation of one of the faces 120°/240° around the C_3 axis. It should be noted that either the top or the bottom face is subject to this rotation and depending on which face is rotated, transitions between different geometrical isomers can occur.

An alternative mechanism could, however, involve the dissociation of one of the dmso molecules. This bond-rupture

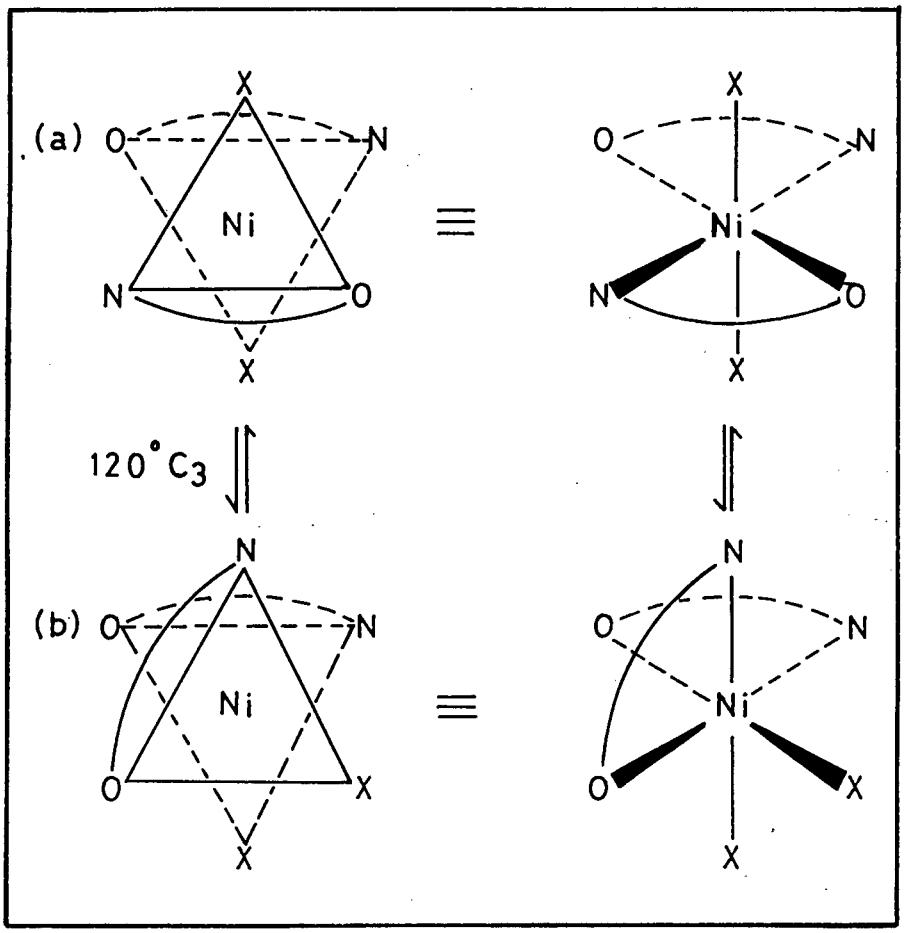

Fig. 5.6 Bailar twist mechanism; (a) = *trans*(X), *trans*(N), *trans*(O) (b) = *cis*(X), *cis*(N), *cis*(O) where X = dmso.

process most likely proceeds through a trigonal bipyramidal transition state, several of which are illustrated in Fig. 5.7. Hence, the isomer that is formed is dependent on both the intermediate and the side at which the dmso molecule enters. An example of this mechanism involving two of these possible trigonal bipyramidal intermediates is given in Fig. 5.8. The route (given in this diagram) can account for the formation of all the possible isomers except the *trans*(X), *cis*(N), *cis*(O) isomer. The latter would involve the trigonal bipyramidal transition state given by Fig. 5.7(e).

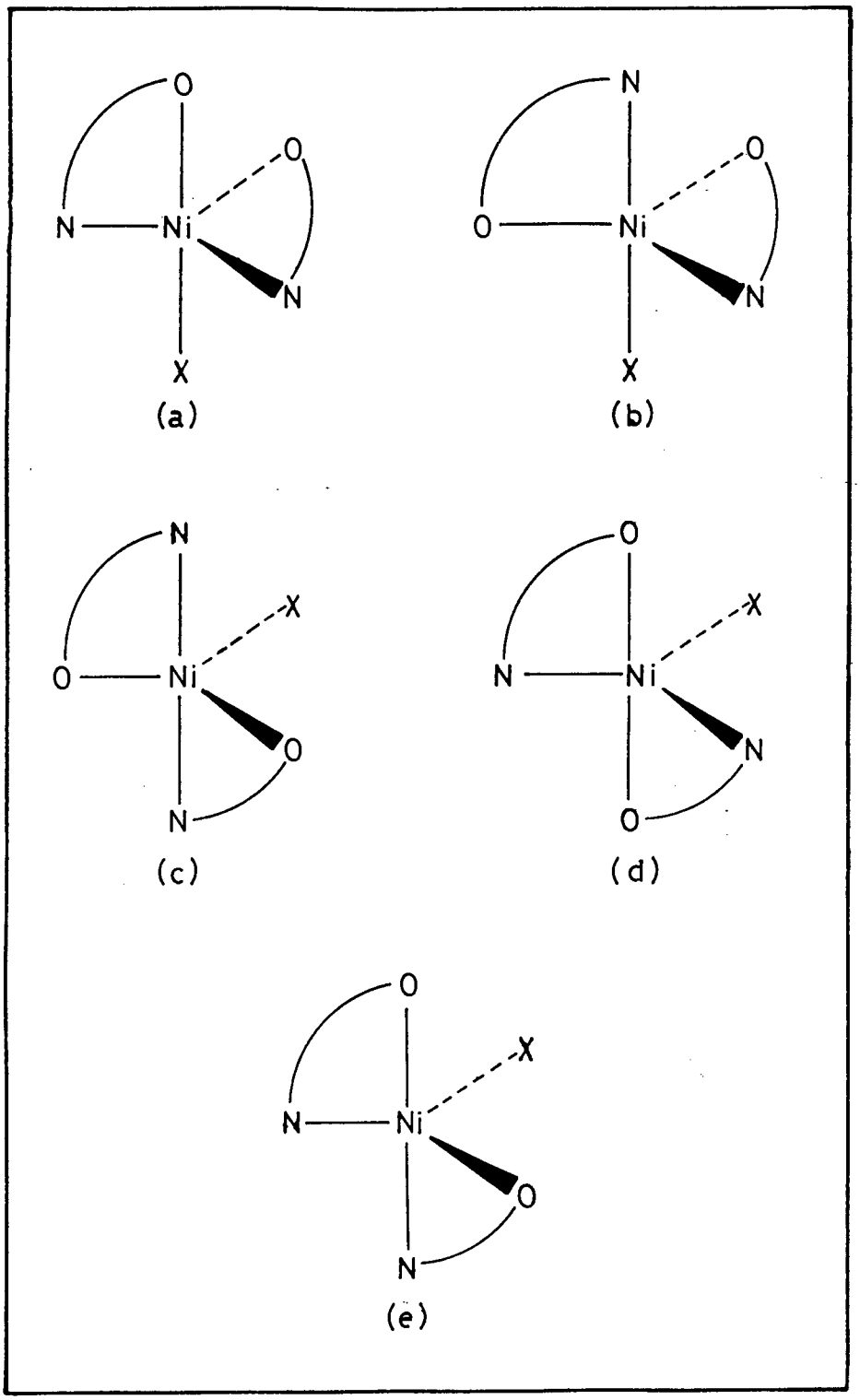

Fig. 5.7 Possible trigonal bipyramidal intermediates (X = dmso).

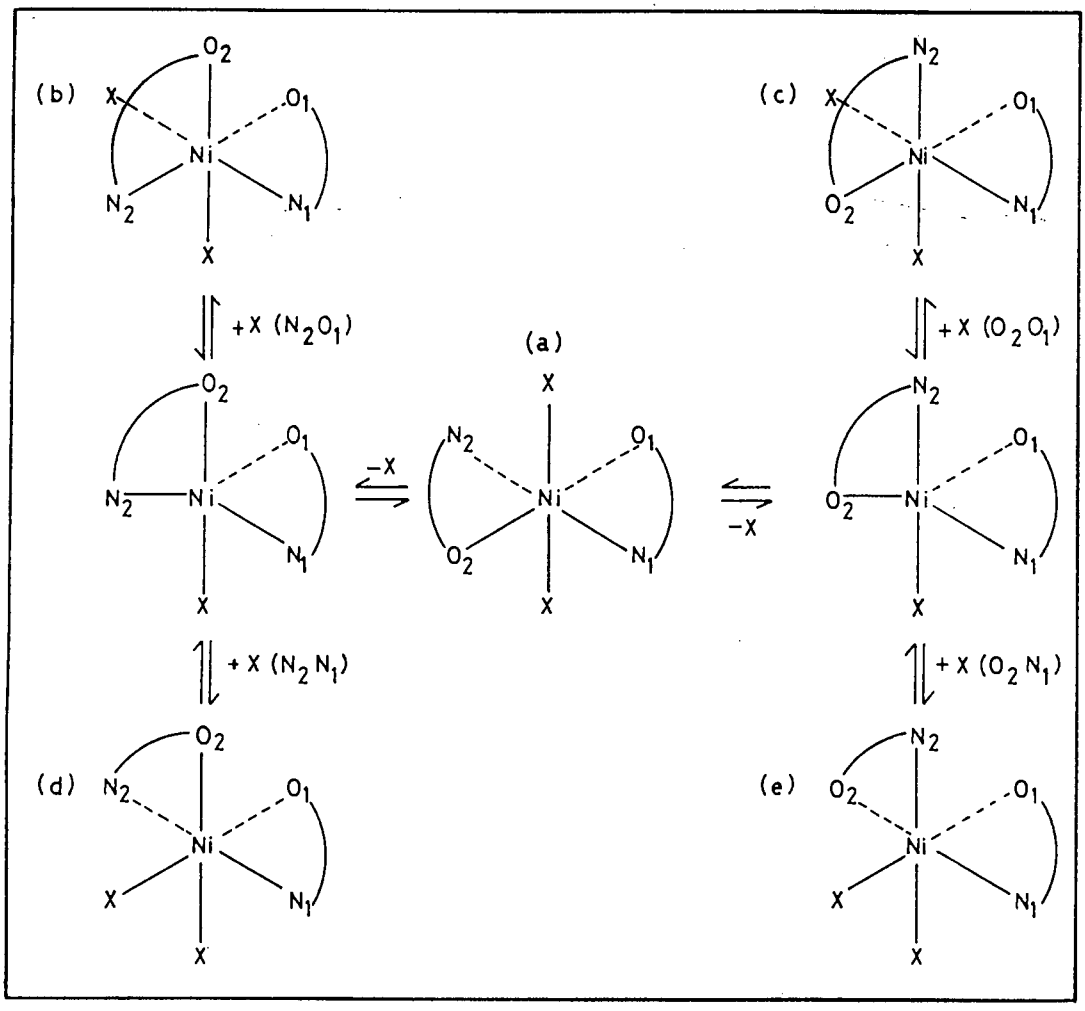

Fig. 5.8 (a) = *trans*(X), *trans*(N), *trans*(O) (b) = *cis*(X), *cis*(N), *cis*(O) (c) = *cis*(X), *cis*(N), *trans*(O) (d) = *cis*(X), *trans*(N), *cis*(O) (e) = *cis*(X), *cis*(N), *cis*(O) where X = dmso.

Note: (b) and (e) are mirror images.

X enters between the two letters given in parentheses.

5.4.3 *INDO spin density calculations*

Net spin density can arise on the ligand of a paramagnetic metal complex as a result of electron transfer from either the metal atom to the ligand or the ligand to the metal atom. If a whole electron is transferred from the metal atom to the ligand, then an anionic ligand radical with unpaired spin density in a previously (empty) antibonding orbital of the ligand is produced. If, however, the transfer is from the ligand to the metal, a cationic radical with unpaired spin density in a previously fully occupied (bonding) orbital is produced. A comparison of the NMR contact shifts (and hence experimentally determined spin densities and hyperfine coupling constants) for a complex with the calculated cationic or anionic spin densities can suggest the direction of electron transfer, and moreover, the type of ligand orbital containing the transferred spin density.

The observed isotropic hyperfine coupling constants (calculated from the observed contact shifts) for Ni(oxine) and Ni(5,7-diBr-2-Me-oxine) complexes with the calculated isotropic hyperfine coupling constants for the cationic and anionic species are given in Tables 5.4 and 5.5 respectively. The INDO calculations predict a downfield shift for all the protons except H-6 for the cationic species and a downfield shift for all the protons for the anionic species as is experimentally observed. Hence, the correlation between the calculated and observed hyperfine coupling constants is better in both sign and magnitude for the anionic ligand radical. This indicates that spin delocalization involves

Table 5.4

Calculated and observed hyperfine coupling constants for the oxine cation and anion.

Species	Nucleus ^1H	A_H(Gauss)	A_H(rel.)
		Calculated	
cation	2	-0.931	0.321
	3	-0.033	0.011
	4	-2.903	1.000
	5	-7.449	2.566
	6	0.644	-0.222
	7	-3.410	1.175
anion	2	-2.299	0.324
	3	-0.755	0.106
	4	-7.104	1.000
	5	-3.076	0.433
	6	-0.288	0.041
	7	-0.663	0.093
		Observed	
	^1H		
	2	$\sim$-1.067	$\sim$6.063
	3	-0.054	0.307
	4	-0.176	1.000
	5	-0.070	0.398
	6	-0.048	0.273
	7	-0.002	0.011

Table 5.5

Calculated and observed hyperfine coupling constants for the 2-methyl oxine cation and anion.

Species	Nucleus ^1H	A_H(Gauss)	A_H(rel.)
		Calculated	
cation	2	-	-
	3	0.256	-0.092
	4	-2.781	1.000
	5	-6.911	2.485
	6	0.108	-0.039
	7	-2.824	1.015
	2-Me	1.982	-0.713
anion	2	-	-
	3	-0.462	0.064
	4	-7.259	1.000
	5	-3.035	0.418
	6	-0.244	0.034
	7	-0.652	0.090
	2-Me	4.392	-0.605
		Observed[a]	
	^1H		
	2	-	-
	3	-0.042	0.199
	4	-2.211	1.000
	5	-	-
	6	-0.041	0.194
	7	-	-
	2-Me	0.024	-0.114

[a]Figures estimated from the spectrum of the complex Ni(5,7-diBr-2-Me-oxine)

the transfer of spin from the metal into the antibonding orbital (π^*) of the ligand. It is noteworthy that the agreement between calculated and observed values for H-2 is particularly poor. One would expect this proton to be the most affected (and hence the most shifted) by spin delocalization because of its close proximity to the metal as has been experimentally observed. However, INDO calculations for the anionic ligand radical predict that H-4 should shift the most from its diamagnetic position. This discrepancy may be due to the fact that the Ni(R-oxine) complexes are not purely octahedral as dmso molecules occupy the axial positions. If there is distortion from an idealized octahedral symmetry, one can no longer assume that the isotropic shifts are purely contact in origin. There may be a significant dipolar contribution to the shift which will attenuate as the distance from the metal is increased. This could explain why H-2 is shifted significantly more than is theoretically expected [6]. An alternative explanation is that considering the ligand as either a cation or anion, as is in our case, is an oversimplication. Such an observation has been reported by Scarlett *et al.* [9]. The neglect of the metal orbitals in the INDO calculations is only justifiable if the relative energies of the ligand orbitals do not change upon complexation.

The observed hyperfine coupling constants are numerically smaller than the calculated hyperfine coupling constants. INDO calculations are performed on the assumption that a whole electron is transferred. It is therefore possible

to estimate the percentage electron transferred by comparing the magnitude of the observed and calculated hyperfine coupling constants. In the Ni(oxine) complex, the percentage electron transferred was estimated[a] to be 3%.

INDO spin density calculations can also predict the type of spin delocalization (σ or π) in a selected system. Spin density in the p_z orbitals of the ligand atoms indicates a π-bonding mechanism, whereas if the spin density is concentrated mainly in the s, p_x and p_y orbitals of the ligand atoms, spin delocalization *via* a σ-bonding mechanism is implied. INDO spin densities for the oxine cation and anion ligand radical are given in Table 5.6. Comparison of the calculated spin densities in the carbon p_y and p_z orbitals for the anionic ligand radical reveals that spin density is concentrated mainly in the p_z orbitals. From this it appears, that delocalization occurs predominantly *via* a π-mechanism. This could arise from π-bonding through the nitrogen atom. There is no evidence for π-bonding through the phenolic oxygen atom as H-7 hardly shifts at all from its diamagnetic position.

It was originally proposed [24,35] that certain features of a paramagnetic spectrum were unique to either a σ- or π-spin delocalization. These characteristic features could therefore assist in the interpretation of spectra. For example, in systems exhibiting σ-spin delocalization, proton resonances were thought to all shift in the same direction, upfield for delocalization of positive (antiparallel) spins and downfield for negative spin delocalization. Isotropic

---

[a]On the basis of H-4.

shifts attenuate rapidly with increasing distance from the paramagnetic metal. On substitution of a proton by a methyl group, the methyl group protons are all shifted in the same direction as the substituted proton, but the shifts are generally smaller. π-Delocalization was thought to be characterized by both up- and downfield shifts which alternated in direction between adjacent positions [36]. In addition, these shifts are not as rapidly attenuated. Often the largest shifts occur at positions far removed from the coordination site.

In contrast to the above discussion, Scarlett and colleagues [9] have recently shown that the manner in which the spin density is distributed through the ring system may not necessarily be indicative of a particular spin delocalization mechanism. These workers have shown that in the pyridine *N*-oxide cation, the unpaired spin density lies in a σ-orbital, even though the sign of the spin density alternated through the conjugated system. In agreement with this observation, we have shown above that a π-spin delocalization mechanism is predominant in the Ni(oxine) complex even though the ^{1}H-NMR spectrum of this complex suggests a σ-spin delocalization mechanism.[a] Evidence for π-spin delocalization stems from the ^{1}H-NMR spectrum of the Ni(5,7-diBr-2-Me-oxine) complex. The replacement of H-2 by a methyl group caused an upfield shift which is in the opposite direction to the unsubstituted proton. This observation has been shown to be characteristic of π-spin delocalization [6].

---

[a]All six proton resonances are shifted downfield from their diamagnetic positions.

Table 5.6

INDO spin densities for the oxine cation and anion.[a]

Species:	Nucleus	ρ_{INDO}	
	C	C_{p_y}	C_{p_z}
cation	2	0.0002	0.0238
	3	-0.0014	-0.0007
	4	0.0038	0.1149
	5	0.1050	0.3274
	6	-0.0061	-0.0315
	7	0.0029	0.1392
	8	-0.0029	0.1720
	9	-0.0003	-0.0033
	10	-0.0044	-0.0641
anion	2	-0.0009	0.0466
	3	-0.0025	-0.0358
	4	0.0087	0.3274
	5	0.0043	0.1486
	6	-0.0013	0.0035
	7	-0.0006	0.0243
	8	0.0025	0.1428
	9	-0.0021	-0.0487
	10	-0.0035	-0.0607

[a]Positive spin density indicates α-spin density.
Negative spin density indicates β-spin density.

REFERENCES

1. I.E. Dzyaloschinskii, *Z. eksptl. i teoret. Fiz.*, 33 (1957) 1454.

2. E.O. Fischer and H. Leipfinger, *Z. Naturforsch*, 10 (1955) 353.

3. G.M. Schwab and J. Voitländer, *Z. physik. Chem.*, 3 (1955) 341.

4. J. Volger, F.W. de Vrijer and C.J. Corter, *Physica*, 13 (1947) 635.

5. M. Hadders, P.R. Locher and C.J. Gorter, *Physica*, 24 (1958) 839.

6. G.N. La Mar, W. deW. Horrocks and R.H. Holm (Eds.), *N.M.R. of Paramagnetic Molecules* [Academic Press] London (1973).

7. R.J. Fitzgerald and R.S. Drago, *J. Amer. Chem. Soc.*, 90 (1968) 2523.

8. J.A. Pople and D.L. Beveridge, *Approximate Molecular Orbital Theory* [McGraw-Hill] New York (1970).

9. M.J. Scarlett, A.T. Casey and R.A. Craig, *Aust. J. Chem.*, 23 (1970) 1333.

10. D.R. Eaton, W.D. Phillips and D.J. Caldwell, *J. Amer. Chem. Soc.*, 85 (1963) 397.

11. G.N. La Mar, *Mol. Phys.*, 12 (1967) 427.

12. M.S. Sun, F. Grein and D.G. Brewer, *Canad. J. Chem.*, 50 (1972) 2626.

13. M.J. Scarlett, A.T. Casey and R.A. Craig, *Aust. J. Chem.*, 24 (1971) 31.

14. G.E. Jackson and L.G. Scott, *S. Afr. J. Chem.*, 36 (1983) 120.

15. L.G. Scott, *B.Sc. (Honours) Project*, 1982.

16. P. Roychowdhury, *Acta Cryst.*, B34 (1978) 1047.

17. G.N. La Mar, J.P. Jesson and P. Meakin, *J. Amer. Chem. Soc.*, 93 (1971) 1286.

18. E.L. Muetterties, W. Mahler, K.J. Packer and R. Schmutzler, *Inorg. Chem.*, 3 (1964) 1298.

19. J.P. Fackler, J.A. Fetchin, J. Mayhew, W.C. Seidel, T.J. Swift and M. Weeks, *J. Amer. Chem. Soc.*, 91 (1969) 1941.

20. E.L. Muetterties, W. Mahler and R. Schmutzler, *Inorg. Chem.*, 2 (1963) 613.

21. N. Baggett, D.S. Poolton and W.B. Jennings, *J. Chem. Soc. Dalton Trans.*, 8 (1979) 1128.

22. K.J. Laidler and J.H. Meiser, *Physical Chemistry* [Benjamin-Cummings] California (1982).

23. W.G. Jackson and A.M. Sargeson, *Inorg. Chem.*, 17 (1978) 1348.

24. G.A. Lawrance and S. Suvachittanont, *Aust. J. Chem.*, 33 (1980) 1649.

25. A.M. Bond, B.S. Grabaric and J.J. Jackowski, *Inorg. Chem.*, 17 (1978) 2153.

26. W.G. Jackson, *Aust. J. Chem.*, 34 (1981) 215.

27. K. Uchida and Y. Takinami, *Bull. Chem. Soc. Japan*, 53 (1980) 3522.

28. M. Schumann and H. Elias, *Inorg. Chem.*, 24 (1985) 3187.

29. D.J. Darensbourg and A.H. Graves, *Inorg. Chem.*, 18 (1979) 1257.

30. D.J. Darensbourg, *Inorg. Chem.*, 18 (1979) 14.

31. A. Peloso and L. Volponi, *Gazz. Chim. Ital.*, 100 (1970) 825.

32. J.E. Brady and D. Thompson, *Inorg. Nucl. Chem. Lett.*, 6 (1970) 663.

33. N. Serpone and D.G. Brickley, *Progr. Inorg. Chem.*, 17 (1972) 391.

34. J.C. Bailar, *J. Inorg. Nucl. Chem.*, 8 (1958) 165.

35. R.W. Kluiber and W. DeW. Horrocks, *J. Amer. Chem. Soc.*, 87 (1965) 5350.

36. J.A. Happe and R.L. Ward, *J. Chem. Phys.*, 39 (1963) 1211.